

**T-Pos69** EXAMINATION OF THE ACCURACY OF THE DERJAGUIN APPROXIMATION FOR THE ELECTROSTATIC DOUBLE LAYER INTERACTION BETWEEN CURVED SURFACES BEARING CONSTANT POTENTIALS. Eytan Barouch, Department of Mathematics, Egon Matijevic, Department of Chemistry, Clarkson University, Potsdam, NY 13676; Adrian Parsegian, NIH, Bethesda, MD 20205.

The difficulty of solving equations for the forces between curved surfaces has prompted the use of a clever and widely used superposition method, originally due to Derjaguin, to relate the force between curved surfaces to the interaction energy between parallel planar surfaces of corresponding material properties. In this paper, we use a recently derived exact result for the interaction of two unlike spheres to examine the relation  $F_{sp}(d) = 2 R_c E_{sp}(d)$  for the force  $F_{sp}$  between a plane and a sphere of radius  $R_c$  with the interaction energy per unit area  $E_{sp}$  of two  $sp$  planes. For bodies bearing equal surface potential, the Derjaguin approximation works  $sp$  remarkably well even at high potentials. For bodies bearing unequal potential either at separations  $d$  approaching contact or approaching infinite separation, the approximation again appears valid. However, at intermediate separations and particularly in regions where force and energy go through extrema, there is a qualitative difference between planar energies computed exactly and those inferred from the approximation. This difference can persist even to bodies of macroscopic dimensions. However, the larger the radii of curvature compared to the Debye length, the smaller the range of distances over which a disparity exists. Thus there is not always an automatic conversion to be assumed in converting forces between curved surfaces and the theoretical examination of such interactions in planar geometry.

**T-Pos70** EVIDENCE FOR COMPLEX INTERACTIONS OF CALCIUM BINDING PROTEINS IN RAT UTERUS PLASMA MEMBRANES. A.K. Grover (Sponsored by Dr. E.E. Daniel). Neurosciences Department, HSC-4N49, McMaster University, Hamilton, Ontario, Canada. L8N 3Z5.

The plots of log of residual pH-dependent Ca-binding by the rat myometrium plasma membrane vesicles vs radiation dose were nonlinear. The autoradiography of 45-Ca-stained electroblobs of SDS-polyacrylamide gel electrophoresis on the same membranes showed that several proteins of different molecular weights were labelled. The radiation inactivation pattern could not be explained as a simple sum of 1-hit, 1-target decays of the component proteins. The data could, however, fit optimally either a 2-hit model or a 3-target model with apparent decay constants of 2.50 and 2.66 Mrdas, respectively. These correspond to apparent target sizes of 256 and 241 kDa, respectively. Since most of the Ca-binding proteins observed with the SDA-gel electrophoresis were much smaller in size, these must be involved in energy-transduction. Therefore, it is concluded that the Ca-binding proteins in this membrane, complex with each other and/or with other membrane components so as to allow this energy transduction resulting in the observed radiation inactivation pattern.

Supported by M.R.C.

**T-Pos71** PROPOSED EXPERIMENTAL APPROACH TO IMMORTALITY IN PLANTS AND ANIMALS, R. Rössler, Medical Policlinic, University of Tübingen, K. Wegmann, Institute for Chemical Plant Physiology, and O.E. Rössler, Institute for Physical and Theoretical Chemistry, University of Tübingen, 7400 Tübingen, W. Germany

Aging is a morphogenetic process. This is because a re-scaling in length of the adaptive viability-as-a-function-of-age curve (Medawar) is recurrently necessary on evolutionary grounds ("temporal French-flag problem"). Unlike ordinary morphogens, which act by providing a positive gradient in space, the present temporal morphogens ("gerogens") act by providing a negative gradient in time. Otherwise, the well known "wooden barrel on a flooded staircase" model of Meinhardt on the irreversible activation of genetic states by a transient morphogen (H. Meinhardt, Models of Biological Pattern Formation, London, Academic Press 1982, p. 113) is directly applicable: A new set of genetic switches is being set as a function of morphogen concentration, with the possibility of a new morphogen (gerogen) taking over at that point. The latter then again acts as a decreasing hourglass until the next threshold is reached. The theory is easy to test by a new type of parabiosis experiments. Two genetically identical macroorganisms (acetabularia, in the simplest case) are connected by a tissue bridge. One of the two twins is then replaced by a new specimen of constant initial age at regular intervals. Aging should thereby be delayed indefinitely in the invariant partner. The experiment is "robust" in the sense that a positive outcome will directly lead to a procedure for the localization, enrichment, identification, and testing of the chemical gerogen involved.

**T-Pos72** SEQUENCE HOMOLOGIES BETWEEN THE MITOCHONDRIAL OUTER-MEMBRANE PORE-PROTEIN AND INNER-MEMBRANE TRANSPORT PROTEINS. C.A. Mannella and I.E. Auger (Intr. by D.S. Berns), Wadsworth Center for Laboratories and Research, N.Y. State Dept. of Health, Albany, NY 12201

The primary structure of the 30,000-d pore-forming protein of the mitochondrial outer membrane (called VDAC or porin) has recently been derived from the cDNA sequence of yeast (Mihara and Sato 1985 *EMBO J* 4:769). The VDAC sequence exhibits very limited local homologies with available sequences of bacterial porins, the 34-37,000-d pore-formers in outer envelopes of gram-negative bacteria. However, there are significant similarities between the VDAC sequence and those of two 30,000-d (ca.) mitochondrial inner-membrane proteins: the ADP/ATP carrier (AAC) and the "uncoupler protein" (UCP) or "thermogenin" of adipose tissue. Homology with VDAC is especially strong for AAC in a segment of over 50 amino acids near the C-terminus (247-301 in the AAC sequence, 212-268 in VDAC), and for rat UCP in a segment of over 110 amino acids (38-153 in the UCP sequence, 39-155 in VDAC). These findings suggest that the three mitochondrial proteins, which all have membrane transport functions but which differ in specificity and location, may be derived from a common ancestral transport protein, perhaps unrelated to that of bacterial porins. Also, regions of highest homology in the mitochondrial protein sequences may be involved in the functional property which the proteins have in common, i.e. forming a transmembrane aqueous channel. (Supported by NSF grant PCM 83-15666).

**T-Pos73** A STUDY OF MUTUAL ENTRAINMENT AS A MECHANISM OF SYNCHRONIZATION IN THE SINUS NODE. DC Michaels, EP Matyas, and J Jalife, SUNY/Upstate Medical Center, Syracuse, NY 13210

Synchronization in the sinoatrial node (SAN) may involve electrical communication of cells via low-resistance nexuses. A mathematical model based on voltage clamp data was used to study synchronization of SAN cells with different intrinsic frequencies. Up to 400 "cells" were connected through ohmic resistances to form a two-dimensional sheet. Intrinsic frequencies and coupling resistances ( $R_c$ ) could be adjusted for each cell. A "dominant" pacemaker region was simulated by increasing the intrinsic frequency of a small cluster of cells in one region. With weak coupling, cells mutually entrained (1:1) to a common frequency that was intermediate between intrinsic frequencies, but different from the mean. In addition, the sheet exhibited "apparent" conduction where coupling intervals increased with increasing distance from the dominant region. At higher values of  $R_c$ , apparent conduction time increased, simulating first degree intranodal block. Under these conditions, "reentry" phenomena were seen. In another set of simulations, intrinsic frequencies were assigned randomly. Again, cells mutually entrained and one region became the "dominant" pacemaker. Increasing  $R_c$  did not alter the pattern of activation sequence except to increase coupling intervals. As noted in previous studies with two coupled pacemakers, over the range in which 1:1 mutual entrainment was maintained, increases in  $R_c$  produced decreases in the common frequency of the synchronized sheet. We conclude that the mathematical simulations provide a realistic model for the SAN. Furthermore, results indicate that mutual entrainment mediated by phase-dependent electrotonic interactions between coupled pacemakers can account for synchronization of electrical activity of SAN.

**T-Pos74** ELECTRON EXCHANGE ALONG FLEXIBLE POLYMERS Robert Bittl and Klaus Schulten, Dept. of Physics, Technical University of Munich, 8046 Garching, Fed. Rep. Germany

The recent solution of the structure of the photosynthetic reaction center of *Rh. viridis* by Deisenhofer and Michel revealed that the chromophores which are involved in the primary electron transfer make contact with each other through the chromophore's aliphatic side chains. We investigate the exchange interaction between the ends of such side chains by means of the stochastic Liouville equation for the spin motion of paramagnetic end groups of aliphatic polymers. Applying our solution to recent observations by Weller et. al. of magnetic field effects on electron transfer reactions between the ends of aliphatic polymers of various length we determine that the exchange interaction is "through space" with a spatial dependence close to that suggested earlier by deKanter et. al. The stochastic folding motion of the polymer has a strong influence on the exchange interaction. This influence can be described by Kubo's spectral function of the exchange interaction  $J(r(t))$ ,  $r$  denoting the end-end distance of the polymer, which accounts for the effect of stochastic variations of  $r$ . Similarly, the rate of electron transfer should be affected by the stochastic motion inside the reaction center.

**T-Pos75** LIMIT CYCLE MODELING OF CIRCADIAN OSCILLATORS: PHASE SETTING EFFECTS

Van D. Gooch; Division of Science and Math  
University of Minnesota-Morris, Morris MN; 56267

Limit cycles have been very useful in circadian rhythm research in discussing the phase shifting effects of pulses of light and temperature. However, there has been much less investigation of the entraining and phase setting effects of a master driving oscillator on a free running limit cycle oscillator. Such an investigation is particularly important in trying to understand how natural daily cycles entrain the circadian rhythms of organisms.

For purposes of an initial approach, a mathematically circular limit cycle has been used. It is assumed that a change in light or temperature affect the reaction kinetics such that the singularity of the limit cycle also becomes altered. Computer simulation, using this model, qualitatively imitates actual results of several experimental formats. Hold-release experiments have been most intensely investigated. An example of such an experiment would be that after full entrainment of cycles of 12 hrs light - 12 hrs dark, different groups of organisms would be held under constant light for varying amounts of time (0,1,2,...72 hrs) and finally released into constant dark; the phase relationship of the resulting phase relative to the release time is determined. Actual experiments have been carried out with *Neurospora* and *Gonyaulax* using light and temperature. These results and published results compare favorably with the modeled results. The computer modeling also suggests new, interesting experiments that should be performed, including a new way of determining singularity.

**T-Pos76** MONTE CARLO CONVOLUTION AND SIMULATION OF FLUORESCENCE SINGLE PHOTON COUNTING DECAY DATA

Joseph M. Beechem and Ludwig Brand. Biology Dept. of The Johns Hopkins University, Baltimore MD.

A Monte Carlo procedure is developed for the simulation (& analysis) of fluorescence decay curves. The essential feature of this approach is that no analytical mathematical form for the proposed decay law is required or assumed. In this way, complex fluorescence decay schemes, in which no analytical forms for the impulse response function exist, can be analyzed. A flow chart for this algorithm can be summarized as follows:

- 1) input excitation profile  $E(t)$
- 2) convert  $E(t)$  to probability distribution function  $E_p(t)$
- 3) calculate decay probability distribution from initial guess(es)  $D_p(t)$
- 4)  $i = 1$ , total number of counts desired in decay curve
- 5) use random number generator with distribution  $E_p(t)$  to obtain a single "start" channel ( $t_2(i)$ )
- 6) use random number generator with distribution  $D_p(t)$  to obtain a single "stop" channel ( $t_1(i)$ )
- 7) apply physical model ( $P(t_2-t_1)$ ) which directly mimics spectroscopic experiment with random number generators
- 8) physical model determines the survival of photon  $i$
- 9) if photon  $i$  survives, increment channel  $i$  by 1.

In this way, decay curves are simulated (one photon at a time), which may contain "square root of time" or other more complicated relationships without any explicit analytical formulation. The convolution is exact, and no noise needs to be added to the simulation. NIH grant #GM11632.

**T-Pos77** DETERMINATION OF REFLECTION COEFFICIENT FROM SCATTERED LIGHT INTENSITY IN OSMOTIC SHOCK EXPERIMENTS. Kevin R. Smith, James Myslik and James A. Dix, Department of Chemistry, State University of New York, Binghamton, NY 13901

A common method to study the solute permeability of biological membranes is to challenge a cell with a hyperosmotic solution, then monitor light scattering intensity as a function of time; the light scattering properties of the cell can then be related to cell volume. In principle, the three relevant membrane parameters (the filtration coefficient,  $P_f$ , the solute permeability coefficient,  $P_s$ , and the reflection coefficient,  $\sigma$ ) along with an overall amplitude and offset can be determined from a detailed analysis of the total time course of light scattering. We have investigated the feasibility of using total time course analysis to determine the reflection coefficient. We find that the amplitude and baseline parameters are orthogonal and can be determined from the line shape with good precision. However, the three membrane parameters are tightly coupled and precise measurements of the reflection coefficient necessitate precise independent measurements of  $P_f$  and  $P_s$ . Inclusion of artifactual changes in scattering light intensity due to solute-induced index of refraction changes (Mledokay et al, *J. Gen. Physiol.* 81, 239-253, 1984) affects primarily the determination of  $P_s$ . Supported in part by HL29488.

**T-Pos78** INTERACTIVE COMPUTER-AIDED INTERPRETATION OF SEDIMENTATION DATA. T.M. Laue & S.L. Pelletier, Department of Biochemistry, University of New Hampshire, Durham, NH 03824.

A commercially-available microcomputer-based spreadsheet program is used to ease the interpretation of analytical ultracentrifuge data in three ways: 1) protein amino acid composition is used to calculate a monomer molecular weight, partial specific volume, as well as values for the anhydrous spherical radius, frictional, sedimentation and diffusion coefficients. These same values may be calculated for user input models in which the molecule's degree of hydration ( $d'$ ) and ellipsoid axial ratio ( $a/b$ ) are varied. 2) Solvent density and viscosity are estimated from the temperature and molar concentrations of the buffer components. Thus, observed sedimentation coefficients may be normalized automatically to standard conditions ( $S_{20,w}^0$ ), and good estimates of the reduced molecular weights  $M(1-\bar{v}_e)w^2/RT$  may be obtained. 3) Experimentally determined value of  $S_{20,w}$  may be interpreted in terms of the degree of hydration or ellipsoid axial ratio. To do this, a model is entered in which one of these two parameters is held fixed; the program then calculates the second parameter. The use of the spreadsheet provides a uniform interactive environment for the expansion of the program to encompass more complex systems.

**T-Pos79** POSSIBILITY OF PROTON SUPERFLUIDITY AT THE WATER-MEMBRANE INTERFACE. Michael Conrad, Depts of Computer Science and Biological Sciences, Wayne State University, Detroit, MI  
Numerical estimates suggest that mobile  $H^+$  bonds at the water-membrane interface can be paired by propagating electronic oscillations in the polar side groups of the membrane. The model is dual to the BCS theory of electronic superconductivity in that 1) mobile protons hopping chiefly between oxygen atoms in the layer of bound water play the role of conduction electrons and 2) the pairing interaction has its origin in electronic excitations rather than lattice vibrations, as in Little's proposed room temperature organic superconductor. The hopping of a proton into the vicinity of a membrane electron can be treated as a transient alteration in the potential in which the electron moves. This produces a transient alteration in its ground state energy and consequent transient alterations in the potential of neighboring membrane electrons. Spectroscopically these excitations would be observable only as a blurring of the UV spectral lines. The pairing interaction is facilitated by high salt and polyelectrolyte concentrations since these screen the Coulomb repulsion. The mobility of  $H^+$  bonds is principally a fluctuation phenomenon, whereas the velocity of conduction electrons in a metal is principally a consequence of the Pauli exclusion principle. However, an  $H^+$  hopping motion lasts long enough for the induced electronic oscillation to establish a pairing interaction that can persist as a distortional correlation with a relaxation time greater than the mean time between hops. Condensation of proton pairs is possible since the water-membrane interface is a surface of finite thickness and is favored by the fact that the density of states is higher than in the metal case. The existence of a condensate might be detectable as a zero voltage proton current analogous to the DC Josephson effect.

**T-Pos80** WAVE AND PARTICLE AS THE PHYSICAL ANALOGUES OF PHENOTYPE AND GENOTYPE, Stanford Goldman, Dept. of Electrical Engineering and Computer Sciences, Univ. of California, San Diego, La Jolla, CA 92093.

The author has found a pervading mimicry between biology and physics, and the subject of this paper is an important example. The mimicry becomes particularly clear when physics is expressed in terms of relativistic quantum mechanics. In the latter, a particle is expressed in terms of quantized values of conserved observables, and a particle need not be physically small. In alternation of generation in biology, e.g. humans, there is the generation of man (or woman) in which the emphasis is on phenotype characteristics, and the generation of sperm (or ovum) in which the emphasis is on genotype characteristics. There is an analogue of alternation of generation in interactions in physics. These alternating generations may be called the isolation and interaction generations. In the former, there is motion of particles from place to place, while in the latter there is interchange of conserved observables between particles. Entities are in waveform in isolation generations, and in particle form in interaction generations.

**T-Pos81** NON-EQUILIBRIUM STATE OF ENZYMATIC PROTEINS AND AGING PROCESSES. M.-T. Klonowska, W. Klonowski, Brandeis University, Department of Chemistry, Waltham, MA 02254.

We have advanced a hypothesis that because of the very mechanism of protein biosynthesis, some proteins at the moment when biosynthesis is completed are in a non-equilibrium meta-stable state and that aging of such macromolecules is a process of internal equilibration. We suggest that the "fast" proteins i.e. ones, having rather short turnover half-times, of the order of 10-100 min., belong to this class of proteins.<sup>1</sup> Certainly, mechanisms of aging of proteins having similar molecular weights but differing by factors of  $10^2$  in the turnover half-time (for "slow" proteins it is of the order of  $10^4$ - $10^5$  min) must be different. If our hypothesis is true, then an artificial reconstruction of such "fast" proteins having intrinsic internal non-stability is just impossible but eventually by genetic engineering methods. The "fast" proteins also may not be renatured as they natural non-equilibrium state may not be reproduced after achieving an equilibrium denatured state.<sup>2</sup> Similar considerations may concern tertiary structure of some proteins, which may be non-equilibrium as a whole even if built up of equilibrium subunits.<sup>3</sup> The hypothesis also suggests the possible importance of tunneling effects in enzymatic catalysis. Scrupulous investigations of "fast" protein primary structure and its correlations with turnover half-time and ability of being renatured are to be desired.

1. M.-T. Klonowska, W. Klonowski, *J. Bioelectr.* 4, 93 (1985).
2. W. Klonowski, M.-T. Klonowska, *Biomathematics* 80, 28 (1982).
3. W. Klonowski, M.-T. Klonowska, *Spec. Sci, Technol.* 6, 258 (1983).

**T-Pos82** LATIN HYPERCUBE SAMPLING AND THE ANALYSIS OF MONTE CARLO MODEL PARAMETER SENSITIVITY. Susan K. Seaholm, Shu-Chen Wu, and Eugene Ackerman, Division of Health Computer Sciences, University of Minnesota, Minneapolis, MN 55455.

Monte Carlo simulations of stochastic models are useful in exploring phenomena in the biophysical and biomedical sciences, such as infectious disease epidemics, which involve many probabilistic, interacting input parameters. However, due to the variety of model input and outcome variables, the testing of hypotheses and the analysis of outcome sensitivity to the parameter values can be difficult. Large numbers of lengthy simulations may be required. Hence the methods used to sample from the parameter space must be efficient while providing adequate estimates of model parameter sensitivity. Latin Hypercube Sampling has been used to reduce the number of required input sets, and to allow finer sampling within intervals given the same number of simulations, as compared to simple stratified sampling. Use of Latin Hypercube Sampling methods in the simulation of viral epidemics in human populations will be discussed, including automated generation of the samples and simulations, observed effects of data transformations and general relationships between input and outcome variables, and the construction of response surfaces for further sensitivity analysis of Monte Carlo simulation models from such samples.

**T-Pos83** **OCTOPUS RHODOPSIN AND ITS PHOTOPRODUCTS- A RESONANCE RAMAN STUDY.** C.Pande, A.Pande\*, R.Callender, T.Ebrey\* and M.Tsuda#. Physics Department, City College of New York, N.Y.; \*Department of Physiology and Biophysics, University of Illinois at Urbana-Champaign, Urbana, IL.; †Universitatsspital Zurich, Switzerland; #Department of Physics, Sapporo Medical College, Sapporo, Japan.

We have measured the resonance Raman spectrum of octopus (*Mizudaco, Paroctopus defleini*) rhodopsin by the flow technique, and with a pump beam, down-stream from the probe beam, to regenerate rhodopsin from the photoisomerized sample. Spectrum, predominantly due to acid-meta rhodopsin, was obtained in the stationary state in the absence of the pump beam. Raman spectra have also been measured at low temperatures and under various illumination conditions to produce photo-stationary states of differing composition. These data were used to extract the spectra of batho- and iso-rhodopsin by algebraic manipulation.

Even though the chromophore chemical-extraction data shows that the octopus rhodopsin, like the bovine rhodopsin, contains the chromophore in the 11-cis isomeric form, there are marked differences in the finger-print region of their resonance Raman spectra. This suggests that the nature of the chromophore-protein interaction may be quite different in these two systems. Data obtained for the other photoproducts will also be compared with those already available for the bovine case, and the possible structural implications will be discussed.

**T-Pos84** **RHODOPSIN CONFORMATIONAL REFOLDING DETECTED BY FTIR SPECTROSCOPY**

K.J. Rothschild, W.J. de Grip and J. Gillespie

*Depts. of Physics and Physiology, Boston University, Boston, MA 02215 (KJR, JG)*

*Dept. of Biochemistry, University of Nijmegen, Nijmegen, The Netherlands (WdG)*

FTIR-difference spectroscopy has been used to characterize the conformational changes occurring in photoreceptor membrane during the bleaching process. Spectral features in the 1700-1770  $\text{cm}^{-1}$  region have been previously detected which reflect alterations in the state of carboxyl groups. (De Grip *et al.*, *BBA* (1985), 809;97-106) By the Meta I intermediate, only those buried carboxyl groups which are inaccessible to water are altered. Meta II formation produces additional changes in exposed carboxyl groups which undergo deuterium/hydrogen exchange. In order to examine subsequent changes in photoreceptor membrane, we utilized kinetic FTIR-difference spectroscopy with one minute time resolution. Photoreceptor membrane as well as rhodopsin reconstituted into a number of different lipids, including ether-PC which does not contain an ester carbonyl group, were studied at a variety of temperatures. Our results indicate that alterations in carboxyl groups by Meta II are partially reversed during the subsequent decay of Meta II, reflecting a refolding of the rhodopsin conformation to allow for rebinding of the 11-cis retinal chromophore. Additional peaks in the difference spectrum can be assigned to other protein moieties. Evidence is also presented for alterations in unsaturated lipid bonds during the Meta II decay. This research was sponsored by NIH-NEI grant EY05499 to KJR, the Netherlands Organization for the Advancement of Basic Research ZWO-SON to WdG, and a NATO research grant to WdG and KJR.

**T-Pos85** **FINGERPRINT ASSIGNMENTS IN RESONANCE RAMAN SPECTRA OF VISUAL PIGMENTS: IMPLICATIONS FOR CHROMOPHORE STRUCTURE AND ENVIRONMENT.** I. Palings and R.A. Mathies, Chemistry Dept., University of California, Berkeley; and J. Pardoen, C. Winkel, J. Courtin, P. Mulder and J. Lugtenburg, Chemistry Dept., Leiden University, The Netherlands.

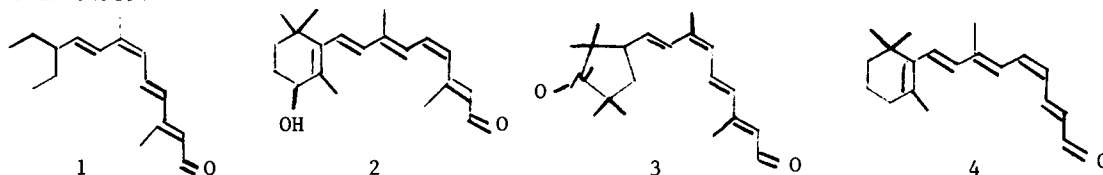
To investigate the molecular basis of wavelength regulation in the visual pigment rhodopsin and energy storage in its primary photoproduct bathorhodopsin we have compared the vibrational properties of the retinal protonated Schiff bases (RPSB) in solution and bound inside the pigments. The C<sub>8</sub>-C<sub>9</sub>, C<sub>10</sub>-C<sub>11</sub>, C<sub>12</sub>-C<sub>13</sub> and C<sub>14</sub>-C<sub>15</sub> single bond stretches of the chromophores have been assigned using <sup>13</sup>C and <sup>2</sup>H labeled chromophore derivatives. These assignments confirm that the normal modes in the fingerprint region of rhodopsin, isorhodopsin, and bathorhodopsin, which are correlated with normal modes in the 11-cis, 9-cis, and all-trans RPSB model compounds, contain the same dominant single bond stretching coordinate. The assignments also indicate that all single bonds between C<sub>8</sub> and C<sub>15</sub> are s-trans in all three pigments. These data are inconsistent with models suggesting s-cis single bond structures between C<sub>8</sub> and C<sub>15</sub>. Significant protein-induced frequency changes are observed for the C<sub>8</sub>-C<sub>9</sub> and C<sub>14</sub>-C<sub>15</sub> stretching modes in bathorhodopsin which are shifted up by 12 and 19  $\text{cm}^{-1}$ , respectively. This is suggestive of protein perturbations, either electrostatic or conformational, that are involved in energy storage. In contrast, the frequencies of the fingerprint modes of rhodopsin in the region C<sub>8</sub> through C<sub>15</sub> are unperturbed by the protein. In particular, the localized C<sub>14</sub>-C<sub>15</sub> stretching mode at 1190  $\text{cm}^{-1}$  shifts by <2  $\text{cm}^{-1}$ . This result appears to be inconsistent with the presence of a negative protein charge near C<sub>13</sub>, which is held to be responsible for the "opsin shift" of rhodopsin. Such a perturbation is expected to significantly increase the C<sub>14</sub>-C<sub>15</sub> bond order.

**T-Pos86 LIPID DEPENDENCE OF LUMIRHODOPSIN AND METARHODOPSIN KINETICS.** Richard W. Morton, Martin Straume, James L. Miller, and Burton J. Litman. Department of Biochemistry, University of Virginia School of Medicine, Charlottesville, VA

Flash photolysis measurements were performed on sonicated, retinal rod disks and on dilution reconstituted, rhodopsin-phospholipid vesicles, composed of phosphatidyl choline (PC) and variously with phosphatidyl serine (PS) and cholesterol. Flash photolysis was performed on a microsecond time scale at 380nm and 420 nm and 10, 25 and 37°C. Computer-assisted analysis was used to derive amplitudes and rate and equilibrium constants for the lumi-metarhodopsin I (MI) and MI-metarhodopsin II (MII) forward and reverse reactions. The lumi-MI rate constant is increased with respect to disks by PC more than by the addition of PS to PC, but cholesterol added to either lipid system had no further effect. In all systems studied, increasing temperature increases the A<sub>380</sub> contribution of MI, independent of lipid environment, interpreted as a blue shift of the MI absorbance spectrum. Addition of PS increases equilibrium concentrations of MII, but cholesterol added to either PS-PC or to PC alone favors MI. In no recombinant system is MII formation as favorable as in rod discs. Our results suggest that the photochemistry of rhodopsin is dependent on both phospholipid head group composition and membrane acyl side chain ordering. Supported by grants NSF PCM 8316858 and NIH EY 00548.

**T-Pos87 THE IMPORTANCE OF THE CHROMOPHORE RING IN METARHODOPSIN FORMATION,** Rosalie K. Crouch and Geoff Renk, Ophthalmology, Medical University of South Carolina, Charleston, SC

Photosensitive pigments have been formed with opsins of various species and numerous retinal analogues. The structural and isomeric requirements for pigment formation are that a) the polyene side chain contain a *cis* double bond in the 7,9 or 11 position; b) some portion of the cyclohexyl ring be present including at least one of the three ring methyl groups; c) the length of the polyene chain be preserved, and d) the terminal aldehyde group be present. The involvement of these synthetic retinals in the bleaching process and physiology role of rhodopsin is not as well elucidated. The goals of these studies are to determine the facility of formation of metarhodopsin I and II and study the rhodopsin catalyzed G-protein GTP-binding using these synthetic rhodopsins. Pigments formed with 1-4 were studied using spectrophotometric identification of the meta I and meta II states and a nonhydrolyzable GTP analogue, GTPYS, to measure the G proteins GTP binding. The cyclohexyl ring was found to play a critical role. Supported by NIH grant EY-04939.



**T-Pos88 DO DIFFUSION RATES IN THE CYTOPLASM OR THE MEMBRANE LIMIT THE RESPONSE SPEED OF THE VERTEBRATE ROD?** Erich S. Phillips and Richard A. Cone, The Department of Biophysics, Johns Hopkins University, Baltimore, MD. 21218.

Phototransduction in the rod involves reactions between photoactivated rhodopsin and membrane associated proteins in a light activated enzyme cascade. This is followed by the diffusion of an intracellular transmitter through the cytoplasm of the rod outer segment (ROS). Thus, either diffusion rates in the membrane or diffusion rates in the cytoplasm might limit the response speed of the rod. If cytoplasmic diffusion rates limit the response speed, then the photoresponse should slow in exact proportion to any increase in cytoplasmic viscosity. In contrast, if membrane diffusion rates limit the response speed, then changes in cytoplasmic viscosity should have little effect on the speed of the photoresponse. With intact frog ROS, we used fluorescence recovery after photobleaching (FPR) to monitor the lateral diffusion rates of either 6-carboxyfluorescein, a cytoplasmic probe or iodoacetamide-fluorescein labelled rhodopsin, a disk membrane probe. We added glycerol to vary the cytoplasmic viscosity, and found that it slowed cytoplasmic diffusion by the same factor that it slows diffusion in water. In contrast, glycerol hardly slowed diffusion in the membrane (less than 10% of the cytoplasmic change). Next, we examined the effects of glycerol on the photoresponse of rods. The photocurrent from isolated frog rods with attached ellipsoids was recorded by aspirating the outer segments into tight fitting suction pipettes (T=21-23 °C). In 20% glycerol (w/v) rods showed no marked change in their response amplitude or light sensitivity compared to rods in normal solution, but their photoresponses took on average 1.7 times longer to reach peak ( $1.68 \pm .11$ , mean  $\pm$  S.E.M.). The 20% glycerol solution was 1.7 times more viscous than water ( $1.72 \pm .08$ , falling ball viscometry). Therefore, to within experimental error, 20% glycerol slowed the photoresponse in the same proportion that it increased the cytoplasmic viscosity. Thus, our results are consistent with the hypothesis that the response speed of a rod is limited almost entirely by diffusion rates of molecules in the cytoplasm rather than diffusion rates of molecules in the membrane. (NIH 2R01EY00520 & 2T32GM07231)

**T-Pos89 MEASUREMENT OF METABOLIC FLUXES AND POOL SIZES OF CYCLIC GMP, ATP, AND GTP IN THE INTACT TOAD RETINA BY  $^{18}\text{O}$  LABELING.** S.M. Dawis, R.A. Heyman, M.J. Causton, T.F. Walseth, R.M. Graeff, D.A. Burkhardt, and N.D. Goldberg, Depts. of Pharmacology and Psychology, University of Minnesota, Minneapolis 55455

The metabolic pool sizes and hydrolytic rates for cGMP, ATP, and GTP were measured in intact, isolated toad retinas by monitoring  $^{18}\text{O}$  incorporation from ( $^{18}\text{O}$ )- $\text{H}_2\text{O}$  into the phosphoryls of retinal nucleotides. Pool sizes were calculated from  $^{18}\text{O}$  distribution after isotopic equilibrium was reached. Metabolic pools have a binomial distribution of  $^{18}\text{O}$  whereas non-metabolic pools exhibit negligible  $^{18}\text{O}$  labeling. In the dark, 40% of the retinal GTP is involved in cGMP metabolism; this is equivalent to all the GTP in the rod outer segment participating in cGMP metabolism. Of the total retinal ATP, 80% is metabolically active, and a discrete pool of phosphate subserves this metabolically active ATP. From rates of  $^{18}\text{O}$  incorporation before reaching isotopic equilibrium it is estimated that in the dark at 22° photoreceptor cGMP is hydrolyzed at a rate of 3  $\mu\text{mol}\cdot\text{mg}\cdot\text{prot}^{-1}\cdot\text{sec}^{-1}$  and  $\gamma$ -phosphoryls of retinal ATP are labeled at a rate of 183  $\mu\text{mol}\cdot\text{mg}\cdot\text{prot}^{-1}\cdot\text{sec}^{-1}$ . With increasing intensities of illumination (40 sec), cGMP flux increases by more than 4-fold and cGMP levels remain unchanged or increase up to 25%. Over this same range of intensities,  $\gamma$ -ATP labeling rate remains relatively constant. The cGMP metabolic flux is estimated to account for 7% of the rate of photoreceptor  $\gamma$ -ATP labeling in the dark and increases to over 30% with photic stimulation. Adaptation to high light intensities is characterized by decreases in cGMP metabolic flux and photoreceptor cGMP concentration and no change in the rate of retinal  $\gamma$ -ATP labeling. These results indicate that cGMP generation and hydrolysis is a tightly coupled and major energy-consuming process in the photoreceptor engaged during photoexcitation. NIH EY04877, GM28818, EY00406.

**T-Pos90 IDENTIFICATION OF ROD OUTER SEGMENT cGMP BINDING PROTEINS BY DIRECT PHOTOAFFINITY LABELING.** P.S.T. Yuen, T.F. Walseth, S.S. Panter, S.R. Sundby and N.D. Goldberg, (Intr. by D. Levitt), Dept. of Pharmacology and Dight Institute for Human Genetics, University of Minnesota, Minneapolis 55455

Cyclic GMP binding proteins in the toad rod outer segment were examined by direct photoaffinity labeling (PAL) with  $^{32}\text{P}$ -cGMP (specific activity >5000 Ci/mmol). Eight cGMP specific bands representing six components were labeled; apparent molecular weights ( $MW_{app}$ ) were 110/105, 94/90, 58, 50, 47, and 41 kDa. The 94/90 kDa doublet corresponds to the  $\alpha$  and  $\beta$  subunits of the phosphodiesterase (PDE) by comparison with authentic  $\text{PDE}_{\alpha,\beta}$  and by several of its cGMP binding characteristics. GTP (10  $\mu\text{M}$ ) inhibits the labeling of the 94/90 kDa doublet, but this effect is lost when transducin is removed during purification. Labeling of the 94/90 kDa doublet is stimulated by 3-isobutyl-1-methylxanthine (30-300  $\mu\text{M}$ ) and by  $\text{PDE}_{\gamma}$  represented by heat-denatured PDE. These are properties of the labeling of non-catalytic sites of PDE. The specificity of this non-catalytic site for cGMP analogs is  $R_p\text{-cGMPs} > S_p\text{-cGMPs} > \text{cGMP} > 8\text{-Br-cGMP}$ . An inactive form of PDE eluted from disc membranes can be detected and distinguished from an active form by PAL. Extended UV exposure accentuates labeling of the 110/105 kDa doublet, which exhibits an identical response to cGMP analogs, GTP, IBMX, and  $\text{PDE}_{\gamma}$  as the 94/90 kDa doublet. The 110/105 kDa doublet behaves as  $\text{PDE}_{\alpha}$  and  $\text{PDE}_{\beta}$  photocrosslinked to  $\text{PDE}_{\gamma}$  ( $MW_{app}$  of 16 kDa). The 58, 50, 47, and 41 kDa bands do not appear to derive from the 94/90 kDa doublet by several criteria. The 50 and 47 kDa components may be related to the regulatory subunits of cAMP-dependent protein kinase, but 58 and 41 kDa components which exhibit exclusive binding properties represent unique cGMP-specific components for which a function has yet to be identified. (Supported by NIH grant GM 28818.)

**T-Pos91 ON THE ACTIVATION AND DESACTIVATION MECHANISM OF THE PHOTORECEPTOR PHOSPHODIESTERASE (PDE) - A Light Scattering Study.** R.Wagner, H.Desel & R.Uhl, intr. by W.Stühmer, MPI für biophysikalische Chemie, Am Faßberg, D-3400 Göttingen, F.R.G.

Light scattering changes accompanying the light-induced interaction between disk membranes and peripheral disk membrane proteins have been characterized using a Multi Angle Flash Photolysis Apparatus.

Bovine ROS with completely intact plasma membrane show regular P- or Binding-Signals (Uhl *et al.* (1977) *Biochim. Biophys. Acta.* 469, 113-122, Kühn *et al.* (1981) *Proc. Nat. Acad. Sci. US* 78, 6873-6877), both in the presence and absence of GTP. GTP can be introduced either by permanently destroying the plasma membrane, using freeze/thawing or a short exposure to a medium of low osmolarity (70 mOsmol/l), or by a new method that only transiently permeabilizes the cell envelope. It employs the use of n-alkylglycerols, which can be readily washed out. In all three cases no Dissociation-signals (Kühn *et al.* 1981) are observed. Instead, an amplified P-Signal occurs, which saturates at bleaches below 0.1% and is completely abolished in the presence of micromolar amounts of GTP- $\gamma$ -S. Thus, even in intact ROS, light scattering signals can be correlated with the rapid interaction of many G-proteins with a single photolysed rhodopsin, i.e. the primary amplification step involved in the light activation of the rod PDE.

The amplification is significantly reduced in the presence of ATP, but this effect can be completely overcome by vanadate.

Preliminary results, basing on parallel measurements of PDE activity and light scattering signals, suggest that the PDE quench by ATP is guarded by two independent mechanisms: one, which reduces the initial velocity and can be turned off by vanadate, and one, being independent of vanadate, which is responsible for the deactivation of rhodopsin after a certain delay.

**T-Pos92 EFFECT OF SONICATION ON NUCLEOTIDE DEPENDENT LIGHT SCATTERING CHANGES IN ROD OUTER SEGMENT SUSPENSIONS**

J.W. Lewis, L.E. Schaechter, and D.S. Kliger, Division of Natural Sciences, University of California, Santa Cruz, CA 95064

Near infrared light scattering from suspensions of rod outer segment fragments reflects light activated changes in peripheral membrane proteins in visual cells. Limited sonication of suspensions has been shown to increase the amplitude of light induced turbidity changes in the presence of guanosine triphosphate (GTP) by a factor of two. Further sonication led to a decrease in the signal amplitude by an order of magnitude. This reduction was puzzling since the activity of the GTP-binding protein (as measured by GTP turnover number) was unaffected by the range of sonication used.

We investigated this effect of sonication using a novel, Reticon based apparatus which measures the angular distribution of scattered light from samples as small as one microliter. The results show that even at high rhodopsin concentrations (125 micromolar, path length 1 mm), significant amounts of unscattered light are transmitted by samples. Analysis of the results using a simple, phenomenological theory which assumes a constant change in scattering power (15%) independent of amount of sonication, explains the effect of sonication on the angle dependence data as well as the original turbidity data. The results have general relevance for optimization of light scattering studies of membrane systems.

**T-Pos93 cGMP INTERACTIONS WITH ROD OUTER SEGMENT MEMBRANES.** J.C.Tanaka<sup>++</sup>, R.E. Furman<sup>\*</sup>, J.M.Rendt<sup>+</sup>, A.Sitaramayya<sup>+</sup>, W.H.Cobbs<sup>+</sup>, and P.H.Mueller<sup>++</sup>. Depts of Anatomy<sup>+</sup>, Biochemistry<sup>++</sup>, Neurology<sup>+</sup>, and Physiology<sup>+</sup>, Univ of Pennsylvania, Philadelphia, PA.

Isolated bovine rod outer segment (ROS) membranes, stripped of >90% of the phosphodiesterase activity were incubated at increasing concentrations of 3H-cGMP (1-100uM), with and without 2mM cGMP. Bound ligand was separated from free by centrifugation; membrane pellets were digested and counted. The binding had a large linear component, as expected; the saturable component was best described by a sigmoidal relationship suggesting cooperative association of the ligand. The half-maximal concentration is about 30uM and the binding site density 50-100 pmol/mg membrane protein (2-4 per thousand rhodopsin).

ROS membranes were fused into POPE/POPC planar bilayers painted across a 150um orifice; a 500/200 cis/trans gradient of NaCl was used to promote fusion. After 30', cis application of cGMP resulted in the following: 1) when 100uM cGMP was perfused onto the membrane there was an immediate and reversible increase in membrane current noise. 2) At 1uM cGMP we saw occasional brief noise bursts; the duration and amplitude of this bursting activity increased at 30uM and was almost constant at 100uM cGMP. The noise varied in amplitude from .5 to 10 pA at -100mV. 3) Occasionally there were increases in the average current which rectified at potentials >0 in cGMP. Bilayer currents were compared with currents from frog ROS excised patches. A similar I/V relation and increased noise was seen in pulled patches after cGMP application. In summary, we observed cGMP-dependent increases in the electrical activity of ROS membranes but the activity was not resolved as discrete, quantized current transitions in either bilayers or excised ROS patches.

**T-Pos94**

**HYDROLYSIS OF 8-BROMO-cGMP BY THE LIGHT-SENSITIVE PHOSPHODIESTERASE OF TOAD RETINAL RODS**

A. E. Barkdoll, III, A. Sitaramayya & E. N. Pugh, Jr.  
Depts. of Psychology, Biochemistry & Psychology, Univ. of Pennsylvania

Light-activated rod disk membrane phosphodiesterase was assayed with the pH-electrode technique in medium containing 150 mM KCl, 2 mM MgCl<sub>2</sub>, 1 mM MOPS. Whole toad retinas were vortexed to remove rods, which were syringed to permeabilize plasma membranes. At pH = 8, a 5% flash bleach in presence of GMP-PNP triggered a pH equivalent to total hydrolysis of added cyclic nucleotide, either cGMP or 8-Bromo-cGMP. (The latter was assayed with HPLC, and found to contain less than 1% cGMP contaminant.) V<sub>max</sub> for cGMP as PDE substrate was c. 75-fold greater than that for 8-Bromo-cGMP. From reciprocal plots of initial hydrolytic velocity in mixture experiments we estimated K<sub>i</sub> = 440 uM for competitive inhibition of cGMP hydrolysis by 8-Bromo-cGMP, nearly equal to the estimated k<sub>m</sub> for cGMP, 360 uM. Given that 8-Bromo-cGMP opens the light-sensitive conductance, and that reduction of cytoplasmic free nucleotide is required for a photocurrent, these findings predict a large shift in light sensitivity in a rod into which 8-Bromo-cGMP has been infused. Supported by NIH grant EY-02660.

**T-Pos95      cGMP + 8-Br-cGMP INFUSED INTO RODS INCREASES O.S. hv-MODULATED CURRENT  
AND PRODUCES TWO COMPONENTS OF PHOTOCURRENT OF DIFFERING LIGHT SENSITIVITY**  
E. N. Pugh, Jr. & W. H. Cobbs, Departments of Psychology & Neurology  
University of Pennsylvania, Philadelphia, PA 19104

Salamander rods held in suction pipettes were infused via whole-cell voltage-clamp pipettes with cGMP, 8-Bromo-cGMP and mixtures of same. (1) 5 mM cGMP or 0.5 mM 8-Br-cGMP in clamp pipette caused a 10- to 20-fold increase in the hv-modulated current (photocurrent) of the o.s. membrane in 10-15 secs. (2) After 15 secs 0.5 mM 8-Br-cGMP infusion the velocity (dJ/dt) of normalized flash photocurrent (1000 isomerizations) was less than 1% of the velocity of pre-infusion control photocurrent, or of photocurrent 15 secs after 5 mM cGMP infusion. (3) After 8-Br-cGMP infusion, flashes 1000-fold more intense than controls were required to produce photocurrent with velocity equal to controls. (4) When a binary mixture of 4.5 mM cGMP and 0.5 mM 8-Bromo-cGMP was infused into a rod, photocurrent velocity showed two distinct components: a fast component whose velocity was about that of the pre-infusion control flash response, and a very slow component whose velocity was approximately that observed when 8-Bromo-cGMP alone was infused. Given the independent observation that the  $V_{max}$  of o.s. light-activated PDE for 8-Br-cGMP as substrate is c. 1% that for cGMP (Barkdoll, Sitaramayya & Pugh, these abstracts), the hypothesis that lowering of o.s. [cGMP] by light activated PDE causes the photocurrent predicts phenomena (2)-(4). Supported by NIH grant EY-02660.

**T-Pos96      TWO COMPONENTS OF OUTER SEGMENT MEMBRANE CURRENT IN  
SALAMANDER RODS AND CONES**

W. H. Cobbs & E. N. Pugh, Jr. Departments of Neurology & Psychology  
University of Pennsylvania, Philadelphia, PA 19104

Outer segment membrane currents were isolated with combined external suction and tight-seal whole-cell recording electrodes. Saturating 20 usec flashes evoked two components of o.s. current. Velocity (dJ/dt) of the fast component ( $C_1$ ) increased with flash intensity over a 100-fold range; the slower component ( $C_2$ ) remained invariant. In 5 mM external  $Ca^{++}$   $C_1$  amplitude diminished to about 1/3 the value in 1 mM  $Ca^{++}$  and  $C_2$  increased about 2-fold. Cyclic GMP (5 mM) in the patch pipette increased amplitude and duration of both components, in both 1 mM and 5 mM external  $Ca^{++}$ . Under each experimental condition relaxation of component 2 was much faster in cones than in rods.  $C_1$  results from suppression of the light-modulated cGMP-dependent conductance, reported to admit both Na and Ca in rods. If  $C_2$  is decay of electrogenic Na/Ca exchange current, reflecting decline of o.s.  $Ca^{++}$ , then this process is much more rapid in cones. A faster decline of o.s.  $Ca^{++}$  in a cone would be expected because of the c. 40-fold smaller o.s. cytoplasmic volume of a typical cone as compared with a rod having about the same light-modulated current. More rapid decay of o.s.  $Ca^{++}$  in cones could provide a mechanism for regulating the more rapid recovery kinetics of cone photocurrent. Supported by NIH grant EY-02660.

**T-Pos97      RECONSTITUTION OF RHODOPSIN INTO A CA ATPase MEMBRANE.**

Warren Scherer and Arlene Albert, Department of Biochemistry, SUNY/Buffalo Medical School, Buffalo, New York 14214.

Purified bovine rhodopsin was incorporated into sarcoplasmic reticulum (SR) vesicles from the white hind leg muscles of New Zealand white rabbits. These SR vesicles contained as their major protein component a Ca Mg ATPase. The reconstituted membranes formed a single tight band upon sucrose density gradient centrifugation. It was shown by polyacrylamide disc gel electrophoresis that they contained the Ca Mg ATPase and rhodopsin as the major protein components. Electron micrographs indicate that the reconstituted membranes are in the form of unilamellar vesicles. These vesicles are capable of energy dependent calcium uptake and subsequent, rapid light-induced, calcium release. It was found that approximately 6-9 calcium ions were released per rhodopsin bleached upon sequential bleaching up to a 50% bleach. This represents 6% of the total calcium pumped into the vesicle by the ATPase. SR vesicles without rhodopsin sequestered calcium but did not release calcium upon illumination. Calcium released by the reconstituted membranes could be resequenced in the vesicles upon the addition of more ATP. Vesicles which had sequestered calcium were treated with the calcium ionophore A23187. It was found that the ionophore released approximately 30% of the total sequestered calcium. This would indicate that the light induced calcium release pathway differs from that of the ionophore. This also indicates the presence of a substantial amount of "free" calcium within the vesicles. (Supported by EY03328)

**T-Pos98** POOLING OF CALCIUM IN TOAD ROD OUTER SEGMENTS. W.H. Schröder and G.L. Fain, Institut für Neurobiologie, KFA Jülich, D-5170 FRG and JSEI, UCLA, Los Angeles, CA 90024 USA.

Using laser micro-mass analysis (or LAMMA) of quick-frozen rods from the intact retina of *Bufo marinus*, we have previously shown that rod outer segments (OS) contain 4-5 mmoles total Ca per  $1 \mu\text{m}^3$  tissue volume, which exchanges very slowly with extracellular Ca in darkness (J. Physiol. in the press). Since the plasma membrane of rods has been shown to be quite permeable to Ca in darkness, the slowness of exchange suggests that most of the OS Ca is sequestered, perhaps within the discs. To explore this possibility, we have measured Ca exchange by exposing rods (which normally contain 97%  $^{40}\text{Ca}$ ) to high concentrations of the stable isotopes  $^{42}\text{Ca}$  and  $^{44}\text{Ca}$ . In Ringer with 5, 10, & 20 mM  $^{44}\text{Ca}$ ,  $^{44}\text{Ca}$  accumulated within the rod OS, at a rate which increased with increasing  $^{44}\text{Ca}$ . However, the entering  $^{44}\text{Ca}$  appeared not to exchange with the  $^{40}\text{Ca}$  originally present in the rod, since the increase in OS  $^{44}\text{Ca}$  was not accompanied by a decrease in  $^{40}\text{Ca}$ . As further evidence for pooling, rods were exposed for 15 min to 20 mM  $^{42}\text{Ca}$  to load their OS, and the retinas were then placed in 20 mM  $^{44}\text{Ca}$ . After 1 min in the  $^{44}\text{Ca}$  Ringer, nearly all of the previously loaded  $^{42}\text{Ca}$  exchanged with  $^{44}\text{Ca}$  (apparently as the result of Ca-Ca exchange across the plasma membrane) at a rate exceeding  $10^8$  Ca per OS per sec. However, the rapid exchange of  $^{42}\text{Ca}$  with  $^{44}\text{Ca}$  occurred with almost no effect on the  $^{40}\text{Ca}$ . We suggest that when rods are exposed to high Ca, the Ca accumulating in the OS enters the cytoplasm and remains free to exchange rapidly across the plasma membrane but cannot exchange with the Ca originally present in the OS, because this Ca is contained within the discs and the disc membrane has little permeability to Ca in darkness.

**T-Pos99** EFFECTS OF THE INTRACELLULAR CALCIUM BUFFER QUIN-2 ON THE PHOTOCURRENT RESPONSES OF TOAD RODS. D.L. Miller and J.I. Korenbrot, Dept. of Physiology, Univ. of Calif., San Francisco, CA 94143.

Using the suction pipette method for measuring current fluctuations through the outer segment membrane of intact rods from *Bufo marinus* in response to light, we have determined the effects of the intracellular calcium buffer QUIN-2 on the kinetics and the sensitivity of the photocurrent. We determined photometrically that rod cells incubated with AM-QUIN accumulated QUIN intracellularly to levels of approximately 0.5 mM. We also determined photometrically that the intracellular  $\text{Ca}^{2+}$  activity in the dark is  $170 \pm 69$  nM in 0.1 mM  $\text{Ca}^{2+}$ , and is  $220 \pm 70$  nM in 1.0 mM  $\text{Ca}^{2+}$ . Both values are close to the  $pK$  of the QUIN- $\text{Ca}^{2+}$  complex, approximately 100 nM.

The most dramatic effects of intracellular QUIN are on the kinetics of the photocurrent. The time-to-peak of the photocurrent is slowed in the presence of the buffer. The initial rate-of-rise of the photocurrent in response to bright light flashes was unchanged. For a given saturating light flash, the period of photocurrent saturation was lengthened in the presence of QUIN. Upon recovery of the dark current an overshoot occurred whose amplitude was a function of flash intensity. The recovery phase of the dark current was hastened in the presence of the buffer. We found that in the presence of 1.0 mM extracellular  $\text{Ca}^{2+}$  the light sensitivity of QUIN-loaded cells was enhanced, while in the presence of 0.1 mM  $\text{Ca}^{2+}$  it is not discernably shifted from that of non-loaded cells. Incubation of cells with AM-ANIS, a molecule similar to QUIN in structure but unable to bind  $\text{Ca}^{2+}$ , was without effect on photocurrent kinetics or sensitivity. Thus it appears that internal  $\text{Ca}^{2+}$  activity transients may be involved in the control of kinetics, gain, and recovery of photocurrents.

**T-Pos100** CALCIUM CURRENT AND AEQUORIN SIGNALS IN ISOLATED SALAMANDER RODS  
L. Cervetto, P.A. McNaughton and B.J. Nunn (Intr. by S.B. Hladky)  
Physiological Laboratory, University of Cambridge, Cambridge CB2 3EG, U.K.

Whole-cell recordings were obtained from the outer segments of salamander rods and the Ca-sensitive photoprotein aequorin was incorporated into the cell by injection into the whole-cell pipette, which was then withdrawn after 6-8 min. The light-sensitive current was recorded using a suction pipette and the free  $\text{Ca}_i$  was simultaneously determined from the rate of aequorin consumption. The resting level of  $\text{Ca}_i$  in the outer segment in darkness was below the detection limit of  $\sim 1 \mu\text{M}$ , but on application of the phosphodiesterase inhibitor IBMX (0.5 mM) an increase in both light-sensitive current and  $\text{Ca}_i$  were recorded. A bright flash of light suppressed the current and reduced  $\text{Ca}_i$  to below detectable levels. The total Ca influx could be measured from the current recorded during exposure to a solution containing IBMX in which Ca (77.5 mM) is the only permeant ion. In these conditions  $\text{Ca}_i$  rose in proportion to the integral of the Ca influx but was smaller by a factor of about 10, showing that about 90% of the Ca influx was rapidly buffered within the cell. A bright flash suppressed the Ca influx and halted the rise in  $\text{Ca}_i$ , but in the absence of external Na little decline in  $\text{Ca}_i$  was recorded. Restoring  $\text{Na}_o$  caused a rapid decrease in free  $\text{Ca}_i$ , with a maximum rate of decline of  $70 \mu\text{M/s}$ . The restoration of  $\text{Na}_o$  also activated a light-insensitive inward current; the time course of the integral of this current is similar to the decline in  $\text{Ca}_i$  and the total charge transferred is about half that of the preceding Ca influx, consistent with a Na:Ca exchange pump operating with a 3:1 stoichiometry. We conclude that the Ca influx occurs principally through light-sensitive channels in the rod outer segment, and that a Na:Ca exchange is the main mechanism of Ca extrusion.

**T-Pos101** EFFECTS OF RAISED INTERNAL SODIUM ON THE Na/Ca EXCHANGE IN ISOLATED RETINAL RODS OF THE SALAMANDER. B.J. Nunn, A.L. Hodgkin and P.A. McNaughton (Intro. by R.D. Keynes). Physiological Laboratory, University of Cambridge, Cambridge CB2 3EG, U.K.

We have examined the properties of the Na/Ca exchange current in single rods after several minutes of continuous exposure to  $Ca_o \ll 10^{-6}$  M. In this solution  $Na_i$  is raised and the time-constant of the Na/Ca exchange current is slowed from the usual value of 0.1-0.2 sec to over 1 sec. A brief exposure to  $Ca_o \gg 1$  mM applied soon after a saturating flash, while the light-sensitive channels are still closed, has a dramatic effect in delaying recovery from the flash. Further, the exposure to raised  $Ca_o$  results in an inward, light-insensitive exchange current on return to low  $Ca_o$ . These results suggest that when  $Na_i$  is raised Ca can enter the outer segment by reversal of the Na/Ca exchange pump. In contrast, a brief exposure to raised  $Ca_o$  on the plateau of a saturating flash response in Ringer ( $Ca_o = 1$  mM) has no effect on the subsequent recovery from the flash.

**T-Pos102** EVIDENCE FOR Na/Ca-EXCHANGE IN 'FORWARD' AND 'REVERSE' DIRECTIONS IN LIMULUS VENTRAL PHOTORECEPTORS. Peter M. O'Day and Mark P. Keller, Inst. of Neuroscience, Univ. of Oregon.

Na/Ca-exchange in *Limulus* ventral photoreceptors has been proposed to account for a rise in  $[Ca]_i$  and the decline in sensitivity to illumination when  $[Na]_i$  is raised or  $[Na]_o$  reduced (Lisman and Brown, 1972. *J.Gen.Physiol.* 59:701; Brown and Mote, 1974. *J.Gen.Physiol.* 63:337; Waloga *et al.*, 1975. *Biol.Bull.* 149:449). These effects require  $(Ca)_o$  and are presumably due to Ca-entry.

To examine Na/Ca-exchange further, we induced similar changes in sensitivity by changing  $[Na]_o$  (Li substitution). We found: A. Reduction of  $[Na]_o$  from dark-adapted (DA) cells caused a desensitization that increased with decreasing final  $[Na]_o$ . Complete Na-removal from DA cells bathed in low Ca (0.1mM) caused a small, fully reversible, loss of sensitivity. B. Reintroduction of normal  $[Ca]_o$  (10mM) to DA photoreceptors bathed in 0-Na, low Ca caused a slow, but thorough, desensitization (7 log units). Subsequent reduction of  $[Ca]_o$  to 0.1mM did not increase sensitivity (30 min); however, subsequent reintroduction of normal  $[Na]_o$  led to recovery (detected within 5 min, complete in 60 min). C. In low  $[Ca]_o$ , removal of  $(Na)_o$  caused a greater reduction in sensitivity under moderate illumination than under dim or bright illumination.

Our results are consistent with a model in which  $(Na)_o$  is exchanged for  $(Ca)_i$  (forward exchange) and  $(Na)_i$  for  $(Ca)_o$  (reverse exchange), analogous to squid axon (DiPolo, 1979. *J.Gen.Physiol.* 73:91). When interpreted in terms of current models, our results suggest that both forward and reverse exchange occur in these photoreceptors and can be separated experimentally. It is not clear whether forward and reverse Na/Ca-exchange arise from separate processes or from a single reversible exchanger. Supported by NSF:BNS 84204463.

**T-Pos103** EFFECTS OF BARIUM UPON SODIUM PUMP ACTIVITY IN TOAD ROD PHOTORECEPTORS. B. Oakley II and H. Shimazaki, Depts. of Electrical Engrg. & Biophysics, Univ. of Illinois at Urbana-Champaign.

Stimulation of rods by light leads to a net uptake of extracellular  $K^+$ ; the active uptake of  $K^+$  by the rods'  $Na^+/K^+$  pump exceeds the reduced passive efflux of  $K^+$  from the rods. The net uptake of  $K^+$  leads to a decrease in  $[K^+]_o$ . During maintained illumination, the activity of the rods'  $Na^+/K^+$  pump decreases and  $[K^+]_o$  reaccumulates. Superfusion with  $Ba^{++}$  blocks this reaccumulation of  $[K^+]_o$ , as do treatments that decrease pump activity. We sought to determine how  $Ba^{++}$  blocks the reaccumulation of  $[K^+]_o$ . Superfusion with Cs<sup>+</sup> and TEA<sup>+</sup> decreases rod membrane conductance and unmasks an electrogenic component of membrane voltage (e.g., Torre, *J. Physiol.* 333, 1982). Under these conditions, 0.5-4.0 mM  $Ba^{++}$  produces membrane depolarization and a large decrease in this electrogenic component, suggesting that  $Ba^{++}$  decreases membrane  $K^+$  conductance ( $g_K$ ) and decreases pump activity. The concentration dependence of this effect is identical to that of the effect upon the reaccumulation of  $[K^+]_o$ . We hypothesize that  $Ba^{++}$  blocks all types of  $g_K$  in rods, thus reducing the  $K^+$  efflux. Following superfusion with  $Ba^{++}$ , the active uptake of  $K^+$ , combined with decreased efflux, would increase  $[K^+]_i$ , and thus decrease pump activity. Consistent with this idea, superfusion with Cs<sup>+</sup>, TEA<sup>+</sup> and Co<sup>++</sup>, which block 3 specific  $g_K$  in rods, decreases the electrogenic component of membrane voltage and blocks the reaccumulation of  $[K^+]_o$ , effects identical to  $Ba^{++}$ . Thus, we suggest that  $Ba^{++}$  blocks all 3 types of  $g_K$  in rods, which ultimately decreases pump activity. This mechanism explains why  $Ba^{++}$  blocks the reaccumulation of  $[K^+]_o$  during maintained illumination. Overall, these experiments have provided insight into the  $K^+$  conductances of the rod membrane and the rods'  $Na^+/K^+$  pump, as well as the effects of  $Ba^{++}$  upon rods. (Supported by NIH grant EY04364.)

**T-Pos104 ION TRANSPORT ACROSS THE DISK MEMBRANE**

H.Desel &amp; R.Uhl, intr. by J.Fernandez,

MPI für biophysikalische Chemie, Am Faßberg, D-3400 Göttingen, F.R.G.

Using light scattering, field-, pH-, and calcium-sensitive dyes we have been able to provide evidence for the existence of a number of proteins in the disk membrane of vertebrate photoreceptors, which are all involved in the transport of ions:

- 1) A Mg-ATPase, responsible for an electrogenic proton transport into the disk interior,
- 2) an anion transport protein, inhibited by DIDS, which couples a chloride cotransport to the proton translocation, and
- 3) a channel for monovalent and possibly divalent cations, which is open in the presence of an electric field across the disk membrane and whose conductance is transiently increased by light ( $T(1/2, \text{activation}) < 10$  ms,  $T(1/2, \text{desactivation}) = 10$  s).
- 4) a field driven antiport system, probably an electrogenic  $\text{Na}^+/\text{Ca}^{2+}$ -antiport, that uses the ATP-generated field gradient for the pumping of  $\text{Ca}^{2+}$  into the disk interior.

Since the ion fluxes promoted by the above transport units are small compared to the  $\text{Ca}^{2+}$ -movements across the plasma membrane and to the proton concentration brought about by the hydrolysis of cGMP, their possible significance appears to lie not in the regulation of cytosolic ion concentrations, but rather in that of the intradiskal space. This would point to a functional importance of the disk compartment for the mechanism of visual transduction.

**T-Pos105 EQUILIBRATION RATES OF IONIC CONTENTS OF FROG RETINAL RODS.**

Margaret C. Foster and W.A. Hagins. Lab. of Chemical Physics, NIADDK, N.I.H., Bethesda, Md. 20892.

Equilibration rates of ionic contents of rods were measured (a) in order to interpret electrical studies in which Ringers are switched, (b) to see if  $\text{Cl}^-$  distribution could be used to indicate membrane potential, (c) to provide a measure of permeabilities of the rod membrane other than those due to light-modulated sites, and (d) to look for slowly equilibrating ions. Ionic contents were determined by microprobe analysis of dark-adapted frog retinas freeze-dried after various incubation times in altered Ringers. Extracellular space was marked with  $\text{ScEDTA}^-$ . In Rb ethane sulfonate Ringers (In mM: 110 Rb  $\text{EtSO}_3^-$ , 0.5  $\text{CaCl}_2$ , 0.5  $\text{MgSO}_4$ , 10  $\text{NaScEDTA}$ ) rods lose most of their Na in less than 3 minutes, perhaps via the Na/K pump. The rapid Na loss confirms predictions from studies of voltage responses mediated by changes in external  $[\text{Na}^+]$  (Torre, V. (1983) *J. Physiol.* 333, 315). In 3 minutes, a time comparable to that for loss of light response in ouabain, K, Cl, and Rb are half-equilibrated. Thus more than 3 minutes must be allowed for Cl equilibration if the  $[\text{Cl}_o]/[\text{Cl}_i]$  ratio is to be used to estimate rod membrane potentials. Since rod outer segment membranes have negligible Cl permeability, (Cobbs, W.H. & Hagins, W.A. (1974) *Fed. Proc.* 33, 1576; Chabre, M. & Cavaggioni, A. (1975) *BBA* 382, 336), and negligible conductivity through non-light-modulated sites (Baylor, D.A. & Lamb, T.D. (1982) *J. Physiol.* 328, 49), K, Cl, and Rb permeabilities must reside in inner segment membranes. Time courses for equilibration could not be described by single exponentials. After 20 m. in Rb  $\text{EtSO}_3^-$  Ringers, 5 to 10 mM Na, K and Cl remained in the rods. 7 mM Cl and 20 mM K remained in rods on retinas incubated for 2 hours in a Ringers with  $\text{Br}^-$  and  $\text{Rb}^+$  substituted for  $\text{Cl}^-$  and  $\text{K}^+$  (In mM: 105  $\text{NaBr}$ , 2.5  $\text{RbCl}$ , 0.2  $\text{CaCl}_2$ , 0.5  $\text{MgSO}_4$ , 10  $\text{NaScEDTA}$ ). Broken isolated rod outer segments incubated for 5 min. in K-free iso-osmotic Ringers also retained about 15 mM K. These slowly equilibrating ions could be in intradisk volume or bound to disk membranes.

**T-Pos106 WHOLE-CELL CLAMP OF DISSOCIATED PHOTORECEPTORS FROM THE EYE OF LIMA SCABRA.**

Enrico Nasi, Department of Physiology, Boston Univ. Sch. Medicine, Boston, MA 02118

The photoreceptors of the file clam Lima Scabra transduce and directly encode light stimuli in the form of propagated action potentials, since the retina of this organism lacks second-order neurons. The eyes can be enzymatically dissociated, yielding solitary photoreceptors which occasionally display a short axon stump, but most often consist only of the cell body with a seemingly intact rhabdomeric lobe, as seen in light and scanning microscopy. Voltage clamp stimulation in the dark by means of a patch electrode reveals the presence of several voltage-dependent conductances that could account for the spiking behavior evoked by light. Depolarizing pulses elicit a fast, inactivating inward current followed by a delayed, sustained outward current. The outward current could be almost completely abolished in a reversible fashion by perfusion with TEA (50 mM) and 4 A-P (5 mM), revealing that the inward current activates at rather high voltages (about -20 mV), peaks as early as 4-5 ms after stimulus onset, and does not show a clear reversal at potentials up to +70 mV. Its kinetics suggest a Na conductance, although it appears to be only marginally sensitive to TTX at concentrations up to 10  $\mu\text{M}$ , and it is suppressed incompletely by Na replacement with TMA. Linear leak subtraction of current traces recorded in the presence of K-channel blockers also shows a small sustained inward current which reaches its maximum amplitude at higher voltages (+50 mV or more) and is presumably carried by Ca ions. However, the large and often irreversible increase in leakage current observed with elimination of Ca from the bath as well as with addition of the Ca-channel blocker  $\text{Cd}^{++}$  (500  $\mu\text{M}$ ) thus far has prevented an unambiguous characterization of this conductance. Supported by NSF grant BNS-8419942.

**T-Pos107** CIRCADIAN RHYTHM IN SUNFISH ERG. Allen Dearry and Robert B. Barlow, Jr. (Marine Biological Lab, Woods Hole, MA; Univ. of California, Berkeley; Syracuse Univ., NY).

Cone photoreceptors of the green sunfish, *Lepomis cyanellus*, exhibit a circadian rhythm (CR) in retinomotor movement (*Invest. Ophthalmol. Vis. Sci.* 25: 539-545, 1984). We have examined the electroretinogram (ERG) of green sunfish kept in constant darkness to see if retinal sensitivity also exhibits a CR. Fish were adapted to the ambient light/dark cycle for at least 3 weeks. They were anesthetized, spinalized, and immobilized in an aquarium so that water circulated through their mouths and over their gills but their eyes remained above the water level. The ERG was recorded differentially between a conductive thread electrode contacting the cornea and a wick electrode contacting the body of the fish. Calibrated diffuse light flashes of 10 msec were delivered every 30 min to the eye while the fish was in constant darkness. The amplitude of the ERG b-wave elicited by a constant intensity stimulus of 640 nm increased at expected dusk, remained high during subjective night, and decreased at expected dawn. ERG amplitude was lower during subjective day than subjective night although a secondary increase was often seen at mid-day. The ERG intensity-response function indicated that light of higher intensity was required to elicit a given response during subjective day than subjective night. The difference between day vs. night I-R curves indicated a 3- to 10-fold increase in retinal sensitivity at night. An ERG CR was still evident after unilateral optic nerve section. Our results demonstrate that green sunfish exhibit a CR in retinal sensitivity as well as cone retinomotor movement. [Supported by a Grass Foundation Fellowship in Neurophysiology to A.D., by NSF grant 8320315, and by NIH grants EY00667 and EY03575.]

**T-Pos108** CHOLESTEROL EXCHANGE BETWEEN UNILAMELLAR VESICLES AND ROD OUTER SEGMENT DISK MEMBRANES. Arlene Albert and Ken House Department of Biochemistry, SUNY/Buffalo School of Medicine, Buffalo, New York 14214.

The concentration of cholesterol in disk membranes is quite low when compared to most plasma membranes. It is well known that cholesterol will readily exchange between erythrocyte ghosts and small unilamellar vesicles. We have now studied this exchange between disk membranes and small unilamellar vesicles to determine if a thermodynamic equilibrium plays a role in determining the cholesterol content of disks. Disk membranes were incubated with small unilamellar phospholipid vesicles which contained cholesterol and with vesicles which contained no cholesterol. Aliquots were removed at various times, the disks and the vesicles separated by centrifugation and assayed for phospholipid and cholesterol content. Our studies indicate that while cholesterol can be exchanged out of the disk, additional cholesterol (above normal levels) will not enter the membrane. The exchange of cholesterol between phospholipid vesicles and extracted disk lipids was also examined. Our experiments suggest that the phospholipid content is a primary factor in determining the cholesterol content the native disk membrane. (Supported by EY03328.)

**T-Pos109** IMMUNOFLOUORESCENT STAINING OF MICROTUBULES IN FROG ROD OUTER SEGMENTS

M. Kaplan, R. Iwata and R. Sears. Neurological Sciences Institute & Dept. of Ophthalmology, Good Samaritan Hospital & Medical Center, Portland, OR 97210.

Disk membranes in rod outer segments (ROS) of frogs maintained in cyclic lighting are shed when they reach a particular position on the outer segment axis rather than a particular age [Kaplan (1984) *Vision Res* 24:1163]. We have investigated the possibility that the length of ciliary microtubules (MTs) may determine the appropriate position for disk shedding. ROS were isolated in MT-stabilizing medium (5mM EGTA, 15mM Mg<sup>2+</sup>, and 2mM GTP or 4M glycerol), plated on poly-L-lysine coated slides, and fixed in paraformaldehyde/PIPES buffer. Cells were then made permeable with 1% Triton X-100 solution, treated with monoclonal mouse anti-tubulin, and labeled with sheep anti-mouse Ig conjugated to Texas Red fluorophore. Stained ciliary MTs were viewed in an epifluorescence microscope equipped with an SIT video system. They appeared as a single, bright, tapered stripe oriented parallel to the ROS axis. For frogs on 12h:12h light/dark cycles, mean ROS length was 46µm, and mean length of stained ciliary MTs was 26µm, or 57% of ROS length. Occasionally MTs as long as 90% of the ROS length were observed. By maintaining frogs in constant darkness for several weeks, normal disk shedding was inhibited, and mean ROS length increased to 60µm. In such ROS mean length of stained MTs was 33µm. Pre-incubating ROS with colchicine to prevent artifactual MT elongation had no significant effect upon mean MT length. We therefore conclude that the immunolabeled ciliary MTs in frog ROS typically extend slightly over half the length of the ROS, and it is therefore unlikely that MT length is correlated with the axial position of normal disk shedding. Supported by USPHS EY01779 & Oregon Lions Sight Foundation.

**T-Pos110** PHOTOMECHANICAL COUPLING IN THE FROG IRIS HAS NO THRESHOLD AND IS NOT MEDIATED BY A MEMBRANE POTENTIAL CHANGE OR BY EXTRACELLULAR CALCIUM ENTRY. Lloyd Barr and Fanji Gu, Dept. of Physiology and Biophysics, University of Illinois, Urbana.

Iris isolated from a variety of vertebrates from eels to mammals contract when light is shined on them. The smooth muscle itself contains rhodopsin and the response is apparently triggered by bleaching rhodopsin resident in the cell membrane. The amplitude of the photomechanical response is attenuated but the time course is not altered when normal bathing solutions are replaced by solutions containing 120 mM K, no added Ca and 10 mM EGTA. Microelectrode studies have not revealed any electrical event associated with the photomechanical response. Over a range of three and a half log units, as light stimuli are reduced the amplitude of photomechanical responses are proportional to the 0.8 power of the product of the light intensity and flash duration. This corresponds to response forces of the order of a few micrograms. Amplitudes were measured by averaging large numbers of individual responses. Our working hypothesis is that a second messenger is released by bleached rhodopsin and in turn releases calcium from an internal store. It is interesting that cGMP does not seem to be involved in this mechanical response while cAMP inhibits it. In this regard iridial smooth muscle is similar to other smooth muscle.

**T-Pos111** PROSTAGLANDINS INDUCE CONE ELONGATION AND RPE PIGMENT GRANULE AGGREGATION IN GREEN SUNFISH RETINAS. Brian Cavallaro and Beth Burnside (University of California, Berkeley).

We have been investigating the regulation of photoreceptor and retinal pigmented epithelium (RPE) retinomotor movements in teleost retinas. In the green sunfish, *Lepomis cyaneellus*, photoreceptors and RPE pigment granules move in responses to change in light conditions and to an endogenous circadian rhythm. At dark onset (dusk) cones elongate, rods contract and pigment granules aggregate to the base of the RPE cells. At light onset (dawn) these movements are reversed. We report here that prostaglandin E<sub>1</sub> (PGE<sub>1</sub>), in the presence of 0.2 mM IBMX, induced movements characteristic of dark onset in both cones and RPE in isolated light-adapted retinas cultured in the light. The extent of PGE<sub>1</sub>-induced cone and RPE movements were dose dependent with maximal movement occurring at 250-500 nM; higher concentrations were not as effective. Incubations with PGE<sub>2</sub>, PGE<sub>3</sub>, and PGD<sub>2</sub> also induced dark-adaptive cone and RPE retinomotor movements, but PGF<sub>2α</sub> did not. Treatments which inhibit endogenous prostaglandin synthesis interfered with dark-induced movement. Indomethacin (50 μM) completely blocked and acetylsalicylic acid (50 μM) partially inhibited dark-induced movement. Light-induced retinomotor movements were not effected by 100 μM indomethacin. Our results suggest that *in vivo*, prostaglandins play a role in mediating the induction of retinomotor movements in cones and RPE by darkness. [Supported by NIH grant EY03575.]

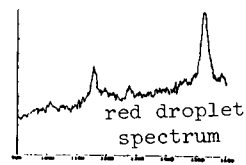
**T-Pos112** RAMAN MICROSCOPIC STUDIES OF INTACT TURTLE CONE OIL DROPLETS

A. Harootunian, R. Barber, A. Lewis, H. Zwick and S. Schuschereba. Applied Physics, Cornell University, Ithaca, N.Y. 14853 and The Letterman Army Institute of Research, Presidio, San Francisco, Ca. 94128

Resonance Raman spectra of single, intact cone oil droplets of turtle (*Pseudemys Scripta*) retina were obtained with a microscope connected to a multichannel Raman Spectrometer. The spectra, such as the red droplet spectrum shown below, were taken while the organelles were still associated with the retina. Instrumental limitations imposed on absorption techniques by the high optical density of the droplets are not a problem due to the backscattering geometry of the microscope. The spectra, when compared to previously published Raman spectra of polyenes<sup>1</sup>, indicate the presence of astaxanthin in both the red and orange oil droplets. This result is in agreement with absorption studies on droplets swollen with mineral oil<sup>2</sup>. The clear droplets do not appear to contain carotenoids measurable by Raman spectroscopy at visible wavelengths. The Raman spectra give detailed information which allows the determination of the mechanisms involved in achieving the super optical densities in oil droplets. Support from U.S. Army Contract #DAMD-79-C-9014 is gratefully acknowledged.

(1)Salares *et al.* J. Ram. Spec. 6,282 (1977)

(2)Liebman and Granda, Nature 253,370 (1975)



**T-Pos113**    **EFFECTS OF SUFFUSION OF IBMX AND SULFHYDRYL REAGENTS ON CONE RECEPTOR POTENTIALS**  
J. Sherwood Charlton and Emily A. Adams, Depts. of Elec. Engr. and Zoology  
University of Arkansas, Fayetteville, Arkansas 72701

Isolated, retinal slices of the larval tiger salamander eye were suffused with Ringer's containing 3-isobutyl-1-methylxanthine (IBMX) in concentrations of 100 $\mu$ M. to 5mM. Single and double cones were impaled with intracellular electrodes and receptor potentials monitored before, during and after chemical application. IBMX application caused a rapid (60 second), reversible depolarization of the dark potential, accompanied by light responses which were of greater magnitude and slower than control responses recorded before and after chemical application. The effects on the light response were only partially reversible. These data are similar to those obtained from rods and suggest a similar mechanism for the two photoreceptor types. The rod data have been interpreted as due to an inhibitory action of IBMX on rod cGMP phosphodiesterase. The application of sulfhydryl reagents N-ethylmaleimide (NEM) and p-chloromercuribenzoic acid (PCMB) causes at least a triphasic response. The first phase is similar to results of IBMX application. A depolarization of the dark potential is accompanied by a slowing of the photoresponse. With NEM application there is also a photoresponse magnitude enhancement. The initial depolarizing phase is followed by a hyperpolarizing phase and loss of photoresponse. The third phase was an irreversible depolarization. The initial effect of the SH reagents is similar enough to the IBMX data to suggest a similar reaction mechanism.

**T-Pos114** ACTIVE TETRAMERS OF  $3\alpha,20\beta$ -HYDROXYSTEROID DEHYDROGENASE FROM *STREPTOMYCES HYDROGENANS*: A PRELIMINARY REPORT OF THE X-RAY CRYSTALLOGRAPHIC INVESTIGATION. D. Ghosh, J. S. Punzi, C. M. Weeks and W. L. Duax, Medical Foundation of Buffalo, Inc., 73 High St., Buffalo, New York 14203

The NADH dependent steroid metabolizing enzyme  $3\alpha,20\beta$ -hydroxysteroid dehydrogenase (EC 1.1.1.53), from *Streptomyces hydrogenans*, has been crystallized in the active tetrameric form in the presence of NADH. The space group is  $P4_32_12$  or its enantiomorph and the cell dimensions are  $a = 106.4(3)\text{\AA}$  and  $c = 203.4(5)\text{\AA}$ . The asymmetric unit contains a tetramer of identical subunits of approximately 25,000 daltons each. The data collection is being carried out by the oscillation method at the Cornell High Energy Synchrotron Source. A complete native data set at  $2.5\text{\AA}$  resolution has been recently collected. Data collection on two isomorphous heavy atom derivatives, prepared with  $K_2Pt(CN)_4$  and  $KAu(CN)_2$ , is in progress. Latest results will be presented. Supported by grant AM26546 from NIH.

**T-Pos115**

Structure of rabbit skeletal muscle aldolase at  $2.8\text{\AA}$  resolution. J. Sygusch, D. Beaudry, M. Allaire, Dept. de Biochimie, Faculté de Médecine, Université de Sherbrooke, Sherbrooke, Qué., Canada J1H 5N4.

Fructose-1,6-diphosphate aldolase (EC.4.1.2.13) is an ubiquitous glycolytic enzyme which catalyzes the reversible aldol cleavage of fructose-1,6-diphosphate to glyceraldehyde-3-phosphate and dihydroxyacetone phosphate. Aldolase from rabbit skeletal muscle is a tetramer (M.W.158000) and crystallizes as a catalytically active conformer (space group  $P2_1$ ; one tetramer/asymmetric unit). A polypeptide chain corresponding to the molecular architecture of the aldolase monomer was traced from a  $2.8\text{\AA}$  resolution electron density map calculated on the basis of SIR phases modified by constraints imposed upon the computed electron density map. The SIR electron density map was subjected to iterative solvent levelling, molecular 222 symmetry averaging of the aldolase tetramer and restraint phase refinement. Three cycles of phase improvement yielded in a final figure of merit of 0.78. The high resolution electron density map confirmed the low resolution study showing the subunits tetrahedrally assembled in the enzyme. The molecular architecture of an aldolase monomer resembles a twisted  $\beta$  sheet connected through  $\alpha$  helices forming for the most part a repeating  $\alpha\beta$  motif similarly found in pyruvate kinase, triose phosphate isomerase, and bacterial aldolase. The flanking helices of the  $\beta$  barrel mediate virtually all intersubunit contacts. The fitting of the amino acid sequence to the computed electron density map is currently in progress. (Supported by MRC Canada grant MT-8088).

**T-Pos116** SMALL ANGLE X-RAY SCATTERING MEASUREMENTS OF CALCIUM-BINDING PROTEINS IN SOLUTION

<sup>1</sup>S.R. Hubbard, <sup>1</sup>S. Doniach, <sup>2</sup>P.C. Leavis, <sup>3</sup>K.O. Hodgson, Departments of <sup>1</sup>Applied Physics and <sup>3</sup>Chemistry, Stanford University, Stanford, CA 94305, and <sup>2</sup>Department of Muscle Research, Boston Biomedical Research Institute, 20 Staniford Street, Boston, MA 02114

Small angle X-ray scattering measurements have been made on solutions of the calcium-binding proteins parvalbumin and troponin C. Data have been collected at the Stanford Synchrotron Radiation Laboratory on the metal-free proteins, parvalbumin with two bound Ca(II), and troponin C with two and four bound Ca(II). For parvalbumin, we have measured a small but definite difference in the scattering curves of the metal-free and Ca(II)-loaded protein in the small angle region out to  $s = 0.04\text{\AA}^{-1}$  ( $s = 2\sin(\theta/2)/\lambda$ ), which indicates that the metal-free protein is less compact than the protein with two bound Ca(II). Data on troponin C provide a measure of the protein's tendency to form dimers as a function of the number of Ca(II) bound.

**T-Pos117** THE X-RAY STRUCTURE OF THE BLUE PROTEIN FROM *A. FAECALIS* S-6 AT 2.4Å  
 E.T. Adman, R. Bramson, S. Turley, Dept. of Biological Structure, Univ. of Washington, Seattle, Wash. 98115 and T. Beppu and H. Watanabe, Dept. of Agricultural Chemistry, Univ. of Tokyo, Bunkyo-ku, Tokyo 113, (Intr. by John Prothero, Department of Biological Structure, Univ. of Washington)

The blue protein from *Alcaligenes faecalis* strain S-6 is a Type I blue copper protein (cupredoxin) which is specifically required for transfer of electrons to a copper containing nitrite reductase, both in the normal electron transfer pathway whereby nitrates are converted to  $N_2$ , and in an abortive pathway whereby the reductase is inactivated in the presence of  $O_2$ .

This cupredoxin crystallizes in space group  $P6_5$ , with cell dimensions  $a = b = 50.06\text{\AA}$ ,  $c = 98.72\text{\AA}$ ,  $\beta = 120^\circ$ . The structure has been solved with a uranyl derivative to 2.4Å, and a platinum derivative to 2.7Å. The overall figure of merit is 0.78. The recently determined chemical sequence has been fit to the electron density map, and refinement of the model is in progress. The protein folds into a  $\beta$ -sandwich as do the related proteins, azurin (Az) and plastocyanin (Pc). A large deletion in the sequence occurs between the first two of the four ligands (His, Cys, His, Met) to the copper; in the structure this deletion corresponds to the 'back flap' of Az and the 'negative patch' of Pc responsible for the interaction of P700 with Pc. In the present protein there are an additional 30 or so residues at the C-terminus relative to Az and Pc which occupy the same spatial region as the 'back flap' of azurin.

This work is supported by NIH grant GM31770.

**T-Pos118** THE STRUCTURE OF THE PROTEIN CRAMBIN FROM X-RAY DIFFRACTION AT 140 K.  
 Martha M. Teeter, Department of Chemistry, Boston University, Boston, MA 02215 and Dr. Hakon Hope, University of California at Davis, Davis, CA 95616.

Diffraction data on crystals of crambin, a small, hydrophobic plant protein (MW = 4700), have been collected to 0.83 Å at 140 K. Vibrational motion of molecules at ambient temperatures will increase uncertainty in atomic position. Systematic errors occur in protein data collection because the capillary tube and the liquid of crystallization can scatter anisotropically.

In order to minimize these errors, the method of H. Hope for working with air sensitive crystals has been adapted to proteins. Crystals of crambin were mounted without a capillary and rapidly transferred into a cold  $N_2$  stream on the P21 diffractometer. The 26,970 observations observed at 0.83 Å ( $\sinh/\lambda = 0.6$ ) represent 81% of the accessible data at this resolution.

The starting model used was that refined at 0.945 Å without hydrogens. Konnert-Hendrickson restrained least squares refinement proceeded (by stepwise addition of data with lower limit 1.5 to 1.0 Å) in 12 cycles to a R value of 14.0% (10.0 - 1.0 Å data.) A difference map at this stage revealed additional waters and the anisotropic motion of the protein. Of the strongest 29 peaks, 40% (12) were assigned to waters, 31% (9) to protein motion and 28% (8) to alternate water positions. Ultimately, 15 new waters were located; 4 former water molecules were changed to alternates; 39 additional water alternates were located; and 2 new ethanols were modelled. The total amount of solvent at this stage is 72 waters with 60 alternates and 4 ethanols. Hydrogens at calculated positions have been added and anisotropic motion of has been allowed.

The peptide geometry, hydrogen bonding networks of water in this refined model will be discussed.

**T-Pos119** THE CRYSTALLOGRAPHIC STRUCTURE OF LYSOZYME AT 1000 ATMOSPHERES. Craig E. Kundrot and Frederic M. Richards, Dept. of Molecular Biophysics and Biochemistry, Yale University, New Haven, CT.

Data has been collected from tetragonal hen egg-white lysozyme crystals in 1.4 M NaCl at 1 atm and 1000 atm to 2.0Å nominal resolution. The crystals, crystallized in .86 M NaCl, require 1.4 M NaCl in the stabilizing solution to prevent cracking at pressures higher than a few hundred atmospheres. The crystals show no measurable hysteresis when cycled through several 1-1000 atm transitions. While the intensities relax to their new values within 1 min. upon pressurization, they require about 90 mins. to relax to the 1 atm values when pressure is released. The unit cell volume decreases 1.1% at 1000 atm. The 1 atm and 1000 atm structures are currently being refined and presently have R-factors of 15% and 18% respectively. Preliminary examination indicates that the structural transition in response to pressure is a continuous, plastic deformation extending anisotropically through the entire molecule. The atomic displacements are on the order of tenths of Ångstroms. The overall deformation leads to a compression of the molecule and the individual isotropic temperature factors of the protein atoms are lower in the 1000 atm structure. To a first approximation, secondary structures such as  $\alpha$ -helices move as rigid bodies. Detailed analysis of the structural response to pressure will follow the completion of refinement. (Supported by grant GM-22778 from NIH).

**T-Pos120** INTERPRETATION OF CONNECTIVE TISSUE X-RAY SCATTERING PROFILES IN TERMS OF LATERAL MOLECULAR INTERACTIONS AND DISORDER. Eric F. Eikenberry, Daniel L. Broek and Barbara Brodsky. Departments of Pathology and Biochemistry, UMDNJ - Rutgers Medical School, Piscataway, NJ 08854.

The x-ray scattering profiles of most connective tissues demonstrate a broad equatorial maximum near 1.5-1.6 nm arising from the lateral arrangement of collagen molecules. This scattering maximum varies in position in different types of tissue. For example, the maximum in non-crystalline tendons (i.e., those other than tail tendons) is near 1.46-1.49 nm, whereas that of skin is near .53 nm, and that of demineralized bone is 1.50-1.65 nm. This maximum represents the sampling of the collagen molecular transform by the interference function derived from the correlation in molecular positions. To interpret the observed maximum in terms of molecular arrangement, the profiles of scattered intensity were deconvoluted for the collagen molecular structure factor (obtained from R.D.B. Fraser and T. McRae). The maxima of the resulting interference functions for various tendons and demineralized bones all occurred at 1.42 nm which represents the center-to-center distance between molecules at closest approach. This result is consistent with the presence in these tissues of molecules of the same diameter and showing the same types of interactions. The variations in peak positions seen in the original x-ray profiles are due to the variations in breadth of the interference maxima. Such effects are explicable by differences in degree of lateral disorder and molecular packing density.

We are calculating pair distribution functions for these and other tissues to characterize more fully the molecular positions, packing density, and degree of order. Perturbations caused by changes in ionic strength, pH, and osmotic pressure are being examined to define the nature of the molecular interactions.

**T-Pos121** SMALL ANGLE NEUTRON SCATTERING STUDIES OF RABBIT MUSCLE PYRUVATE KINASE. Thomas G. Consler, Gerard J. Bunick, and James C. Lee, Department of Biochemistry, St. Louis University School of Medicine, St. Louis, MO 63104, and Biology and Solid State Divisions, Oak Ridge National Laboratory, Oak Ridge, TN 37831.

Rabbit muscle pyruvate kinase (PK) is an important regulatory enzyme in the glycolytic pathway. The mode of regulation is through an allosteric transition induced by the binding of an inhibitor, L-phenylalanine (Phe). The observable effect of this transition is the shifting of the steady-state kinetic behavior from a hyperbolic to a sigmoidal dependence on the substrate, phosphoenolpyruvate (PEP), concentration with a concomitant conformational change. Steady-state kinetic and small angle neutron scattering (SANS) studies were initiated to identify the solution variables which affect the allosteric behavior of PK and to more fully characterize the structural changes. Kinetic data imply that the presence of Phe and high pH favor the inactive (T) state of the enzyme whereas the presence of PEP,  $Mg^{++}/K^{+}$  and low pH favor the active (R) state. Under similar experimental conditions, SANS results showed that the radius of gyration ( $R_G$ ) increased by 0.6-1.5 Å and decreased by the same magnitude under conditions that favor the T and R state, respectively. Further analyses yielded length distribution profiles for PK. These profiles indicate subtle changes in the molecular dimensions and the gross hydrodynamic structure of PK. The T state is represented by an expansion of the molecule and the R state by a contraction. These changes may reflect movements of domains in PK. (Supported by NIH Grants NS-14269 and AM-21489)

**T-Pos122** X-RAY DIFFRACTION STUDIES OF MUTANTS OF STAPHYLOCOCCAL NUCLEASE  
Patrick J. Loll and Eaton Edward Lattman, Department of Biophysics,  
Johns Hopkins University School of Medicine, Baltimore, MD 21205  
Telephone (301) 955-8388.

Many workers are currently employing physico-chemical and genetic means in studies of the extracellular nuclease from *S. aureus* (E.C. 3.1.4.4) in attempts to elucidate both its mechanism of action and the nature of its folding pathway. Structures of the apoenzyme and of an inhibited, calcium-ligated complex have previously been determined by x-ray diffraction methods in the laboratories of Cotton, Hazen and colleagues (1). To provide a structural basis for these studies we have grown single crystals of a number of mutant forms of the enzyme. These exhibit phenotypes which differ markedly from that of the wild type enzyme; however, mutant and wild-type crystals appear to be isomorphous. X-ray diffraction analysis of these mutant protein structures is underway. In addition, we are engaged in least-squares coordinate refinement of high resolution crystal structures of both wild-type crystal forms. This work was supported by NIH BRS grant RR5378.

1. Tucker, P.W. et al., MOL. CELL. BIOCHEM. 22 67 (1979).

**T-Pos123** COMPACT DOMAINS IN PROTEINS.

Micheal H. Zehfus and George D. Rose, Department of Biological Chemistry, Pennsylvania State University, Milton S. Hershey Medical Center, Hershey, PA 17033.

An explicit measure of geometric compactness, called the coefficient of compactness, is introduced. This single value figure of merit identifies those continuous segments of the polypeptide chain that have the smallest solvent accessible surface area for their volume. These segments are the most compact units of the protein, and they correspond well with regions described in the literature as domains, subdomains, or modules. These units exist in a hierarchic organization that suggests possible folding pathways.

The coefficient of compactness is used to find the constituent compact units in 20 proteins. Listings of these units and displays of their hierarchic organization are presented for individual proteins. The entire collection of units is also analyzed for the presence of commonly used structural elements. These common elements include familiar structures, such as beta-alpha-beta and beta-turn-beta units. Also seen are unfamiliar units, composed only of loops and turns, with little regular secondary structure.

**T-Pos124** MOLECULAR DYNAMICS OF PROTEIN SOLVATION: THE CYTOCHROME C' DIMER. John J. Wendoloski and F. Raymond Salemme, E. I. du Pont de Nemours & Company, Central Research & Development Department, Experimental Station, Wilmington, DE 19898.

Molecular dynamics simulations of the cytochrome c' dimer from *Rhodospirillum molischanum* are reported. Cytochrome c' is a hemeprotein of molecular weight 28,000 that crystallizes with a functional dimer in the crystallographic subunit. As a result, subunit monomers are situated in different lattice environments. Here we report a molecular dynamics simulation of the dimer that examines the role of solvent intensities which are observed to differ in the two monomers. These calculations have been carried out with the dimer fully solvated in a box of water. Predicted B values are compared with the 1.67Å resolution structure of P. C. Weber et al. (*J. Mol. Biol.* 1985, in press), and the effect of lattice constraints on the B values is examined.

There are also a relatively large number of solvent water molecules bound in the 1.67Å structure of cytochrome c', some of which may be "structural" in nature. The predicted water geometry in the area of these "structural" waters is examined. Several alternative side chain conformations observed experimentally are also analyzed in terms of the molecular dynamics trajectories.

**T-Pos125** THE ROLE OF A  $\text{GLU } 2^- \cdots \text{ARG } 10^+$  SALT BRIDGE IN STABILIZING THE ISOLATED C-PEPTIDE HELIX, Kevin R. Shoemaker\*, Peter S. Kim\*, Eunice J. York#, John M. Stewart#, and Robert L. Baldwin\*, \*Department of Biochemistry, Stanford University School of Medicine, Stanford, CA 94305, #Department of Biochemistry, University of Colorado School of Medicine, Denver, CO 80262.

There is a large charged-group effect on the stability of the isolated C-peptide helix (residues 1-13 of ribonuclease A). Previous work has shown that  $\text{Glu } 2^-$  and  $\text{His } 12^+$  stabilize the helix [Shoemaker et al. (1985) *PNAS* 82, 2349-2353]. The charge on the N-terminal residue also has a large effect on helix stability (to be published). Experiments are reported here which test the role of a possible  $\text{Glu } 2^- \cdots \text{Arg } 10^+$  salt bridge in stabilizing the helix. This salt bridge is present in the X-ray structure of native RNase A. When  $\text{Arg } 10^+$  is replaced by Ala, two effects are seen: (i) there is little change in helix stability at pH 5, but (ii) the effect on helix stability of titrating  $\text{Glu } 2^-$  disappears. It appears, therefore, that a principal role of  $\text{Glu } 2^-$  in stabilizing the helix is via a  $\text{Glu } 2^- \cdots \text{Arg } 10^+$  salt bridge. pH titration of peptides containing  $\text{His } 12^+$ , and also replacement of  $\text{His } 12^+$  by Ala, both indicate that  $\text{His } 12^+$  stabilizes the helix, but the role of  $\text{His } 12^+$  remains to be clearly defined. A helix dipole explanation remains possible, since previous work has shown that  $\text{His } 12^+$  does not stabilize the helix via a  $\text{Glu } 9^- \cdots \text{His } 12^+$  salt bridge. These results indicate that the nature of the charged-group effect on helix stability is complex.

## T-Pos126 POSSIBLE SALT BRIDGE BETWEEN LYS7+ AND GLU11- IN THE HELIX FORMED BY A C-PEPTIDE ANALOGUE

Jannette Carey<sup>1</sup>, Eunice York\*, John M. Stewart\*, and Robert L. Baldwin<sup>1</sup> Dept. of Biochemistry; <sup>1</sup>Stanford University, Stanford, CA, 94305, and \*University of Colorado, Denver, CO, 80262.

The helix formed by the isolated C-peptide (residues 1 - 13) of ribonuclease A shows two striking properties: (1) the helix is much more stable than predicted by the Zimm-Bragg equation and host-guest data, and (2) charged groups play a special role in determining the stability of the helix. In studying analogues of C-peptide made by chemical synthesis, we found that the substitution Glu11 → Glu in the peptide AcAlaGluThrAlaAlaAlaLysPheGluArgGlxHisAlaNH<sub>2</sub> enhances helix stability. This result was surprising, because the negative charge of Glu11 might be expected to counteract the helix-stabilizing effect of His12<sup>+</sup> found in previous work.

A possible explanation for the helix-stabilizing effect of Glu11<sup>-</sup> is that it forms a Lys7<sup>+</sup>---Glu11<sup>-</sup> salt bridge, since the side chains of Lys7 and Glu11 are close together in the x-ray crystal structure of ribonuclease. This explanation is now being tested by synthesis of a peptide with the additional substitution Lys7 → Ala, and by finding out if a γ-peptidyl linkage between the -COO<sup>-</sup> group of Glu11 and the -NH<sub>3</sub><sup>+</sup> group of Lys7 can be made using a water-soluble diimide. The results will be presented.

T-Pos127 THE DIELECTRIC CONSTANT OF AN ALPHA HELICAL PROTEIN Michael Gilson and Barry Honig  
Dept. of Biochemistry and Molecular Biophysics, Columbia University, New York, NY 10032

The dielectric constant of proteins is a crucial variable in a variety of problems associated with protein structure and function. Here we present a method to determine the dielectric constant of proteins, and describe results for alpha-helical proteins. Our approach starts with the Kirkwood-Frohlich dielectric theory for polar liquids. The theory must be modified to account for the fact that dipolar groups in a protein are constrained, unlike dipoles in a liquid, which rotate freely. This leads to the introduction of C, the factor of constraint, which is 1 for liquids and larger than 1 for proteins. A generalized dielectric theory results, which may be applied to proteins, liquids, and polar molecular solids. A new formula is used to calculate the dielectric constant of a hypothetical alpha helical protein. In this calculation, the constraint factor (C) and Kirkwood's correlation factor (g) are determined by normal mode analysis of an alpha-helix, along with a Taylor series expansion of the helix dipole moment. Similar calculations permit the calculation of thermal factors, for comparison with X-ray data. The results indicate that the dielectric constant of an alpha helical protein probably lies in the range 2.5 - 4.0 [Supported by NIH 5-30354.]

## T-Pos128 ION PAIRS IN THE INTERIORS OF PROTEINS ARE STABLE ONLY IN POLAR SITES. F. Sussman and A. Warshel, Dept. of Chemistry, University of Southern California, Los Angeles, CA 90089

The absolute energies of several internal ion pairs (salt bridges) in papain, trypsin and LADH are evaluated using the Protein Dipoles Langevin Dipoles (PDL) model<sup>1,2</sup>. This microscopic model converts the actual X-ray structure of proteins to the corresponding energies without any adjustable parameter. It is found that in all cases the sites of the salt bridges are very polar and the ionized groups are surrounded by oriented dipoles (C=O, groups H-bonds etc.). Repeating the calculations for non polar sites, (by removing the polar groups destabilizes the ion pairs by more than 15 kcal/mol. This supports previous studies<sup>3,4</sup>. Since model calculations may be considered as theoretical exercises rather than facts we suggest a simple experiment to support our findings. That is, one can mix polar (hydrophilic) and non-polar (hydrophobic) solvents that form two separate phases, and add a charged Zwitterion to the system. The partition of the Zwitterion between the two phases will demonstrate the preference of ion pairs to be in polar environments.

## References:

1. A. Warshel and S. Russell, Quart. Rev. of Biophys. 17, 283 (1984).
2. S. Russell and A. Warshel, J. Mol. Biol. (1985), in press.
3. A. Warshel, Proc. Natl. Acad. Sci. 75, 2558 (1978).
4. A. Warshel, Acc. Chem. Res. 14, 284 (1981).

**T-Pos129**    **TITLE:** EXPLORING ENZYME BINDING SITE BY FORCED LIGAND MOTION.  
**AUTHORS:** Boryeu Mao, T.K. Sawyer, S. Thaisvirongs, The Upjohn Company, Kalamazoo, Michigan, 49001.

**ABSTRACT:** A method has been developed to computationally probe the potential energy hypersurface of a protein-ligand complex. The neighborhood of the binding geometry in the multi-dimensional space is explored by a forced motion of the ligand; a measure of the size of the binding site for the given ligand is obtained in terms of the sum total of all the interactions within the complex. In addition, the method yields information on other characteristics of the complex such as the stability of the ligand at the given binding site.

The active site in models of human renin complexed with fragments of its natural substrate, one of 8 amino acid residues in length (W. Carlson, Mass General Hospital, private communication) and of two residues, have been explored with the methodology. In addition, the structure of several potent analogues of the Renin Inhibitory Peptide bound in the active site of renin have also been constructed and the enzyme-ligand interactions investigated with the forced ligand motion method.

A quantitative measure of the size of binding site experienced by individual ligands can be used to estimate the entropic contribution to the free energy of binding. In complexes where structure information is not yet available this method is useful in guiding the modeling of the ligand-enzyme interactions. In its present application, the forced ligand motion method explores the potential energy hypersurface in the immediate neighborhood of a binding geometry; the range of surveying can be extended so that a docking operation can be achieved.

**T-Pos130**    **GEOMETRY OF PROLINE AND HYDROXYPROLINE:** An analysis of X-ray crystal structure; semi-empirical and quantum chemical calculations. V.N. Balaji††, M. Jagannatha Rao‡ and V. Sasisekharan‡ (†Allergan Pharmaceuticals, 2525 Dupont Drive, Irvine, CA92715; ‡ Molecular Biophysics Unit, Indian Institute of Science, Bangalore, India 560 012)

We have computed and analyzed the geometries of proline and hydroxyproline residues in terms of bond lengths, bond angles, dihedral angles and deviations from planarity at atomic centers in small cyclic and acyclic peptides as found by X-ray crystal structure determination retrieved from the Cambridge Crystal Structure Data Base. We observe that the nitrogen atoms have considerable pyramidal character. This pyramidal character at the nitrogen atom in the pyrrolidine ring has been examined for model compounds as part of conformational energy calculations using CNDO/2, MNDO and GAUSSIAN80 methods. The predictions from these methods are compared with the results obtained from X-ray diffraction studies. It is shown that these theoretical calculations are in good agreement with observations. The present study indicates that the pyramidal distortion at the nitrogen atom of the pyrrolidine unit may have to be taken into consideration, in addition to the variations in the dihedral angles  $\phi$  and  $\psi$ , when modeling structures with proline and hydroxyproline rings.

**T-Pos131**    **COMPUTER GRAPHICS AND ARTIFICIAL INTELLIGENCE METHODS  
IN PROTEIN STRUCTURE PREDICTION**

D. Kneller, I. D. Kuntz, F. Cohen, R. Abarbanel, T. E. Ferrin and R. Langridge  
Computer Graphics Laboratory, University of California, San Francisco, 94143

We are integrating computer graphics and exploratory programming to study and refine protein tertiary structure prediction. Using a Symbolics Lisp Machine, rules based on amino acid sequence are invoked to predict tertiary structure and an abstract representation of the possible packing arrangements are illustrated and manipulated. Three dimensional views of the tertiary structure are displayed and manipulated on an Evans & Sutherland PS350 or Silicon Graphics IRIS 2400 connected by an Ethernet link to the Lisp Machine. The rules for prediction are generated and modified using KEE, the knowledge engineering environment, from IntelliCorp. Currently, we use a sequence pattern matcher to identify turns and secondary structural regions, though any of several methods may be used. This combination of hardware and software permits rapid and informative experimentation. Supported by NIH grants RR-1081 and GM-31497 and US Army Research Office grant DAAG29-83-G-0080.

**T-Pos132** ELECTRIC BIREFRINGENCE OF TROPOMYOSIN. Charles A. Swenson and Nancy C. Stellwagen, Department of Biochemistry, University of Iowa, Iowa City, IA 52242.

The electric birefringence of rabbit skeletal tropomyosin has been studied as a function of electric field strength, pulse length and concentration. Orientation occurs primarily by a permanent dipole mechanism. At a concentration of less than 7 ug/ml the molecule behaves as a monomer. Some interaction between molecules is suggested even at these concentrations by the observed increase in decay time with increase in pulse length. A possible explanation is that orientation of this rod-shaped coiled-coil molecule enhances the normal head to tail interaction observed at higher concentration. Estimation of the permanent dipole moment from a combination of reversing field experiments and analysis of the effect of field strength on the steady state value of the birefringence shows that the dipole is smaller than is expected from a straight-forward calculation of the contributions of the peptide dipole moments and the formal charges. Supported by NIH grants GM-29690 and AM-27554.

**T-Pos133** STRUCTURAL MODELING OF THE ICE NUCLEATION PROTEIN OF *PSEUDOMONAS SYRINGAE*. Paul K. Wolber and Gareth J. Warren, Advanced Genetic Sciences, Inc., 6701 San Pablo Ave., Oakland, CA 94608.

The protein product of *inaZ*, the ice nucleation gene of *P. syringae*, has been identified and purified, after cloning and overexpression in *E. coli*. The transformants catalyze ice formation, and the level of activity seen in the transformants correlates with the level of protein expression. Nucleation activity copurifies with the *inaZ* product; therefore, it is likely that the protein is a crucial component of the template structure which catalyzes ice formation. The amino acid sequence predicted from the DNA sequence of *inaZ* supports this contention: the majority of the sequence consists of interlaced 8, 16, and 48 amino acid repeats (in ascending order of fidelity). Two different methods of secondary structure prediction both predict a  $\beta$ -sheet structure for the repeated sequences, punctuated by 5-6 turns per 48-amino acid unit. The repeated unit is reasonably hydrophilic, and is particularly rich in Ser and Thr. The primary sequence suggests that the protein folds into a regular structure built up from the 48-amino acid repeat, and that this structure presents H-bonding side chains in a manner which mimics an ice lattice. The fact that the 48-amino acid repeat is built up from 3 less perfect 16-amino acid repeats, which are in turn built up from two, least perfect 8-amino acid repeats, suggests that the protein structure is formed by a hierarchy of folded domains. Thus, it should be possible to build up the protein structure by a recursive modeling strategy. Models of possible structures of this novel protein will be presented.

**T-Pos134** MEMBRANE PROTEIN SECONDARY STRUCTURE PREDICTION: AN EVALUATION OF EMPIRICAL METHODS. M. Cascio, D.L. Mielke, and B.A. Wallace, Dept. of Biochemistry and Molecular Biophysics, Columbia University, New York, NY 10032.

With the advent of molecular cloning methods, the amino acid sequences of a number of membrane proteins have recently been determined. The paucity of detailed three-dimensional structural information available for these molecules has led to attempts to predict the secondary structures of membrane proteins from their sequences. Empirical prediction schemes had been developed for proteins based on folding motifs found in soluble proteins of known three-dimensional structure and sequence, with the most widely used method being that of Chou and Fasman [Biochem. 13:211 (1974); J. Mol. Biol. 115:135 (1977)]. The goal of the present work was to determine if such prediction schemes, based on soluble protein data bases, could be used to predict membrane protein secondary structures, which are influenced by the hydrophobic and anisotropic lipid environment in which they are embedded. To evaluate the accuracy of the predictive methods, integral membrane proteins and membrane-spanning polypeptides for which both primary and secondary structural information were available were analyzed by the method of Chou and Fasman. The calculated secondary structures were then compared with the secondary structures determined experimentally in either this or other laboratories by a variety of independent physical methods, including circular dichroism, Raman and infrared spectroscopy, image reconstruction, and X-ray diffraction. Chi-square analysis indicated a less than 0.5% correlation between the predicted secondary structures and the experimental results. Thus, such prediction schemes using soluble protein data base appear to be inappropriate for the prediction of membrane protein folding. (Supported by NIH Grant GM27292).

**T-Pos135** MULTIPLE SEQUENCE ALIGNMENT. Wayne F. Anderson, David J. Bacon and Clifford D. Mol, Medical Research Council of Canada Group in Protein Structure and Function, Department of Biochemistry, University of Alberta, Edmonton, Alberta, Canada T6G 2H7.

It has been observed that proteins with little or no amino acid sequence homology may, nonetheless, have regions with similar three-dimensional structure. Can these segments be detected in the amino acid sequences in a statistically meaningful way? Although the information may be present in the amino acid sequences it may not be possible to distinguish the correct segments of two sequences and their proper alignment. One way to improve the signal is to simultaneously align a number of sequences containing the same structural motif. We have devised a computationally feasible method for intercomparing a number of sequences at once. This approach allows the alignment of  $n$  sequences of average length  $L$  in a time proportional to  $n^2$  rather than proportional to  $L^n$ , as required for a brute force search. Two different statistical models are used, making it possible to group protein fragments objectively even when most or all of the inter-relationships are weak. Comparisons among a variety of nucleic acid binding proteins will be presented to illustrate the use of the technique.

(Supported by the Medical Research Council of Canada)

**T-Pos136** FOURIER TRANSFORM INTENSITY MATCHING TECHNIQUE CLASSIFIES AMPHIPHILIC REGIONS IN PROTEIN SEQUENCES Leslie A. Kuhn, Alexander D. Diehl, and John S. Leigh, Jr., Department of Biochemistry and Biophysics, 504 Goddard Laboratories / G4, Philadelphia, PA 19104

Classification of amphiphilic regions in proteins is facilitated by a new Fourier transform technique which identifies protein segments which are similar to model amphiphilic sequences. Fourier intensities measuring how periodic a sequence is at various periods are computed for successive protein segments and weighted by the intensity expected on average in random rearrangements of each segment. Each weighted intensity pattern is then compared to intensity patterns of model sequences periodic at the repeat periods of untwisted and twisted beta strands and  $3_{10}$  and alpha helices in order to identify segments of particular structural interest.

Analyses of the *Electrophorus electricus* sodium channel sequence and other membrane protein sequences are presented, and the implications for their structures are discussed. The sodium channel results are especially interesting because the four most periodic segments in the protein (four homologous regions amphiphilic at the  $3_{10}$  helix period) have been proposed to be channel-forming elements by other researchers.

**T-Pos137** SECONDARY STRUCTURE ORIENTATION OF BACTERIORHODOPSIN AND THE NICOTINIC ACETYLCHOLINE RECEPTOR, Thomas Earnest and Kenneth Rothschild, Departments of Physics and Physiology, Boston University, Boston, MA 02215

Polarized Fourier transform infrared (FTIR) spectroscopy in conjunction with Fourier self-deconvolution and second derivative techniques has been used to investigate the orientation of  $\alpha$  helical and  $\beta$  sheet structures in bacteriorhodopsin (bR) from *Halobacterium halobium* and the nicotinic acetylcholine receptor (AChR) from *Torpedo californica*. Contributions to the amide I (C=O stretch) and amide II (N-H in-plane bend) bands from  $\alpha$  helical and  $\beta$  sheet structures, which occur at different frequencies but show considerable overlap, can be resolved by the use of deconvolution and second derivative methods. Analysis of the infrared dichroism of these bands allows deductions about the orientation of these structures to be made. Bacteriorhodopsin appears to contain anti-parallel  $\beta$  sheet structure in addition to the helical segments proposed from the original electron diffraction maps. Furthermore the dichroism of the amide I bands at  $1640\text{ cm}^{-1}$  and  $1683\text{ cm}^{-1}$  corresponding to anti-parallel  $\beta$  sheet in-plane modes indicates that the orientation of the plane of the sheet is predominantly perpendicular to the membrane plane. The amide I band for  $\alpha$  helices at  $1665\text{ cm}^{-1}$  also shows a strong dichroism perpendicular to the membrane in agreement with earlier work (Rothschild and Clark, *Biophys. J.*, 25:473, 1979). We also find evidence for oriented  $\alpha$  and  $\beta$  structures in AChR. The amide I band at  $1656\text{ cm}^{-1}$  shows that the  $\alpha$  helical segments have a net orientation perpendicular to the membrane plane. In contrast, the in-plane bands for anti-parallel  $\beta$  sheet structure exhibit a dichroism suggestive of a net direction of the C=O bonds parallel to the membrane plane. This is supportive of models of AChR with transmembrane  $\alpha$  helices perpendicular to the membrane and a large extracellular region with extensive  $\beta$  sheet structure. Calculations will be presented which determine the direction of the  $\alpha$  and  $\beta$  structures with respect to the membrane, along with experiments designed to localize the regions of the protein which give rise to the dichroic bands.

**T-Pos138** CHARACTERISTIC PEPTIDE GROUP NORMAL MODE FREQUENCIES OF THE PARALLEL-CHAIN PLEATED  $\beta$ -SHEET. J. Bandekar and S. Krimm, Biophysics Research Division, University of Michigan, Ann Arbor, MI 48109.

Normal mode calculations are providing significant insights into the interpretation of vibrational spectra of peptide systems in terms of their three-dimensional structure (1). We have now computed the normal mode frequencies of a parallel-chain  $\beta$ -sheet, a structure that is commonly found in proteins. The model system was a parallel-chain pleated sheet of poly(L-alanine). Using standard values of bond lengths and angles, this structure has  $n=2$ ,  $h=3.25\text{\AA}$ ,  $\phi=-119^\circ$ ,  $\psi=114^\circ$ , and an interchain distance of  $4.85\text{\AA}$ . Transition dipole coupling was incorporated using ab initio values of dipole derivatives in internal coordinates (2) and eigenvectors from the normal mode calculation. The following amide mode frequencies (in  $\text{cm}^{-1}$ ) were obtained - amide I:  $\nu(0) - 1666$ ,  $\nu(\pi) - 1654$ ; amide II:  $\nu(0) - 1550$ ,  $\nu(\pi) - 1589$ ; amide III:  $\nu(0) - 1234$  (plus 1207),  $\nu(\pi) - 1330$ ; amide V:  $\nu(0) - 712$  (plus 417),  $\nu(\pi) - 706$  and  $628$  (plus 437). The amide I and amide II mode frequencies differ significantly from those of the antiparallel-chain pleated sheet, but the infrared-active modes are very close to those of  $\alpha$ -helical poly(L-alanine). These comparisons will be discussed in detail, as will results on some tripeptides known from crystal structure studies to adopt a parallel-chain pleated sheet conformation. Supported by NSF grants PCM-8214064 and DMR-8303610.

1. S. Krimm and J. Bandekar, *Adv. Protein Chem.* (1986).
2. T.C. Cheam and S. Krimm, *J. Chem. Phys.* 82, 1631 (1985).

**T-Pos139** AN FTIR STUDY OF RED CELL MEMBRANE PROTEIN STRUCTURE.

Bernard Chasan and Eileen Armstrong, Physics Dept., Boston University, Boston, MA 02215

We have used a Nicolet 60 SX FTIR Spectrometer to study the infrared absorption spectrum of the human red cell membrane, with particular emphasis on the secondary structure of the membrane proteins. We have also studied the spectra of two modified red cell membrane preparations; Cabantchik vesicles which are enriched in the integral protein Band 3 by negative purification, and ghost membranes which have been subjected to vigorous proteolysis with pepsin. These membranes were studied as dried or deuterated films. Secondary structure was studied using deconvolution and second derivative techniques to resolve the broad amide I band into its components. The ghost spectra are rich in alpha helix but have considerable amounts of beta sheet and turns as well. The Cabantchik spectra are richer in alpha helix and the pepsin treated membranes richer still. The pepsin treated membranes are largely depleted of extra-membraneous pieces of protein and our results indicate that there is very little beta configuration within the red cell membrane.

**T-Pos140** RESOLUTION-ENHANCED FT-INFRARED SPECTRA OF PROTEINS WITH PARALLEL BETA-CHAINS. Heino Susi and D. Michael Byler (Intr. by Peter L. Irwin)  
Eastern Regional Research Center, Agricultural Research Service, U.S. Department of Agriculture, Philadelphia, PA 19119.

Deconvolved and second derivative Fourier-transform infrared (FT-IR) spectra of the proteins flavodoxin and triose phosphate isomerase have been obtained in the amide I spectral region ( $1620-1690\text{ cm}^{-1}$ ). Both proteins have beta-sheets comprised of parallel chains, as well as helical segments, but contain no antiparallel beta-sheets. Absorption bands are observed in the  $1626-1639\text{ cm}^{-1}$  region (strong) and the  $1670-1680\text{ cm}^{-1}$  region (weak) for the parallel sheets, and close to  $1650\text{ cm}^{-1}$  for the helical segments. The assignments are corroborated by band area measurements which yield quantitative conformational information in reasonable agreement with X-ray diffraction data. The data will be compared with spectra of proteins containing only antiparallel beta-regions and proteins having mixed sheets. To our knowledge these results provide the first unequivocal infrared data on proteins with parallel beta-chains. Apparently, the parallel and antiparallel beta-sheets have quite similar absorption characteristics in the amide I region, but neither conformation exhibits bands which overlap the bands associated with the helices (ca.  $1650-1655\text{ cm}^{-1}$ ). Our results thus suggest that FT-IR spectroscopy permits unambiguous distinction between helical regions and extended chains, but does not clearly differentiate between parallel and antiparallel beta sheets.

**T-Pos141** THE CIRCULAR DICHROISM OF TWISTED BETA SHEETS. Mali P. Illangasekare and Robert W. Woody, Department of Biochemistry, Colorado State University, Fort Collins, CO 80523.

Circular dichroism (CD) spectra have been calculated for twisted  $\beta$  sheets, and the results have been compared with the spectra predicted for planar sheets of the same size. The geometries considered were those generated by Scheraga and co-workers (*J. Mol. Bio.* **162**, 89 (1982); **168**, 389 (1983)) and included both antiparallel and parallel sheets of varying size and extent of twist. Slightly twisted sheets (twist angle  $\delta < 5^\circ$ ), such as those predicted for poly(Ala), have a negative band near 220 nm and a positive band of comparable magnitude at 195-200nm. Parallel and antiparallel sheets are similar in magnitude but the parallel sheets have their extrema shifted to the blue by  $\sim 5$  nm. Strongly twisted sheets ( $\delta > 20^\circ$ ), such as those predicted for poly(Val) and poly(Ile), exhibit a slightly enhanced and red-shifted  $\pi\pi^*$  band but the most spectacular feature is the enhancement of the positive band near 200 nm and the development of a strong negative band near 180 nm. For the antiparallel sheets, the positive band is 3-4 times stronger for the highly twisted sheet than for the planar or slightly twisted sheet. For parallel sheets, the enhancement is about 8-fold. The strong CD of the highly twisted sheets is largely attributable to intrachain interactions, since single strands from the highly twisted sheets are predicted to have CD amplitudes (on a per residue basis) comparable to those of the full parallel sheets. In antiparallel sheets, interstrand interactions partially cancel and intrastrand contributions. In addition to the increased amplitudes, twisting of the sheets causes a red shift of the crossover wavelength on the low-wavelength side of the positive band. (Supported by USPM GM 22994.)

**T-Pos142** GEOMETRY AND CIRCULAR DICHROISM OF CLOSELY-PACKED ANTIPARALLEL BETA SHEETS. Mark C. Manning and Robert W. Woody, Department of Biochemistry, Colorado State University, Fort Collins, CO, 80523.

While the circular dichroism (CD) spectrum of protein secondary structural features, such as the  $\alpha$ -helix and  $\beta$ -sheet, has been widely studied, little attention has been paid to the CD arising from two closely-packed structures, such as face-to-face  $\beta$ -sheets. Exciton model calculations on two idealized flat sheets show that three effects can modulate the CD spectrum. First, the two sheets must approach closer than 10Å to allow intersheet interaction. Second, the CD is very sensitive to  $\Omega$ , the angle between the average strand directions in the two sheets. The negative CD bands maximize at  $\Omega = 30^\circ$  and  $85^\circ$ , coincidental with angles found most often in globular protein structures. Third, deviations from parallelism are unimportant until parts of the sheet approach within 5-7Å. Calculations on real protein structures suggest that the CD is dominated by the extent of intra-strand twisting. Proteins with this double  $\beta$ -sheet structure, such as plastocyanin, prealbumin, concanavalin A, immunoglobulin VRE1, and superoxide dismutase, have mostly highly twisted strands ( $\delta > 25^\circ$ ). Beyond  $\delta = 30^\circ$ , this effect apparently yields no further contribution to the CD, producing  $[\theta]_{\max}$  for the positive  $\pi\pi^*$  band of  $\sim 35000$  deg  $\text{cm}^2 \text{dmol}^{-1}$ . Both the intra- and inter-strand twists were measured for all five proteins. A high positive correlation is observed for the two twists, although some deviations occur. (This work was supported by the National Institutes of Health, GM 22994, and a grant of computer time from the Institute for Computational Studies at Colorado State University.)

**T-Pos143** THE INFRARED SPECTRA OF PROTEINS IN AQUEOUS SOLUTIONS. R. J. Jakobsen and K. B. Smith, National Center for Biomedical Infrared Spectroscopy, Battelle-Columbus Division, Columbus, Ohio 43201-2693.

While the improvement in Fourier transform infrared systems now permits the use of aqueous solutions, most infrared studies of proteins are still done either on the solid protein or in D<sub>2</sub>O solutions. This use of D<sub>2</sub>O as a solvent limits the peptide backbone spectral information available to a single vibration, that of the Amide I vibration. We wish to present an FT-IR study of 10 proteins where the work was carried out in aqueous solutions allowing information to be obtained on the Amide I, II, and III vibrations and on vibrations of amino acid side chains. The use of several peptide backbone vibrations allows more definitive information to be obtained on secondary structure and the assignment of amino acid side chain vibrations not only yields some information on tertiary structure, but aids in deducing which parts of the protein molecule are involved in conformation changes. In addition, the aqueous solution protein spectra have been compared to the solid state spectra and to spectra in D<sub>2</sub>O to both aid in vibrational assignments and in comparing structural differences between the various physical states.

The study has also involved inducing structural changes in the proteins by varying parameters such as pH, pressure, or temperature and by using non-aqueous solvents. The use of such parameter variation coupled with the use of Fourier self-deconvolution techniques (to resolve the broad protein infrared bands) has strengthened the assignment of infrared bands to protein structural features and has shown that FT-IR has great potential as a protein structure probe.

**T-Pos144** STRUCTURAL REQUIREMENTS OF THE ALKALINE PHOSPHATASE SIGNAL PEPTIDE. D.A. Kendall, S.C. Bock and E.T. Kaiser. Laboratory of Bioorganic Chemistry and Biochemistry, The Rockefeller University, New York, NY 10021.

The signal peptide of *E. coli* alkaline phosphatase mediates transport of the enzyme to the periplasm. We are investigating the structural features of this peptide which may facilitate the translocation process. To evaluate the potential role of a hydrophobic  $\alpha$ -helical conformation, we constructed a mutant signal sequence containing nine consecutive leucine residues in its core region (mutant 1). This involved making amino acid substitutions in the natural sequence using site-specific mutagenesis. A multi-copy plasmid containing the alkaline phosphatase gene with either this mutant (mutant 1) or wild type (WT) sequence was then used to transform an *E. coli* host. Transport studies with the mutant strain indicate processing of the precursor form is comparable to wild type and that mature alkaline phosphatase is transported to the periplasm. A second mutant which extends the length of the signal sequence by six additional leucine residues was also characterized (mutant 2). Studies with this mutant indicate that lengthening the hydrophobic segment of this signal peptide slows, but does not entirely inhibit, transport of the enzyme to the periplasm.

WT: MKQSTIALALLPLLFPTVTKA  
mutant 1: MKQSTILLLLLLLLLLLTPVTKA  
mutant 2: MKQSTILLLLLLLLLLLLLLLTPVTKA

**T-Pos145** HYDROGEN ISOTOPE EXCHANGE IN CRYSTALS AND SOLUTION OF BOVINE PANCREATIC TRYPSIN INHIBITOR. Warren H. Gallagher and Clara K. Woodward. Dept. of Biochemistry, Univ. of Minnesota, St. Paul, MN 55108.

Hydrogen isotope exchange of peptide amide NH protons is sensitive to the internal motions of proteins. There is a great deal of interest in comparing the internal motions of proteins in solution with those in crystals. To facilitate a comparison, we have developed methods for monitoring hydrogen isotope exchange of bovine pancreatic trypsin inhibitor (BPTI) in both crystals and solution. Crystals are grown from a saturated solution of BPTI in 1.5M dipotassium phosphate (pH 9.4) at room temperature. To keep crystals stable during crystal exchange, the reaction is carried out in solvents similar to those used for growing the crystals. Under these conditions we monitor the exchange of the slowly exchanging amide protons, primarily those of the  $\beta$ -sheet core region of the protein. Exchange in crystals is initiated by transferring crystals to  $^2\text{H}_2\text{O}$  containing 1.5M dipotassium phosphate at the experimental pH and temperature. At time intervals following the initiation, an aliquot of the crystal suspension is removed and the crystals collected and dissolved in  $^2\text{H}_2\text{O}$  at pH 3.6 and 4°C. This quenches the slowly exchanging sites of further exchange. From assigned resonances in  $^1\text{H-NMR}$  spectra, the extent of exchange for individual amide protons is determined for each time point. Solution exchange experiments are carried out similarly. To initiate exchange, BPTI is dissolved in the same solvent used in the crystal experiments: 1.5M dipotassium phosphate in  $^2\text{H}_2\text{O}$  at the appropriate pH and temperature. Aliquots are removed at various times and the BPTI precipitated by raising the concentration of dipotassium phosphate from 1.5M to 1.9M. The precipitated protein is then collected and dissolved in  $^2\text{H}_2\text{O}$  at pH 3.6 and 4°C. We have obtained rate constants for exchange in crystals at pH 10/35°C, pH 10/22°C, pH 9.2/40°C, and pH 9.0/35°C; and in solution at pH 10/35°C. The rates obtained are for the peptide amide NH's of Ile 18, Arg 20, Tyr 21, Phe 22, Tyr 23, Asn 24, Gln 31, Phe 33, Tyr 35 and Phe 45; and the primary amide protons of the Asn 43 side chain. For all these, the rates are slower in the crystal than in solution. The factor by which they are slowed in the crystal varies from 2 to 350.

**T-Pos146** CONFORMATION OF MgATP BOUND TO PYRUVATE KINASE AND METHIONYL tRNA SYNTHETASE BY HOMONUCLEAR PROTON NOE MEASUREMENTS. B. D. Ray and B. D. Nageswara Rao, Department of Physics, IUPUI, P.O. Box 647, Indpls., IN 46223 and P. Plateau and G. Fayat, Ecole Polytechnique, 91128 Palaiseau, France

Homonuclear proton nuclear Overhauser effect (NOE) measurements were made to obtain conformational information on MgATP bound to two classes of enzymes for which it is a substrate, a phosphoryl transfer enzyme, pyruvate kinase (from rabbit muscle), and an adenylyl transfer enzyme methionyl tRNA synthetase (from *Escherichia coli*). The experiments were performed at 276 and 300 MHz on samples containing 10-20 fold excess of substrate relative to enzyme binding site concentration. The observed NOE is almost entirely due to the bound complex since the bound and free complexes are in rapid exchange and the NOE in free MgATP is negligible under the conditions of the experiment. At different values of delay following the selective inversion of a given resonance using a DANTE pulse, the NOE was measured for all the other resonances using difference spectroscopy. Similar measurements were also made following monochromatic irradiation for different chosen intervals. Initial build-up rates were obtained from both methods for MgATP complexes of the two enzymes and the results are compared. Ratios of distances between protons of adenine and those of ribose obtained from the initial build-up rates indicate a high degree of anti-conformation about the glycosidic bond for both the enzymes and subtle differences in the conformation of the ribose of MgATP in these complexes. (Supported by NSF DMB 83-09120 and Ecole Polytechnique, Palaiseau, France.)

**T-Pos147** HYDROGEN EXCHANGE AND  $^1\text{H}$  NMR STUDIES ON M13 COAT PROTEIN. J.D.J. O'Neil, and B.D. Sykes, Department of Biochemistry, University of Alberta, Edmonton, Alberta, Canada T6G 2H7.

The coat protein of the bacteriophage M13 is inserted into the inner membrane of *E. coli* during infection of the host cell. The protein consists of a 19-residue hydrophobic domain, flanked by N-terminal acidic and C-terminal basic domains of 20 and 11 residues, respectively. In order to obtain information about the secondary structure of this small 'model' membrane protein we have measured amide exchange rates using  $^1\text{H}$  NMR spectroscopy for the protein in perdeuterated sodium dodecyl sulphate micelles from pH 3-9 at 25°C. At pH 3 about 38 amides exchange slowly enough to be observed; 27 of these form a distinct peak of overlapping resonances between 7.5 and 8.5 ppm and a group of 11 hydrogens form a peak between 8.5 and 9.2 ppm. Analysis of the exchange rates by a multiple exponential non-linear least-squares fitting routine shows that the upfield peak of amides consists of about 13 rapidly exchanging hydrogens ( $k=0.9\text{ h}^{-1}$ ), 5 amides with an intermediate exchange rate ( $0.04\text{ h}^{-1}$ ) and 18 slowly exchanging hydrogens ( $k=0.0005\text{ h}^{-1}$ ); the downfield peak of shifted amides can be decomposed into 3-4 rapidly exchanging hydrogens ( $k=1\text{ h}^{-1}$ ), 5 amides with an intermediate exchange rate ( $0.01\text{ h}^{-1}$ ), and 3-4 with a slow exchange rate ( $k=0.0005\text{ h}^{-1}$ ). All of the exchange rates are from 10 to more than 1000 times slower than the rates of exchange of 'freely exchanging', non-hydrogen bonded amides. The conclusion is that, at pH 3, at least 38 of the 50 amides in the protein participate in secondary structural elements such as  $\alpha$ -helix or  $\beta$ -sheet, and that their exchange rates are retarded by internal hydrogen bonding. In addition, the 4 sets of amides with very different exchange rates suggests that the secondary structure consists of at least 4 elements which unfold independently.

**T-Pos148** HYDROGEN EXCHANGE IN M13 COAT PROTEIN (A MODEL MEMBRANE PROTEIN) DETECTED BY  $^{13}\text{C}$  NMR ISOTOPE SHIFTS. G.D. Henry, J.H. Weiner, and B.D. Sykes, Department of Biochemistry, University of Alberta, Edmonton, Alberta T6G 2H7, Canada.

$^{13}\text{C}$  nuclear magnetic resonance (NMR) spectroscopy has been used as an indirect probe of the exchange rates of selected amide protons in the detergent-solubilised coat protein of the filamentous coliphage M13. The 50-residue coat protein comprises three distinct domains, an acidic N-terminus, a basic C-terminal region and a 20-residue hydrophobic core; it spans the inner membrane of *E. coli* during infection. The carbonyl (C1) resonance of a peptide bond experiences a small 2-bond isotope shift (ca 0.09 ppm) upon deuteration of the nitrogen atom of the succeeding residue. Individual CONH and COND peaks are resolved in 1:1  $\text{H}_2\text{O}:\text{D}_2\text{O}$  mixtures if the exchange rate is slow ( $<40\text{ s}^{-1}$  at 75 MHz). Since H-exchange is catalysed by  $\text{OH}^-$ , resonances may be brought from slow to fast exchange conditions by increasing the pH.

Coat protein was biosynthetically labelled at the peptide carbonyls of lysine, proline, phenylalanine, tyrosine and glycine residues. These labels are distributed within both the hydrophilic and hydrophobic domains of the protein, and have been largely assigned. At the N-terminus (ala 7, ala 9 and asp 12) exchange rates were observed to be 10-20x slower than a fully exposed peptide. At the C-terminus, although ala 49 is freely exposed, the cluster leu 41-thr 46 exchanges 500 to 50,000x more slowly. Amide exchange rates can be interpreted in terms of protein secondary structure and/or solvent accessibility. This equilibrium approach allows measurement of very fast rates and the  $^{13}\text{C}$  label provides selection of a given amide proton.

**T-Pos149** DECONVOLUTION ANALYSIS OF HEAT CAPACITY DATA FOR SUPERHELICAL DNAs. Daniel Goldfarb, Interdisciplinary Program in Biophysics, Box 448, University of Virginia, Charlottesville, Va., 22908.

I have melted superhelical p5N DNA under various conditions using high sensitivity differential scanning calorimetry. The plasmid p5N was constructed by inserting into the PstI site of pBR322 an approximately 400 base pair sequence from the 3' end of a glutathione transferase complementary DNA. This insert contains a poly-A sequence about 60 base pairs long. Deconvolution analysis (Freire and Biltonen, *Biopolymers*, 17, 463, (1978).) of the D.S.C. heat capacity melting profile for this plasmid indicates at least 6 to 8 sequential thermotropic transitions for the supercoiled form. The linear form also shows multiple transitions similar to the supercoiled form, with the number of transitions and their enthalpy changes and melting temperatures depending upon conditions. I am currently preparing topoisomers of p5N to investigate the effects of varying the linking number on the melting profile and on the subsequent parameters obtained from deconvolution analysis.

**T-Pos150** FLOW LINEAR DICHROISM OF NUCLEIC ACIDS IN THE VACUUM ULTRAVIOLET. Stephen P. Edmondson and W. Curtis Johnson, Jr., Department of Biochemistry and Biophysics, Oregon State University, Corvallis, Oregon 97331

If the transition dipole directions are known, there are three unknowns in a flow linear dichroism experiment on nucleic acids: (1) the inclination of the bases, (2) the axis around which the bases incline, and (3) the fractional orientation of the nucleic acids in the flow. Extension of linear dichroism spectra into the vacuum ultraviolet region gives enough information to solve for all three unknowns in the case of simple repeating polynucleotides, and the minimum inclination in the case of natural nucleic acids. The minimum inclination for A-form DNA is measured at 17° from perpendicular, close to the X-ray diffraction value. The 10.4 and 10.2 B-forms are found to be only slightly less inclined at about 15° from perpendicular. Specific inclinations and axes of inclination have been determined for poly dA•poly dT, poly d(AT)•poly d(AT), poly dG•poly dC, and poly d(GC)•poly d(GC) in the B-form, and poly d(GC)•poly d(GC) in the Z-form.

**T-Pos151** ROTATIONAL DIFFUSION OF SHORT DNA FRAGMENTS IN POLYACRYLAMIDE GELS. S. Wijmenga and A. Maxwell (Intr. by W.A.Hagins), National Institutes of Health, Bethesda, MD20205

The rotational diffusion in polyacrylamide gels of 5 short DNA restriction fragments ranging in size from 55 to 256 base pairs has been examined by electric birefringence as a function of gel concentration and electric field strength. The recently developed theory of Odijk (1) for the dynamics of slightly flexible rods in a network has been used to interpret our results. The dependence of the observed rotational relaxation time  $T$  on the fragment length  $L$  is given by  $T \propto L^a$  with  $a=1.95 \pm 0.05$  and  $2.01 \pm 0.04$  for 4% and 10% gels respectively, in good agreement with the prediction from the Odijk theory,  $T \propto L^2$ . The rotational relaxation times were found to depend on the gel concentration contrary to the prediction from the Odijk theory. We discuss possible reasons for this. For small electric fields the birefringence decay curves were found to be single exponential, indicating a single relaxation process.

(1) Odijk, T. *Macromolecules* 1983, 16, 1340.

**T-Pos152** TRANSIENT ELECTRIC BIREFRINGENCE STUDIES OF SMALL ION DYNAMICS IN THE VICINITY OF SHORT DNA RESTRICTION FRAGMENTS. Matthew S. Gebhard, Matheen Haleem, and Don Eden, Dept. of Chemistry, San Francisco State Univ., San Francisco, CA 94132

Reverse pulse transient electric birefringence studies were carried out on a short DNA restriction fragment in various aqueous salt solutions to elucidate the dynamics of small ion interactions with the negatively charged DNA. This was accomplished by determining the inherent ionic polarization relaxation time for several counterions. The DNA sample consisted of a 1:1 ratio of 123 and 124 base pair fragments from a HaeIII digest of pBR322 with concentrations between 6 and 10  $\mu\text{g}/\text{mL}$ . The field strength was 1850 V/cm. The solutions with their counterion concentrations were 1mM NaPi, 1mM KPi, 1mM (NMe<sub>4</sub>)Br, 1mM (NBu<sub>4</sub>)Br and 0.5mM Mg(Ac)<sub>2</sub>. The data were analyzed using the slow induced dipole model of Takezoe and Yu (*Biochemistry* **20** 5275 (1981)). In a temperature dependence study on the Na<sup>+</sup> solution, the ionic relaxation time was found to behave linearly on  $\eta/T$ . This indicated that the ionic polarization is most likely a diffusional process. The relaxation times at 4 C were 206ns (Na<sup>+</sup>), 207ns (K<sup>+</sup>), 175ns (NMe<sub>4</sub><sup>+</sup>), 191ns (NBu<sub>4</sub><sup>+</sup>), and 126ns (Mg<sup>++</sup>). One would expect a universal inverse relation between these values and the bulk ionic diffusion constants if only ions with weak interactions with the DNA were important in the polarization. However, this correlation was not observed. The relative trend is observed with the tetra-alkyl ammonium ions when one considers the considerable contribution that may arise from the Br<sup>-</sup>. Given the 45% greater diffusion constant for K<sup>+</sup> relative to that of Na<sup>+</sup> one would expect a faster ionic relaxation time for the KPi solution. A longer relaxation would be expected for Mg<sup>++</sup> relative to that for Na<sup>+</sup>. Furthermore, no universal correlation between the ionic relaxation times and the ionic polarizabilities as determined from the steady state birefringence was observed.

**T-Pos153** COUNTERION DYNAMICS NEAR ROD-LIKE MACROIONS AS DETERMINED BY TRANSIENT ELECTRIC BIREFRINGENCE. Matheen Haleem, Don Eden, and Attila Szabo, Department of Chemistry, San Francisco State Univ., San Francisco, CA 94132 and Lab. of Chem. Phys., NIH, Bethesda, MD 20892.

The dynamic behavior of counterions in the vicinity of macroions in solution is a biologically important phenomenon that has been difficult to measure experimentally as well as to model theoretically. Transient electric birefringence (TEB) experiments may be used to determine ion dynamics in the vicinity of simple polyelectrolyte systems such as solutions of short DNA restriction fragments. Specifically, an electric field drives charge polarization, and charge polarization is coupled to molecular rotation. The time dependent average orientation is measured via the optical property, birefringence. We have developed a new model for TEB resulting from ionic polarization around rod-like macroions in solution, given the assumptions that (1) counterion dynamics can be completely described by a single relaxation time, and (2) counterion motion along the symmetry axis of the rod is the only source of dipole moments. We have rigorously formulated and exactly solved a coupled rotational equation for birefringence in the low field limit for the case of (1) a reversed pulse electric field and (2) an AC field. Unlike previous formulations in which the rotational dynamics were treated stochastically but the ion atmosphere dynamics were treated deterministically, our approach treats both stochastically. The resulting simple analytical expressions for field reversal TEB reduce to the classical limiting response expected of a permanent dipole orientation when the ion-atmosphere relaxation is slow and to the response of a molecule with an instantaneously induced dipole when the relaxation is rapid compared with rotation. The results are used to analyze experimental TEB data on short DNA restriction fragments.

**T-Pos154** NMR STUDIES OF THE INTERACTIONS OF SIMPLE CATIONS WITH DNA.

S. Padmanabhan, C. F. Anderson, M. T. Record, Jr., Depts. of Chemistry and Biochemistry, University of Wisconsin, Madison, WI. 53706.

The interactions of small ions with DNA have large effects on DNA conformational and ligand binding equilibria. We have employed measurements of the NMR relaxation rates of the quadrupolar nucleus <sup>14</sup>N in solutions of various simple cations, including monovalent ammonium and tetraalkylammonium ions, and the divalent polyamines, putrescine and cadaverine. Ion size, charge and hydrogen bonding may all affect the interactions of these ions with DNA. The relaxation rates of the ammonium ion and putrescine are quite sensitive functions of pH in the absence of DNA. At constant pH (~6.0) titrations of NaDNA with ammonium tetraalkylammonium ions, or putrescine, ions gave a single <sup>14</sup>N peak in each case. The longitudinal and transverse relaxation rates obtained from inversion recovery and linewidth measurements, respectively, were found to decrease with increasing amounts of the cation, as has been observed for other quadrupolar ions like, <sup>23</sup>Na<sup>+</sup>, <sup>87</sup>Rb<sup>+</sup> and <sup>39</sup>K<sup>+</sup> in DNA solutions. These titrations are analysed in terms of a two state model for the observed relaxation rate, assuming fast exchange of cations between "bound" and "free" environments. The extents of counterion association with DNA and their relative affinities for DNA can thereby be estimated and correlated with the specific characteristics of these ions.

**T-Pos155** MONTE CARLO SIMULATIONS OF DNA-SALT SOLUTIONS: THE PREFERENTIAL INTERACTION COEFFICIENT. P. Mills, C. F. Anderson and M. T. Record, Jr., Depts. of Chemistry and Biochemistry, University of Wisconsin, Madison, WI. 53706.

Monte Carlo (MC) computations using a grand canonical approach were performed to investigate nonideality in aqueous solutions of NaDNA with NaCl. The solvent was modeled as a dielectric continuum, the small ions as hard spheres, and DNA as an impenetrable cylinder with uniform, continuous axial charge density equal to the mean projected axial charge density of helical B-DNA. At fixed values of the electrolyte chemical potential, variations in the salt concentrations,  $C_3$ , as a function of DNA phosphate concentration,  $C_u$ , were determined by computing the equilibrated number of salt ions in the MC cell as a function of its size. The resulting plots of  $C_3$  vs.  $C_u$  all are linear over extended concentration ranges. The slopes of these plots are directly related to  $\Gamma_{3u}$ , the preferential interaction coefficient, which is the key quality in thermodynamic analyses of the salt-dependence of equilibria involving DNA. The magnitudes and salt-dependence of  $\Gamma_{3u}$  determined by the MC approach are comparable to the corresponding predictions of the Poisson-Boltzmann (PB) cell model, which does not include small ion correlations. The significant salt-dependence of  $\Gamma_{3u}$ , predicted by both MC and PB calculations, has not been observed experimentally. Possible origins of this discrepancy are under investigation. (Supported by NIH grant GM-34351.)

**T-Pos156** CONDENSATION OF DNA BY DIVALENT CATIONS AT ELEVATED TEMPERATURES. David A. Knoll, Michael G. Fried\*, and Victor A. Bloomfield. Dept. of Biochemistry, Univ. of Minn., St. Paul, MN and \*Dept. of Biochemistry, Univ. of Texas, Health Science Center, San Antonio, TX.

Incubation of double stranded (ds) DNA at elevated temperatures in the presence of divalent cations results in the formation of large multimolecular aggregates. Using a solubility assay we have measured the midpoint ( $T_m$ 's) of the aggregation transition. At 1 mg/ml DNA and 50 mM cation, the  $T_m$ 's fall into three categories: alkaline earths (Mg, Ca, Sr, Ba)  $T_m = 80 \pm 10^\circ\text{C}$ , transition metals<sup>II</sup> (Mn, Co, Ni, Cu, Zn, Cd)  $T_m < 70^\circ\text{C}$ , and putrescine (no condensation observed  $< 90^\circ\text{C}$ ). Increasing the divalent cation concentration results in a decrease in the  $T_m$  whereas the nature of the anion and the DNA concentration (1 to 15 mg/ml) have only minor effects on the  $T_m$ . Using static light scattering, we observe large increases in the scattering intensity upon condensation of the viral DNA's -- more than would be expected for monomolecular collapse. When the temperature is lowered, the aggregates do not dissociate. The aggregates can be as large as several microns in diameter as seen by dynamic light scattering and electron microscopy. Thus far we have not found conditions which yield monomolecular (and hopefully reversible) collapse. Our results raise significant questions with respect to current theories of DNA condensation: 1) Divalent cations are not predicted to cause DNA condensation in aqueous solution: the effect temperature on fractional charge neutralization is small. 2) Specific ion effects are pronounced, possibly indicating multiple modes of cation binding. Since divalent cations are expected to stabilize dsDNA with respect to strand separation, we believe our DNA to be double stranded throughout the entire temperature range of our experiments.

**T-Pos157** DISSECTION OF THE SOLVENT ENTROPY CHANGE DRIVING MOLECULAR ASSEMBLY: CHAOTROPIC AND LYOTROPIC ANIONS IN THE MN-INDUCED CONDENSATION OF DNA. Donald C. Rau and V. Adrian Parsegian (Intr. by M.S. Prouty). National Institutes of Health, Bethesda, MD 20892.

The assembly of many macromolecules into biologically interesting structures is frequently an entropically driven process. Collagen fibril formation, DNA collapse, TMV assembly, sickle cell hemoglobin polymerization, tubulin assembly and a great many others are examples of such processes (cf. M. Lauffer, Entropy-Driven Processes in Biology, Springer 1975). In many of these systems, the increased entropy of the ordered phase is presumed due to the release of "bound" water. It is not widely appreciated that the entropy of the bulk water into which these bound water molecules are released is an integral part of the total entropy change. To quantify this contribution we have been investigating the effect of three specific anions ( $\text{SO}_4^{2-}$ ,  $\text{Cl}^-$ , and  $\text{ClO}_4^-$ ), known to differently affect bulk water entropy on the transition to an ordered, attractive array of DNA helices induced by  $\text{Mn}^{2+}$  binding. We use osmotic stress coupled with X-ray diffraction to map the transition as a function of applied osmotic pressure, temperature, and ionic activities. The transition entropy is determined at constant ionic activity using the Clausius-Clapeyron equation. We find that the chaotropic anion,  $\text{ClO}_4^-$ , is particularly effective in increasing the transition entropy. We will also correlate the differences in the transition entropies for the three anions with their known effect on bulk water entropies.

**T-Pos158** WINDING ANGLE AND CD SPECTRAL CHANGES OF B FORM DNA IN ETHANOL:H<sub>2</sub>O SOLVENTS. Steven Ringquist and Sue Hanlon, Dept. Biol. Chem., U of IL Col. of Med., Chicago, IL 60612.

The conformation of highly purified pBR322 DNA has been examined at pH 7.6 in ethanol:H<sub>2</sub>O solvents containing either Mg or Na ions. As the ethanol concentration is increased up to 30%(v/v) the positive CD band above 260nm decreases. The average change in the winding angle, as evaluated electrophoretically with covalently closed DNA, increases in these solvents regardless of which cation is present. The increase in Mg solvents is ca. 3E-3 deg/%EtOH and is 6E-3 deg/%EtOH in Na solutions as the ethanol concentration is increased up to 30%(v/v) ethanol. In 6.6mM MgCl<sub>2</sub> and 28%(v/v) ethanol, linear pBR322 DNA undergoes a temperature dependent reversible conformational transition and condensation between 15° and 50°C. At 27°C and below the DNA is in a B form. Above this temperature the CD spectral properties indicate a transition to a conformation which shows some aspects of an A-like structure. This precedes a reversible aggregation of the DNA. Electron microscopic examination of these aggregates show rod shaped structures with a diameter of ca. 110Å and a variable length. Sodium solutions show none of these effects in the same EtOH range. The results in Mg disagree with the earlier observations of Lee, Mizusawa and Kakefuda (PNAS 78, 2838 (1981)) who found a decrease in the winding angle of pBR322 DNA in mixed organic-H<sub>2</sub>O-Mg solvents. The origin of the discrepancy may be due to the presence of contaminants of RNA and protein in the pBR322 preparation of the latter workers. The present results serve to verify the inverse relationship between changes in the rotational strength of the CD band above 260nm and the winding angle of B form DNA. (Supported by NIH GM30284).

**T-Pos159** THE PRE-DISSOCIATION AND DISSOCIATION DYNAMICS OF GGAATTC W. H. Braunlin and V. A. Bloomfield, Dept. of Biochemistry, University of Minnesota, St. Paul, MN 55108

We find that the NMR linewidths and selective T<sub>1</sub> relaxation rates of the imino proton resonances of the self-complementary octadeoxynucleotide GGAATTC are sensitive to pH and base-catalyst concentrations. At low catalyst concentrations and moderate pH, the linewidths/relaxation rates of the three central imino resonances are nearly equal and exchange occurs primarily through dissociation of the octamer duplex. Under these conditions our measurements allow the determination of k<sub>d</sub>, the salt-dependent duplex dissociation rate constant. For 0.15 M Na<sup>+</sup>, we find k<sub>d</sub> = 2.7 s<sup>-1</sup> at 25 °C and E<sub>a</sub> = 45 kcal/mol. At 0.03 M Na<sup>+</sup> we obtain k<sub>d</sub> = 13 s<sup>-1</sup> at 25 °C and no significant change in E<sub>a</sub>. As the pH or base-catalyst concentration is increased, imino relaxation speeds up and markedly different relaxation rates are observed for the three internal imino resonances. As expected, those resonances nearer the ends of the helix are found to relax faster. Under these circumstances the imino proton relaxation monitors the salt-independent opening reactions of individual base-pairs (which occur prior to complete helix dissociation). Combining the results of our measurements at low and high catalyst concentrations provides a rather detailed picture of the salt-dependent dynamics of pre-dissociation and dissociation of the GGAATTC octamer.

**T-Pos160** IDENTIFICATION OF THREE DIFFERENT CONFORMATIONAL STATES OF PLASMID pUC12.

An Zhi Li\* and Victor A. Bloomfield, Department of Biochemistry, University of Minnesota, St. Paul, MN 55108 \*Permanent Address: Department of Physics, Nankai University, Tianjin, P.R. China

We have investigated the condensation reactions of the plasmid pUC12 by dynamic and static light scattering measurements. At low DNA concentration and low ionic strengths, cobalt hexamine and spermidine cause the plasmid pUC12 (2680bp) to form toroids which are similar in size to the toroids formed by the much larger λ DNA (49,000 bp) (Widom and Baldwin (1983) Biopolymers, 22, 1595-1620). Combining dynamic and static light scattering measurements, three distinct conformational states of pUC12 can be observed. These correspond to transitions from random coil to collapsed coil and from collapsed coil to aggregated coil. Though distinct states are evident, the transitions do not occur in a simple two-state manner. The three different states of DNA are identified by the following approaches: the first approach is to check if the diffusion coefficient is independent of both the concentration of DNA and the concentration of condensing agent. Another approach is to observe the time dependence of dynamic light scattering parameters. The final approach is a method of pattern recognition-cluster analysis. Samples could be identified to be one kind of state according to their location in a pattern space defined by dynamic and static light scattering parameters.

**T-Pos161** FLUORESCENCE CORRELATION SPECTROSCOPY AS A PROBE OF MACROMOLECULAR MOTION, Béthe A. Scalettar, Melvin P. Klein, and John E. Hearst, University of California, Berkeley, CA 94720.

The orientational and translational motions of DNA have important implications for many biological phenomena. Fluorescence correlation spectroscopy (FCS) is a technique that can extract information about these motions by monitoring fluctuations in the total fluorophore emission from a small, open system. FCS can be used to probe the microsecond to second time regime and hence is well suited to a comprehensive study of macromolecular motions. Previous FCS studies of DNA in solution have employed the noncovalently bound intercalator ethidium bromide; they are thus complicated by fluctuations from the on-off kinetics of the probe. We have been able to extend this work by covalently attaching an azide analogue of ethidium, ethidium monoazide, to a variety of DNAs. With our system, translational diffusion constants of oligomeric molecules as well as much longer plasmid and phage DNAs have been accurately determined. We have also begun a study of rotational, bending, and torsional motions of DNA labeled with a small number of dye molecules. These studies are being carried out under conditions of high viscosity and DNA concentration that simulate the nuclear environment. Preliminary results with long DNAs reveal millisecond decays appropriate to longer reorientational DNA motions. Theoretical work on reorientation in concentrated, constrained systems is being used to interpret these experiments. Supported by NIH grant #GM30781 and by DOE under contract #DE-AC03-76SF0098.

**T-Pos162** DNA MINOR GROOVE BINDERS. Luis A. Markey, Robert Ferrante, and Kenneth J. Breslauer. Department of Chemistry, Rutgers University, New Brunswick, NJ 08903

Netropsin and distamycin A both are basic oligopeptides which exhibit antibacterial, antifungal, and antiviral activities. Distamycin A is an analogue of netropsin, possessing one more methyl-pyrrole ring. Both drugs bind in a non-intercalative manner to the minor groove of "B"-form DNA. The resulting drug-DNA complexes are stabilized by contributions from peptide-nucleotide hydrogen bonding, hydrophobic forces, and electrostatic interactions. Previously we have reported on the high affinity binding of netropsin to poly dAT•poly dAT ( $K \approx 10^9$ ) which we showed is enthalpy driven ( $\Delta H = -11.2$  kcal/mol of drug bound).

To investigate the influence of the additional pyrrole ring of distamycin on DNA binding, we have used a combination of temperature-dependent uv absorption spectroscopy, circular dichroism, and batch calorimetry to measure the thermodynamic parameters for the association of distamycin A with poly dAT•poly dAT at low ionic strength. The following observations have been noted: (1) distamycin A increases the thermal stability of the host duplex by  $\sim 30^\circ\text{C}$ , (2) this drug-induced thermal stabilization of the duplex corresponds to a binding constant of  $\approx 10^9$ , (3) this binding constant is of the same order of magnitude as that which we have determined for netropsin under identical conditions, (4) significantly, however, the binding enthalpy for distamycin is  $\approx 7$  kcal/mol more exothermic than the corresponding value for netropsin.

Supported by NIH grant GM 34469.

**T-Pos163** ETHIDIUM BINDING TO DNA AND RNA. Denise Zaunczkowski, Kenneth J. Breslauer, and Luis A. Markey. Department of Chemistry, Rutgers University, New Brunswick, NJ 08903

Ethidium bromide is an important drug whose functions are of considerable biochemical interest. The drug binds to both DNA and RNA by intercalation of the ethidium chromophore between base pairs. Drug binding inhibits DNA synthesis *in vivo* and interferes with DNA-dependent DNA and RNA polymerases *in vitro*. Despite extensive investigations on this drug, important questions remained unanswered. To alleviate this situation, we have employed a combination of spectroscopic and calorimetric techniques to investigate the role of base sequence and helix conformation on the affinity and specificity of ethidium cation binding to DNA. Specifically, we have measured the thermodynamic parameters that accompany the interaction of the ethidium cation with commercially available DNA and RNA polymer duplexes containing various base sequences. The following thermodynamic binding profiles in 10 mM phosphate buffer, pH = 7.0 at  $25^\circ\text{C}$  have been obtained:

polymer	$\Delta G$ (kcal/mol)	$\Delta H$ (kcal/mol)	$\Delta S$ (cal/K-mol)
poly dAT•poly dAT	-9.4	-10.0	-2.0
poly dIC•poly dIC	-9.3	-9.2	+0.5
poly dGC•poly dGC	-8.8	-6.3	+8.3
poly rA•poly rU	-9.1	-9.0	+0.3

Supported by NIH grant GM 34469.

**T-Pos164** SEQUENCE DEPENDENT COOPERATIVE INTERACTIONS IN A/T CONTAINING DUPLEX OLIGO- AND POLYDEOXYRIBONUCLEOTIDES. Robert L. Jones\*, Gerald Zon+ and W. David Wilson\*, Dept. of Chemistry, Georgia State University, Atlanta, Ga. 30303\*, and Division of Biochemistry and Biophysics, Food and Drug Administration, National Institutes of Health, Bethesda, MD, 20892+.

Many intercalators exhibit unusual binding interactions with the nonalternating sequence polymer PolydA.dT relative to the alternating polymer of identical composition, Polyd(A-T)<sub>2</sub>. The unusual effects in PolydA.dT intercalation include: (1) nonstandard hydrodynamic changes,<sup>2</sup> (2) a large positive enthalpy and entropy, (3) temperature dependent cooperativity, (4) a reduced free energy for binding relative to other sequences, and (5) unusual association kinetics. Detection of these five effects requires an interaction probe such as the intercalator propidium. In order to understand the biological significance of the unusual properties of nonalternating A/T sequences, it is necessary to determine how the interaction is modified by the length of the A/T sequence, by breaks in the sequence, and by the composition and sequence of adjacent DNA segments. We have approached these questions through propidium binding and NMR studies with A/T containing oligonucleotides. With the oligomer d(A-T)<sub>6</sub>.d(A-T)<sub>6</sub> binding interactions are similar to those observed with Polyd(A-T)<sub>2</sub>. In the same way dA<sub>10</sub>.dT<sub>10</sub> behaves very much like PolydA.dT, indicating that the unusual properties of nonalternating<sup>10</sup> sequences can occur for short DNA segments. The oligomer d(A<sub>6</sub>-T<sub>6</sub>).d(A<sub>6</sub>-T<sub>6</sub>) has unusual results which appear to require an initial strong binding of propidium to a unique site, followed by binding to a set of sites having a highly cooperative, but weaker, interaction. [ Supported by NIH Grant GM 30267 ].

**T-Pos165** CARCINOGEN-NUCLEIC ACID INTERACTIONS: EQUILIBRIUM BINDING STUDIES OF AFLATOXIN WITH DNA David E. Graves†, Michael P. Stone\*, and Thomas M. Harris\* †Department of Chemistry, University of Mississippi, University, MS 38677, and \*Department of Chemistry and Center in Molecular Toxicology, Vanderbilt University, Nashville, TN 37235

Equilibrium binding is believed to play an important role in directing the subsequent covalent attachment of many carcinogens to DNA. We present detailed studies of the non-covalent interactions of aflatoxin B<sub>1</sub> and B<sub>2</sub> with native DNAs and synthetic specific-sequence polynucleotides. Aflatoxin B<sub>1</sub> is demonstrated to bind in a highly cooperative manner to calf thymus DNA. This positive cooperativity may be explained by the presence of specific high-affinity sites for this carcinogen, which have been postulated to exist on the basis of covalent attachment studies. The effects of ionic strength, temperature, and base-sequence specificity on the cooperative nature of this carcinogen-DNA interaction are investigated.

**T-Pos166** EFFECTS OF INTERCALATING DRUGS ON THE ANTIVIRAL AND INTERFERON-INDUCING ACTIVITIES OF POLYRIBONUCLEOTIDES. James M. Jamison, Pedro J. Bonilla, and Chun-che Tsai, Department of Chemistry, Kent State University, Kent, Ohio 44242 and Department of Microbiology and Immunology, Northeastern Ohio Universities College of Medicine, Rootstown, Ohio 44272

As part of our studies on the perturbation of RNA structure induced by intercalating drugs and its effect on antiviral and interferon-inducing activities, we have designed experiments to systematically examine and quantify the effects of intercalating drugs on the antiviral and interferon-inducing activities of polyribonucleotides (poly r(A-U) and poly r(G-C)) using the human foreskin fibroblast-vesicular stomatitis virus bioassay system. The interferon titers were based on the activity of NIH human fibroblast interferon reference standard and poly (rI).poly (rC) reference standard. A wide range of minor, major, and minor/major groove intercalating drugs have been tested in this study. The role of each intercalating drug in modulating the antiviral and interferon-inducing activities of poly r(A-U) and poly r(G-C) was examined by experiments in which the concentrations of both polyribonucleotides were fixed at 0.05 mM, 0.1 mM or 0.2 mM while the drug concentration was varied to produce variable drug/nucleotide ratios ranging from 1:16 to 2:1. Our experimental results demonstrate that the combination of poly r(A-U) or poly r(G-C) with minor or minor/major groove intercalating drug produced an adjuvant effect on the antiviral and interferon-inducing activities at the drug/nucleotide ratio range of 1/6 to 1/4. These results suggest a synergism between the polyribonucleotide (poly r(A-U) or poly r(G-C)) and the drug (minor or minor/major groove intercalating drug). The combination of poly r(A-U) or poly r(G-C) with major groove intercalating drug did not display this synergism.

**T-Pos167** ULTRAVIOLET RESONANCE RAMAN STUDY OF THE INTERACTION OF CIS- AND TRANS- DICHLORO-DIAMMINE WITH 9-SUBSTITUTED GUANINES. KRZYSZTOF BAJDOR, YANG WANG, AND W.L. PETICOLAS. Department of Chemistry, University of Oregon, Eugene, Oregon 97403. Several years ago it was shown that the carbonyl vibration in 5'-GMP is active in the Resonance Raman spectrum (RRS) taken from the second excited state (200-230nm) but not from the first (240-290nm) (1). We have used this effect to study the interaction of cis- and trans-platin with guanosine and 9-ethyl guanine using 218nm light from a hydrogen shifted YAG laser. The Pt compounds and the bases were mixed 1:1 in D<sub>2</sub>O solution at pD4. Raman spectra were taken of the resulting compounds in deuterium oxide solution as a function of pD. At pD 9 guanosine and their 7-substituted derivatives lose their carbonyl group due to the ionization of the NH-1 hydrogen. This transition occurs at a pD near 7. Thus, careful attention must be given to the pD dependence of the RRS which changes abruptly over the pD range of 6 to 8. The cis-platin and the trans-platin adducts of guanosine and 9-ethyl guanine show a different RRS when taken at 218nm. The carbonyl band is measurably weaker in the cis-adduct than in the trans at pD 4. We interpret this as evidence of weak interaction through an aquo bridge between the Pt and the C=O6 group. However as the pD is raised the trans adduct precipitates out at pD 6.5 giving evidence that the aquo group is replaced by the hydroxide ion. The pK of the cis adduct is lower than the trans presumably due to stabilization of the negatively charged C-O<sup>-</sup> by the Pt. We propose that at neutral pD the cis-Pt adduct is stabilized by an interaction of the Pt with the O6 of the carbonyl by means of a hydroxide bridge. (1) L.D. Ziegler, D.P. Strommen, B.S. Husdon, and W.L. Peticolas (1982), Raman Spectroscopy: Linear and Nonlinear, J. Sascomb and P.V. Huang, ed. John Wiley, New York, 707-8.

**T-Pos168** ANALYSIS OF BINDING DATA FOR THE INTERACTION OF DNA REPAIR PROTEINS WITH DAMAGED DNA  
Sharlyn J. Mazur & Lawrence Grossman, Department of Biochemistry, Johns Hopkins University School of Hygiene and Public Health, 615 N. Wolfe St., Baltimore, MD 21205

The interaction of proteins with specific DNA sites is often studied *in vitro* through indirect measures of the occupancy of the sites. In the study of DNA repair proteins and damaged DNA, the use of these indirect assays is complicated by heterogeneity in the damaged DNA. Exposure of DNA molecules to a damaging agent results in a population of DNA molecules with a distribution in the number of damaged sites per molecule and a distribution in their location. We present methods for analyzing data from indirect assays when there is a distribution in the number of specific sites per molecule. Some assays, such as nitrocellulose filter binding or the conversion of covalently closed circular DNA to nicked DNA, are sensitive only to the first binding event. Others, such as a gel electrophoretic mobility retardation assay or an assessment of changes in the equilibrium topological linking number, are sensitive to the number of proteins bound to the DNA molecule. In addition, the sequence surrounding a site of damage may influence its interaction with the repair protein. The distribution in the sequence-specific location of damaged sites may result in a distribution of binding or kinetic constants. Methods for distinguishing sequence-specific factors from other factors are discussed. These methods of analysis are illustrated by application to data from a variety of assays for the interaction of the *E. coli* uvrABC proteins with DNA damaged by ultraviolet light.

**T-Pos169** NMR STUDIES OF THE EFFECT OF CYCLOSPORINE ON  $^{19}\text{F}$ -LABELED PHOSPHOLIPIDS. Susan R. Dowd<sup>1</sup>, David H. Van Thiel<sup>2</sup>, and Chien Ho<sup>1</sup>. Department of Biological Sciences, Carnegie-Mellon University<sup>1</sup> and Department of Medicine, University of Pittsburgh<sup>2</sup>, Pittsburgh, PA 15213, U.S.A.

The fungal metabolite, cyclosporine (Cs A), is a cyclic undecapeptide that has found extensive use as a specific immuno-suppressive drug in organ transplantation. The X-ray crystal structure of Cs A shows that six of its amino acids are involved in an antiparallel  $\beta$ -sheet conformation while the remainder forms an open loop [Petcher, Weber, and Ruegger, *Helv. Chim. Acta* 59, 1480 (1976)]. The binding of Cs A to lymphocytes has been a subject of intense investigation without the finding of a specific binding site and only a suggestion of non-specific inclusion in the lipid bilayer. We have investigated the effect of Cs A on phospholipid bilayers by using both  $^{19}\text{F}$  and  $^{31}\text{P}$  nuclear magnetic resonance (NMR) techniques.  $^{19}\text{F}$  NMR studies of aqueous dispersions of dimyristoylphosphatidylcholine (DMPC), labeled with a difluoromethylene ( $\text{CF}_2$ ) group at the 4-, 8-, or 12-position of the *sn*-2-acyl chain, have proven to be useful for characterizing the structural and dynamic properties within a lipid bilayer. The addition of a membrane constituent, cholesterol, to  $^{19}\text{F}$ -labeled DMPC has the effect of making the gel state more fluid and the region above the phase transition less mobile. Cs A, like cholesterol, is a fairly rigid hydrophobic molecule. Our  $^{19}\text{F}$  NMR results show a significant but smaller effect than that of cholesterol on the various labeled positions of  $^{19}\text{F}$ -labeled DMPC.  $^{31}\text{P}$  NMR studies suggest that Cs A has no effect on the headgroup region of DMPC. The implication of our NMR results to the interaction between Cs A and DMPC will be discussed. [Supported by a research grant from the NIH (GM-26874)].

**T-Pos170** ROTATING-FRAME SPIN-LATTICE RELAXATION INVESTIGATION OF SLOW MOLECULAR MOTIONS AT KHz FREQUENCY RANGE IN FLUORINE-19-LABELED LIPID BILAYERS. Zheng-Yu Peng<sup>1,2</sup>, Virgil Simplaceanu<sup>1</sup>, Irving J. Lowe<sup>1</sup>, and Chien Ho<sup>1</sup>. Department of Biological Sciences<sup>1</sup> and Department of Physics<sup>2</sup>, Carnegie-Mellon University, 4400 Fifth Avenue, Pittsburgh, PA 15213, U.S.A.

In order to study the slow molecular motions in phospholipid model membranes, we have measured the  $^{19}\text{F}$  rotating-frame relaxation rates ( $1/T_{1\rho}$ ) on multilamellar phospholipid dispersions. Our samples are prepared from dimyristoylphosphatidylcholine (DMPC), labeled with a difluoromethylene ( $\text{CF}_2$ ) group at the 4-, 8-, or 12-position of the *sn*-2-acyl chain, dispersed in  $\text{H}_2\text{O}$ . We have investigated the dependence of the relaxation rate on the locking field strength, temperature, and label position. Our results show, given the fact that  $T_{1\rho} \ll T_1$  on all the samples studied, that the slow molecular motions in the KHz frequency range dominate the relaxation processes. We assume these motions to be the so-called director fluctuations because  $^{19}\text{F}$  relaxation is thought to be dominated by chemical shift anisotropy which is an intra-molecular interaction. The locking-field dependence of the relaxation rate indicates that there is a distribution of correlation times centered around  $10^{-5}$  sec. Effects of temperature and label position will also be discussed in relation to the structural and dynamic properties of multilamellar phospholipid dispersions. [This work is supported by NIH grants (GM-26874 and HL-24525). I.J.L. is a recipient of a Senior Fellowship of the NIGMS (GM-11075)].

**T-Pos171** FLUORESCENCE LIFETIME AND ROTATIONAL BEHAVIOR OF DEHYDROERGOSTEROL IN LIPID BILAYERS. P.L.-G. Chong and T.E. Thompson, Department of Biochemistry, University of Virginia, Charlottesville, Virginia 22908.

A dramatic decrease in fluorescence lifetime with increasing temperature appears to be responsible for the depolarization of dehydroergosterol (DHE) in dimyristoyl phosphatidylcholine (DMPC), and dilauroyl phosphatidylcholine (DLPE) multilamellar vesicles, which is always seen when the bulk lipids become more ordered. Our data suggest that the DHE emission in vesicles is described by two exponential components at temperatures below the phase transition and by one component above the transition. The large change in lifetime may be explained by an increase in thermal quenching of DHE by its neighboring molecules. The rotation of DHE in lipid bilayers can be phenomenologically described in terms of the temperature dependence of the thermal coefficient of frictional resistance offered by the environment. We observe a change in the thermal coefficient at  $19.5^\circ\text{C}$  and  $27^\circ\text{C}$  for 4.8 mole % DHE in DMPC, and at  $26.5^\circ\text{C}$  and  $32.5^\circ\text{C}$  for 4.0 mole % DHE in DLPE. These temperatures correspond to the onset and the completion temperatures of the phase transition of the phospholipid, as determined by differential scanning calorimetry. This coincidence suggests that the critical temperature for DHE rotation in lipid bilayers is correlated with the starting and the end point of the melting of the bulk lipids. The thermal coefficient of DHE rotation in DLPE is much less sensitive to the phase transition of the bulk phospholipids than is diphenylhexatriene. This distinction may be a result of differences in the location of chromophores in bilayers or a result of DHE-enriched domains. (Supported by NIH Grant GM-14628).

**T-Pos172** LATERAL DISTRIBUTION OF A PYRENE-LABELLED PHOSPHATIDYLCHOLINE DETERMINED BY FLUORESCENCE PHASE AND MODULATION DATA. R.C. Hresko, I.P. Sugar, Y. Barenholz, and T.E. Thompson Department of Biochemistry, University of Virginia, Charlottesville, Virginia, 22908.

The lateral distribution of 1-palmitoyl,2-pyrenedecanoyl,3-phosphatidylcholine (PyrPC) was studied in small unilamellar vesicles of dipalmitoyl-, dimyristoyl-, or 1-palmitoyl-2-oleoyl-3-phosphatidylcholine (DPPC, DMPC, and POPC respectively). The DPPC and DMPC experiments were carried out over temperature ranges above and below the matrix phospholipid phase transition temperature ( $T_m$ ). Phase and modulation data were used to determine the temperature dependence of 4 pyrene fluorescence rate parameters. These parameters were then used to interpret plots of the excimer to monomer fluorescence intensity ratio ( $E/M$ ) as a function of temperature and to calculate the concentration of the probe within liquid crystalline ( $C_f$ ) and gel ( $C_g$ ) domains in the phase transition region of DPPC. Our results indicate that PyrPC is randomly distributed in pure gel and liquid crystalline phosphatidylcholine bilayers. In the phase transition region, PyrPC molecules mix less ideally in DPPC than in DMPC bilayers. (Supported by USPHS Grants GM-14628 and HL-17576).

**T-Pos173** DPH FLUORESCENCE LIFETIME DISTRIBUTIONS IN MULTILAMELLAR VESICLES. M. Glaser (\*), R. Fiorini (\*), S. Wang (\*), M. Valentino (\*), E. Gratton (\*\*). (\*) Department of Biochemistry and (\*\*) Department of Physics, University of Illinois, Urbana, IL 61801.

The emission decay of 1,6-diphenyl-1,3,5-hexatriene (DPH) in dipalmitoylphosphatidylcholine (DPPC) and dimyristoylphosphatidylcholine (DMPC) multilamellar vesicles was measured using multi-frequency phase fluorometry. The fluorescence decay, which is conventionally described by a sum of two or three exponentials, was analysed using a continuous distribution of lifetime values. This approach better reflects the heterogeneity of the DPH surroundings and also the rate of exchange of environs during the excited state lifetime. The form of the distribution which better described the decay was lorentzian. In our analysis we have used the sum of two lorentzians to better describe a possible asymmetry of the real distribution. In most cases a simple lifetime distribution accounts for at least 95% of the observed decay. The width as well as the center position of the distribution are related to the structural phase transition in DPPC and DMPC. At temperatures below the phase transition the lifetime distribution is centered at about 10 nsec. The width of the distribution is about 1 nsec FWHM. At the phase transition and higher temperatures the lifetime distribution becomes very narrow (0.2 nsec), meanwhile its central value decreases. We discuss the origin of the lifetime distribution in terms of the dynamics of the lipids around the DPH molecule. Supported in part by National Science Foundation grant NSF PCM84-03107 and the NIH grant GM 21953.

**T-Pos174** FREQUENCY DOMAIN FLUORESCENCE STUDIES OF ROTATIONAL MOTIONS OF DPH IN MULTILAMELLAR VESICLES. S. Wang, M. Glaser, and E. Gratton\*, Department of Biochemistry and \*Department of Physics, University of Illinois, Urbana, IL 61801.

The physical structure of multilamellar vesicles has been studied using the rotational behavior of the fluorescent probe 1,6-diphenyl-1,3,5-hexatriene in dimyristoylphosphatidylcholine and dipalmitoylphosphatidylcholine. The decay of the emission anisotropy was analyzed using two emitting species in correspondence with the observation of two distinct lifetime components in the same system. The major component had an average lifetime value of about 10 nsec below the phospholipid phase transition and it decreased to about 7 nsec above the transition. The second component had a lifetime of approximately 3 nsec independent of temperature and contributed about 5 percent of the total fluorescence intensity. The major emitting component showed restricted motion. The values of the time zero anisotropy ( $r_0$ ), time infinity anisotropy ( $r_\infty$ ), the rotational correlation time and the average aperture of the cone were determined in the temperature range from 10°C to 60°C. Increasing the temperature through the phospholipid phase transition resulted in a large decrease in  $r_\infty$  while the rotational correlation time decreased more gradually. The values of  $r_0$  remained constant over the temperature range investigated suggesting that no other rotational motions were present for the major fluorescent component. It was crucial to include in the analysis two rotational species as suggested by the lifetime components to obtain a constant value of  $r_0$ . The minor fluorescent component had a rotational rate similar to the major component. Supported by NIH GM 21953 and NSF PCM 84-03107.

**T-Pos175** EXCITATION WAVELENGTH DEPENDENCE OF TRANS-PARINARIC ACID FLUORESCENCE LIFETIME AND POLARIZATION ANISOTROPY DECAY: EVIDENCE FOR MEMBRANE STRUCTURAL DOMAINS IN FLUID PHASE BILAYERS NEAR THE PHASE TRANSITION TEMPERATURE, AND THEIR RELATIONSHIP TO CRITICAL FLUCTUATIONS. Anthony Ruggiero and Bruce Hudson. Department of Chemistry, University of Oregon, Eugene, OR 97403.

Recent theoretical [Mouritsen et al., *Europ. Biophys. J.* (1985) 12, 75-86] as well as ultrasonic [Mitaku et al., *Biophys. J.* (1983) 42, 137-144] studies have revealed the existence of long range structural fluctuations in the vicinity of the phase transition point in single-component lipid bilayers. These fluctuations have a relaxation time on the order of 1-100 nanoseconds and a temperature dependence characteristic of critical phenomena. Fluorescence lifetime and time-resolved fluorescence polarization anisotropy measurements will be presented that indicate the presence of structural domains in fluid phase bilayers near the transition temperature on the fluorescence time scale. The relationship between these measurements and the ultrasonic studies, along with their relevance to understanding the nature of the phase transition in lipid bilayers, will be discussed. In addition, second and fourth rank order parameters resulting from the analysis of the anisotropy data in terms of the approximate solution to the rotational diffusion equation developed by Van der Meer et al. [*Biophys. J.* (1984) 46, 515-523] will be presented along with the resulting angular distribution functions.

**T-Pos176** A SEARCH FOR NERNSTIAN DYES TO MEASURE MEMBRANE POTENTIAL IN INDIVIDUAL CELLS. Leslie M. Loew, Benjamin Ehrenberg, Eric Fluhler, Mei-de Wei, and Valerie Burnham, Department of Physiology, University of Connecticut Health Center, Farmington, CT 06032.

Radiolabelled tetraphenylphosphonium (TPP) cation has become widely used as a probe of membrane potential for cells in suspension. The ratio of concentrations inside to outside the cells for this permeant cation is governed by the Nernst equation. We have begun to search for fluorescent permeant cations which, via microfluorometry, can report the membrane potential of individual cells. Since the dye distribution within the cell is directly visualized, this would also have the advantage of allowing direct assessment of contributions to probe accumulation from factors other than plasma membrane potential (e.g., membrane binding or mitochondrial uptake) which are always possible sources of artifact in TPP based measurements. Existing potentiometric dyes undergo a potential dependent change in fluorescence quantum yield and are used to monitor changes rather than measure absolute values of membrane voltage. We have screened over 20 commercially available dyes with HeLa cells and have identified rhodamine 6G as the most reliable. By employing small and cell sized unilamellar vesicles as models, we were able to develop methods for determination of and correction for artifacts due to self-quenching and dye binding. In particular, rhodamine 6G accumulates inside cell-sized vesicles according to the nernst equation after a small correction due to membrane binding.

(Supported by USPHS grants GM35063 and AI22106.)

**T-Pos177** ANALYSIS OF MEMBRANE PENETRATION DEPTH USING FLUORESCENCE QUENCHING BY SPIN-LABELED PHOSPHOLIPIDS. Amitabha Chattopadhyay and Erwin London. Department of Biochemistry, State University of New York at Stony Brook, New York 11794-5215.

Fluorescence quenching of fluorescent groups incorporated into model membranes was measured in two sets of samples: one set in which membranes contained a variable concentration of a phosphatidylcholine (PC) carrying a spin label on the 5 carbon of one acyl chain, and a second set in which the same concentration of PC spin-labeled on the 12 carbon of one fatty acyl chain was present. By combining the results of fluorescence intensity measurements from the two sets, the depth of the fluorescent group can be determined by use of the equation:  $R_5 = -\frac{[\ln(F_5/F_{12})]/[\pi C] - d_{5-12}}{2d_{5-12}}$ , in which  $R_5$  is the distance between the plane of the fluorophor and the 5-position spin-label in units of Å,  $F_{12}$  is fluorescence intensity in the presence of the 12 carbon spin-labeled PC,  $F_5$  is fluorescence intensity in the presence of the 5 carbon spin-labeled PC,  $C$  is the 2-dimensional concentration of the spin-labels in units of molecules/Å<sup>2</sup>, and  $d_{5-12}$  is the distance between the plane of the 5-position spin-label and 12-position spin-label. It can be shown that by combining two experiments in this way the effect of restrictions on the minimum allowed lateral approach of fluorophor and acceptor is cancelled out. Furthermore, the method can be extended to analyze quenching by brominated phospholipids and energy transfer acceptors. Application of this method to determination of the location of fluorescence groups on anthracene labeled fatty acids, dansyl and NBD labeled phosphatidylethanolamines, NBD labeled cholesterol, and gramicidin, will be shown. Supported by N.I.H. grant GM 31986.

**T-Pos178** FLUORESCENT LIFETIME MEASUREMENTS OF THE STEROL PROBE DEHYDROERGOSTEROL  
Greg Smutzer and Philip L. Yeagle, Dept. of Biochemistry, School of Medicine, State University of New York at Buffalo, Buffalo, New York 14214

The fluorescent sterol probe dehydroergosterol has been used to detect sterol-rich regions in lipid bilayers. The fluorescent lifetime of this probe was measured by a mode-locked argon-ion laser capable of sustaining repetitive pulses of approximately 150 psec; all measurements were carried out at the Regional Laser and Biotechnology Laboratories of the University of Pennsylvania. The fluorescent lifetime of dehydroergosterol in organic solvents was a monoexponential decay of approximately 200 psec. When probe levels of dehydroergosterol were incorporated into L- $\alpha$ -dimyristoylphosphatidylcholine (DMPC) multilamellar vesicles that contained no cholesterol, two major lifetimes were observed. In the gel state of DMPC, one lifetime of 1.15 nsec as well as a second lifetime of about 0.1 nsec was observed. The 1.15 nsec component underwent a decrease in lifetime to 0.85 nsec above the  $T_m$  of DMPC. The midpoint of the decrease in lifetime was 23.8 $^{\circ}$  C and occurred over a 2 $^{\circ}$  C span. Both major lifetime components underwent a change in relative amplitude at the  $T_m$  of DMPC. DMPC vesicles that contained 5 mol% cholesterol also possessed two major lifetimes; one component was approximately 0.9 nsec and the second component was near 0.15 nsec. Neither component underwent a change in lifetime or relative amplitude at the  $T_m$  of DMPC. These results are further evidence that dehydroergosterol probes sterol-rich regions in membranes. (Supported by NIH grants HL 23853 and HL 07010).

**T-Pos179** FLUOROMETRIC DETECTION OF BILAYER TO HEXAGONAL PHASE TRANSITIONS IN LIPOSOMES  
Patricia A. Baldwin, Keelung Hong and Demetrios Papahadjopoulos, Cancer Research Institute and Department of Pharmacology, University of California, San Francisco, CA, 94143.

The lipid bilayer to hexagonal phase transition has been detected by several techniques. However, no established technique allows for determination of the transition temperature ( $T_H$ ) in dilute membrane suspensions or analysis of the kinetics of the transition. Recently, we have developed a fluorometric method for detection of  $T_H$  using the fluorescent probes N-(7-nitro-2,1,3-benzoxadiazol-4-yl) phosphatidylethanolamine (NBD-PE) or N-(5-dimethylaminonaphthalene-1-sulfonyl) phosphatidylethanolamine (dansyl-PE).  $T_H$  was detected in PE liposomes (containing 1% of either NBD-PE or dansyl-PE) which had been aggregated by  $Ca^{2+}$  or protons, using front face fluorescence with a short path length cuvette (0.1mm). In general, the fluorescence intensity decreased as a function of increasing temperature except at  $T_H$ , where an increase in fluorescence was observed. For dilute liposome suspensions, the time course of the fluorescence change was monitored at a series of temperatures after injection of a hexagonal phase inducing agent (e.g.  $Ca^{2+}$  or  $H^+$ ). Plots of the maximum fluorescence intensity after injection vs. temperature were similar to those of the preaggregated samples. The bilayer to hexagonal phase transitions detected using this assay on dioleoyl PE and PE from several natural sources (egg, *E. coli*, and transesterified from egg phosphatidylcholine) correlated well with transitions obtained by differential scanning calorimetry (DSC). Using liposomes of dansyl-PE-labeled dioleoylmonomethyl PE (100  $\mu$ M) we detected  $T_H$  at approximately 63 $^{\circ}$ C, close to what has been observed by DSC. In addition, a break in the downward slope of the fluorescence intensity vs. temperature curve was observed at the temperature corresponding to the isotropic NMR signal seen for this lipid (40 $^{\circ}$ C). Dansyl-PE-labeled liposomes also exhibited an increase in polarization and a shift of the fluorescence emission maximum to shorter wavelength (~6 nm) at the transition from bilayer to hexagonal phase. These changes suggest that there is a decrease in the polarity of the environment or a decrease in the motion of the dansyl group (or both) during the transition from bilayer to hexagonal phase. ACS PF-2331

**T-Pos180** PACKING ASYMMETRY IN CURVED MEMBRANES DETECTED BY FLUORESCENCE SPECTROSCOPY

John Bramhall. Microbiology & Immunology Dept., UCLA School of Medicine, Los Angeles, CA 90024.

There are distinct differences in the molecular packing of phospholipid molecules in the inner and outer membrane monolayers of small lipid vesicles; a small radius of curvature results in an asymmetry in the interface between these two monolayers. We have used an amphiphilic fluorescent probe, N,5-dimethylaminonaphthalene-1-sulfonylglycine (dansyl glycine) to determine if these asymmetries in molecular packing can create different environments for fluorescent probes resident in the membrane. Dansyl glycine is highly sensitive to the dielectric constant of its environment and the fluorescence signal from membrane-bound dye is distinct from that in the aqueous medium. When dansyl glycine is first mixed with vesicles it rapidly partitions into the outer monolayer; the subsequent movement of dye into the inner monolayer is much slower. Because of the time lag between the initial partitioning and the subsequent translocation it is possible to measure the emission spectrum from membrane bound dye before and after translocation, thus distinguishing the two potential environments for dansyl glycine molecules. In the outer membrane monolayer of small dipalmitoylphosphatidylcholine vesicles dye fluorescence emission is maximal at 529 nm, corresponding to a dielectric constant of 7 for the medium surrounding the fluorophore. For dye in the inner monolayer emission is maximal at 519 nm, corresponding to a dielectric constant of 4.7. The results suggest that water molecules are excluded more efficiently from the dye binding sites of the inner membrane monolayer than they are from those of the outer monolayer.

**T-Pos181** INTERACTION MECHANISM AND LOCALIZATION OF POTENTIAL SENSITIVE CYANINE DYE BINDING TO BRUSH BORDER MEMBRANES. G. Cabrini and A.S. Verkman, Cardiovascular Research Institute, University of California, San Francisco, CA 94143

Binding of the potential sensitive probe diS-C<sub>3</sub>-(5) (3,3'-dipropylthiodicarbocyanine iodide) to rabbit renal brush border membrane vesicles (BBMV) was examined by phase-modulation and stopped-flow fluorescence, and by quenching of n-(9-anthroyloxy) stearic acid (n-AS) probes. At 622 nm excitation, aqueous diS-C<sub>3</sub>-(5) (D<sub>a</sub>) has a 670 nm emission peak which shifts to 695 nm for membrane-bound monomeric dye (M); bound dimer (D) is non-fluorescent. Rapid mixture of BBMV with diS-C<sub>3</sub>-(5) gives a 6 ms increase in F<sub>695</sub> at high BBMV/Dye, 30-40 ms decrease in F<sub>670</sub> at low BBMV/Dye and 1-1.3 s increase/decrease in F<sub>695</sub>/F<sub>670</sub>, suggesting a 6 ms binding followed by 30-40 ms reorientation/dimerization and 1-1.3 s translocation across the bilayer. Compared to D<sub>a</sub>, M has higher anisotropy ( $r=0.102$ ) and lifetime ( $\tau=2.1$  ns), and hindered rotation ( $R=0.54$  ns<sup>-1</sup>,  $r_{\infty}=0.11$ ). Based on Stern-Volmer and lifetime analyses, M and D quench the fluorescence of the n-AS probes by a collisional mechanism. At low Dye/BBMV ( $[M] \gg [D]$ ), the quenching efficiencies (Q) for the n-AS probes are similar ( $n=2,6,12,16$ ); at high Dye/BBMV ( $[D] \gg [M]$ ), Q increases with n ( $16 \gg 12 \gg 6 \gg 2$ ), suggesting that M is oriented perpendicular, and D parallel to the membrane surface. Stopped-flow mixture of diS-C<sub>3</sub>-(5) with BBMV containing n-AS showed a biexponential fluorescence decrease (Ex 390 nm, Em >450 nm) with time constants 30-40 ms and 1-1.5 s. These findings suggest that diS-C<sub>3</sub>-(5) adheres to the outer membrane surface in 6 ms, binds parallel to the membrane phospholipid in 30-40 ms, dimerizes and rotates 90° in <<30 ms, and translocates to the opposite half of the bilayer in 1-1.3 s. Similar studies performed in BBMV with induced membrane potentials suggest that the translocation step is the potential sensitive reaction.

**T-Pos182** LIFETIME AND DIFFERENTIAL POLARIZATION STUDIES OF BRUSH BORDER MEMBRANE FLUIDITY USING n-(9-ANTHROYLOXY) FATTY ACID PROBES. H.Y. Lin, H.E. Ives and A.S. Verkman. Cardiovascular Research Institute, University of California, San Francisco, CA 94143

Although the application of fluorescence techniques to examine thermotropic phase transitions in pure phospholipid bilayers is well established, it is unclear whether these methods can be applied to cholesterol-containing biological membranes. In a purified biological membrane system, the rabbit renal brush border vesicle (BBV), activation energies for transport of three unrelated compounds (water, diS-C<sub>3</sub>-(5) and urea) sharply increase 3-10 fold at T=31-33°C, suggesting a membrane phase transition at that temperature. We measured steady-state polarization spectra ( $r(\lambda)$ ), lifetimes ( $\tau$ , 18 and 30 MHz) and differential tangents ( $\tan \Delta$ ) for diphenylhexatriene (DPH) and the n-(9-anthroyloxy) probes 2,6 and 12-AS and 16-AP in BBV over the temperature range 5-55°C. Probe rotational rate (R) and limiting anisotropy ( $r_{\infty}$ ) were calculated from  $r$ ,  $\tan \Delta$  and  $\tau$ . In control experiments using dimyristoylphosphatidylcholine vesicles, there were sharp decreases in  $r$  and  $r_{\infty}$  at the known phase transition temperature (24°C); in ethanol and in phosphatidylcholine vesicles, changes in  $r$  and  $r_{\infty}$  were gradual. In BBV, the AS probes underwent excited state reactions whereas DPH and 16-AP did not. Lifetimes were homogeneous for DPH and heterogeneous for the AS probes without sharp changes with T. With increasing T,  $r$  decreased for all probes; changes in the  $r(\lambda)$  shape for the AS probes were gradual. Surprisingly, changes in  $r$  paralleled changes in  $r_{\infty}$  and not in R. At every T,  $r$  and  $r_{\infty}$  decreased with increasing n, suggesting that membrane fluidity increases toward the center of the bilayer. Based on these measurements we question whether biologically important thermotropic transitions can be detected with the present fluorescence methodology.

**T-Pos183** THE INFLUENCE OF CHOLESTEROL ON THE EQUILIBRIUM AND DYNAMIC STRUCTURAL PROPERTIES OF UNSATURATED LIPID BILAYERS. Martin Straume and Burton J. Litman, (Intr. by Jay Fox) Department of Biochemistry, University of Virginia School of Medicine, Charlottesville, VA 22903.

Phase-modulation fluorometric characterization of DPH and TMA-DPH labelled phosphatidylcholine (PC) bilayers was performed on Egg PC, POPC (16:0, 18:1-PC), DOPC (di-18:1-PC), PAPC (16:0, 20:4-PC), and P-22:6-PC (16:0, 22:6-PC) systems. Cholesterol was incorporated into large, unilamellar, octyl glucoside dialysis vesicles at approximately 0, 15, and 30 mol % concentrations. Lifetime analysis was performed by applying a constrained, biexponential decay model. Predominantly long lifetime populations were present for both DPH and TMA-DPH labelled membranes, regardless of the cholesterol content or sample temperature from 5 to 37°C. Cholesterol did, however, cause increases in the intensity-weighted mean fluorescence lifetimes, particularly for TMA-DPH labelled systems. DPH equilibrium distributions were derived according to an orthogonal, bimodal, Gaussian orientational model. TMA-DPH distributions were constrained to a unimodal, Gaussian function. Cholesterol caused increases in lipid molecular ordering and substantial acceleration of probe depolarizing motions. DPH equilibrium distributions also showed significant alterations in the relative populations of the two orthogonal distribution peaks in response to incorporation of cholesterol. Supported by NSF grant PCM-8316858.

**T-Pos184** LATERAL DIFFUSION IN AN ARCHIPELAGO: THE EFFECT OF MOBILE OBSTACLES. Michael J. Saxton (Intr. by John C. Owicki), Plant Growth Laboratory, Department of Agronomy & Range Science, University of California, Davis, California 95616; and Laboratory of Chemical Biodynamics, Lawrence Berkeley Laboratory, Berkeley, California 94720.

Lateral diffusion of mobile species in membranes is hindered by the presence of immobile species. If the obstacles are stationary, their effect may be described by percolation theory, which predicts that the diffusion constant is zero when the area fraction of obstacles is greater than the percolation threshold ( $\sim 0.67$  for a continuum;  $0.41$  for a square lattice). If the obstacles are mobile, the diffusion constant of the tracer particles depends on the area fraction of obstacles and the relative jump rates of tracers and obstacles. Diffusion may occur even above the percolation threshold, at a rate limited by the diffusion rate of obstacles. Monte Carlo calculations of diffusion on a square lattice are presented. Byproducts of the calculations are the tracer diffusion constant and the diffusion constant in the percolation limit. (Supported by DOE Contract AT03-80ER10700)

**T-Pos185** MOTION AND SURFACE ACCESSIBILITY OF SPIN LABELED LIPIDS IN MODEL LIPOPROTEINS OF CHOLESTERYL OLEATE (CO) AND DIMYRISTOYLPHOSPHATIDYLCHOLINE (DMPC). Martha P. Mims and Joel D. Morrisett, Depts. of Medicine & Biochemistry, Baylor College of Medicine, Houston, Tx. 77030.

EPR was used to measure the order parameters and ascorbate reduction rates of a series of doxyl-labeled lipids incorporated into DMPC vesicles and  $\sim 700$  Å CO/DMPC microemulsion particles (MP). Although 5- and 12-doxyl labeled phospholipids (PC) and cholesteryl esters (CE) detected a thermal transition in DMPC vesicles, no transitions were detectable in MP either for the polar surface monolayer or the nonpolar core. Both 5- and 12-doxyl derivatives demonstrated that the surface monolayer was less ordered than the core at  $10-55^\circ$ . Pseudo-first order reduction rates were measured at a series of ascorbate concentrations on vesicles and MP containing 5-doxyl PC or CE. Reduction of PC in vesicles was biphasic, with an outer leaflet reduction rate constant  $\sim 1.88 \times 10^{-1} \text{ sec}^{-1}$  at both  $24$  and  $35^\circ$ . Reduction of CE in vesicles was monophasic with a rate constant of  $4-5 \times 10^{-2} \text{ sec}^{-1}$  assuming CE was equally soluble in, and moved rapidly between both halves of the bilayer. Reduction of 5-doxyl PC and CE in MP was also monophasic; rates were linearly dependent on [ascorbate] and corresponded to a reduction rate constant of  $4-6 \times 10^{-2} \text{ sec}^{-1}$  for PC. For CE, the rate constants were  $3$  to  $4 \times 10^{-3} \text{ sec}^{-1}$  at  $24$  to  $55^\circ$ . The monophasic nature of this reaction indicated that equilibration of CE between core and surface was more rapid than ascorbate reduction. Using reduction of 5-doxyl CE in vesicles as a model for reduction in MP, these rates corresponded to CE partition ratios of  $\sim 11:1$  (core:surface). These data suggest that PC are more restricted in the surface monolayer of the MP than in the vesicle and that CE is more soluble in the monolayer than in the bilayer. Supported by HL27341 and Welch Foundation.

**T-Pos186** ANALYSIS OF NEAREST NEIGHBOR PHOSPHATIDYLETHANOLAMINES BY DIMETHYLSUBERIMIDATE CROSSLINKING. Ruth Welti and Fred L. Smardo, Jr., Div. of Biology, Kansas State University, Manhattan, KS 66506 and Dept. of Biochemistry, Kansas University Medical Center, Kansas City, KS 66103

Binary mixtures of dipalmitoylphosphatidylethanolamine, dioleoylphosphatidylethanolamine, and dipalmitoleoylphosphatidylethanolamine in multilamellar vesicles were reacted with dimethylsuberimide at various reagent concentrations, temperatures, and pHs. The resulting phosphatidylethanolamine dimers were separated by reverse phase high pressure liquid chromatography and quantitated. Higher levels of crosslinking were observed as the pH was increased from  $7$  to  $10$ . In mixtures of dipalmitoylphosphatidylethanolamine and either unsaturated phosphatidylethanolamine, the amount of heterogeneous dimer increased with increasing temperature between  $0^\circ\text{C}$  and  $50^\circ\text{C}$ , indicating that there was more mixing of the molecular species as the amount of fluid phase increased. In each case, the patterns of nearest neighbor species determined by crosslinking are correlated with the phase properties of the mixtures.

**T-Pos187** DIFFUSION IN ERYTHROCYTE MEMBRANE TETHERS. David A. Berk and Robert M. Hochmuth.

Department of Biomedical Engineering, Duke University, Durham, NC 27706. Intr. by P.L. LaCelle.

Plastic deformation of erythrocyte membrane is induced by drawing a thin cylindrical strand of membrane material (a so-called "tether") from the cell. This process is characterized by a yield stress at which plastic flow begins and a viscosity which is a measure of the resistance to the rate of deformation (Evans and Hochmuth, *Biophys. J.* 16:13, 1976). Nevertheless, it is unclear what structural alterations occur during this process and what these deformation and flow parameters signify at the molecular level. To elucidate this matter, a method has been devised to characterize the structural integrity of the membrane material in terms of a measured lateral diffusion rate in the membrane of a tether. In normal erythrocyte membrane, the lateral diffusion of transmembrane proteins is severely hindered by the spectrin cytoskeleton (Koppel et al., *Proc. Natl. Acad. Sci. USA*, 78:3576, 1981). The extent to which the measured diffusion coefficient departs from this retarded value and approaches a maximum value is a measure of cytoskeletal disruption.

Tethers are extracted from red cells in a flow channel with the method of Hochmuth et al. (*Biophys. J.* 13:747, 1973). The tether and adjacent cell body are tagged *in situ* with FITC-labeled Wheat Germ Agglutinin (Sigma) at 2 to 20  $\mu\text{g/ml}$ . A fluorescence photobleaching method is used to determine the rate of diffusion on the membrane of the tether and adjacent cell body. The geometry of the tether facilitates bleaching of a small region and analysis of the fluorescence redistribution process using a one-dimensional model for diffusion. Preliminary results reveal an enhanced diffusion rate in the tether, suggesting that the plastically deformed material has either a disrupted or spectrin-deficient cytoskeleton. (Supported by NHLBI Grant HL 23728)

**T-Pos188** FLUIDITY CHANGES IN HEP-2 CELL MEMBRANES DURING VESICULAR STOMATITIS VIRUS (VSV) PENETRATION. Peter L. Gutierrez and Raveendran Pottathil. University of Maryland Cancer Center, University of Maryland Medical School and Division of Pediatrics, City of Hope Medical Center, Duarte, CA.

Transmembrane penetration of viruses is initiated by the high-affinity binding of virus surface proteins to specific cell surface receptors. The subsequent temperature-dependent uptake of virus particles is a process very similar to receptor-mediated endocytosis. We investigated changes in membrane fluidity in connection with synchronous penetration of Vesicular Stomatitis Virus (VSV) in a laryngeal carcinoma cell line (HEP-2) by Electron Spin Resonance (ESR) spectroscopy. HEP-2 cells were labeled with spin-labeled stearic acid analogs containing a nitroxyl free radical group positioned at the polar I (12,3), middle I (5,10) or hydrophobic I (2,14) region of the fatty acyl chains. Additional HEP-2 cell fluidity studies were made with spin-labeled cholesterol and with membrane-partitioning spin labels, TEMPO, TEMPOL, and TEMPONE. Synchronous entry of VSV into HEP-2 cells resulted in membrane rigidity as measured by ESR parameters of I (12,3) and I (5,10). There was no alteration in membrane fluidity during VSV penetration when cells were labeled with stearic acid analog I (2,14), spin labeled cholesterol or TEMPO, TEMPOL, or TEMPONE. The observed increase in membrane rigidity correlated with transmembrane penetration of  $^{125}\text{I}$ -labeled VSV. VSV infection of HEP-2 cells was also associated with temperature- and time-dependent modifications in fatty acyl chains of phospholipids as determined by the polarity of incorporated radioactive fatty acids in reverse-phase TLC. These data show specific and localized modifications in HEP-2 cell membrane fluidity and composition in connection with receptor-mediated internalization of VSV. The rigidity was more pronounced when the labels were located near the mid-region of fatty acyl chains of phospholipids.

**T-Pos189** KINETICS OF GANGLIOSIDE TRANSFER BETWEEN MEMBRANES. M. Masserini and E. Freire.

Department of Biochemistry, University of Tennessee, Knoxville, TN 37996

The transfer of ganglioside  $\text{GM}_1$  from micelles to membranes and between different membrane populations has been examined using a pyrene fatty acid derivative of the ganglioside. The transfer of gangliosides from micelles to membranes depends on the physical state as well as the molecular composition of the acceptor vesicles. At  $30^\circ\text{C}$ , the transfer of micellar gangliosides to DPPC large unilamellar vesicles ( $T_m = 41.3^\circ\text{C}$ ) is characterized by a rate constant of  $0.01 \text{ min}^{-1}$ ; at  $48^\circ\text{C}$ , however, the rate constant is  $0.11 \text{ min}^{-1}$ . Below the phase transition temperature, the activation energy is 25 kcal/mol whereas above the phase transition, it is 17 kcal/mole. Similar experiments performed with synaptic plasma membranes yielded a rate constant of  $0.05 \text{ min}^{-1}$  at  $37^\circ\text{C}$ . The rate of transfer of ganglioside molecules, asymmetrically located on the outer layer of donor vesicles, to acceptor vesicles lacking ganglioside, depends on the physical state of both the donor and acceptor vesicles. For the transfer of ganglioside from DPPC (donor) vesicles to DMPC (acceptor) vesicles, the rates were essentially zero at  $15^\circ\text{C}$  in which both vesicles populations were in the gel phase,  $0.008 \text{ min}^{-1}$  at  $30^\circ\text{C}$  in which DPPC is in the gel phase and DMPC in the fluid phase, and  $0.031 \text{ min}^{-1}$  at  $48^\circ\text{C}$  in which both vesicle populations are in the fluid phase. The transfer of ganglioside from DPPC vesicles to synaptic plasma membranes was also dependent on the physical state of the donor vesicles and showed an inflection point at the phase transition temperature of DPPC. Finally, in the fluid phase, the addition of excess  $\text{Ca}^{2+}$  (20mM) reduced the rate constant of ganglioside transfer by only 10%. (Supported by NIH grant NS-20636.)

**T-Pos190** EFFECT OF INCREASING FATTY ACYL POLYUNSATURATION ON MEMBRANE LIPID PHYSICAL PROPERTIES. C.D. Stubbs, C.L. Pryor, Y. Nie, T. Taraschi, J. Ellingson and R. Mendelsohn<sup>+</sup>  
Department of Pathology, Hahnemann University, Philadelphia PA 19102, and <sup>+</sup>Department of Chemistry, Rutgers University, Newark NJ 07102

Model membranes and biological membranes with varying levels of *cis*-unsaturation were investigated using 1-palmitoyl, 2-oleoyl (18:1)/linoleoyl/arachidonyl/ or docosahexaenoyl (22:6)-phosphatidylcholines (PC) and dietary supplementation, respectively. From fluorescence polarization measurements using 3, 9, or 12-anthroyl stearates and diphenylhexatriene as membrane fluorophor probes, an increased disordering effect on bilayer structure was shown to correlate with the increase in *cis*-unsaturation. The 22:6-PC, the most unsaturated lipid examined, was found to be in the bilayer configuration over the physiological range using <sup>31</sup>P-NMR. Using Raman spectroscopy the 22:6-PC was found to have a gel-liquid crystalline phase transition at -3°C -- little different from the mono-unsaturated 18:1-PC, which means that the 18:1 and 22:6/PC can be compared at the same absolute temperature and the fluorescence polarization measurements indicate a large difference in lipid order. Thus, the experiments indicate that in natural membranes substantial fatty acid supplementation resulting in elevated levels of the degree of *cis*-unsaturation would result in decreased lipid order. Fish and olive oil dietary supplementation studies using the rat liver microsome as a model showed that, at least as far as bulk overall membrane lipid order is concerned, the effects of supplementation are minimized by a comprehensive reorganization of the membrane fatty acid profile compensating for the elevated level of polyunsaturation.

**T-Pos191** VOLTAMMETRY STUDY OF ELECTRON-CONDUCTING BILAYER LIPID MEMBRANES. Pawel Kryszinski and H. Ti Tien, Membrane Biophysics Lab, Physiology Department, Michigan State University, East Lansing, MI 48824

The electrochemical behavior of electron-conducting lipid membrane (BLM) was tested. BLMs were made electron-conducting by modifying them with so called "organic metal" TCNQ (N,N,N',N' tetracyano-p-quinodimethane) or iodine. It is well known that the BLMs upon suitable modification can serve as a unique model for biological membranes. Since the electron transfer and redox reactions play a key role in energetics of living cells and in a number of systems (e.g., such as the thylakoid or cristae membrane), an attempt has been made at mimicking their functions by electron conducting BLMs. These doped BLMs have been investigated by a voltammetric technique which has shown that suitably modified BLMs can act as electronic conductors, partaking a number of redox reactions at membrane/solution interfaces. Two kinds of experiments with modified BLM were carried out. In the first series of experiments, TCNQ or iodine containing BLMs were investigated in the presence of a variety of redox couples, some of them biologically important. The second set of experiments consisted of the iodine-containing BLM being used as a tool for the voltammetric studies of electron transfer mechanisms of different donor type substances, including some neurotransmitters. From the resulting voltammograms, information about thermodynamic and kinetic parameters of electron translocation, as well as redox reactions may be gained, thereby providing insights into the mechanisms of electron transfer in the system under investigation. These type of studies are also the preliminary step before investigations of BLMs with reconstituted redox proteins from energy transducing natural membrane systems. [Supp. by NIHGM14971]

**T-Pos192** PHASE TRANSITIONS IN LIPID-WATER SYSTEMS USING HIGH RESOLUTION X-RAY DIFFRACTION. P.J. Quinn, Department of Biochemistry, King's College London, London W8 7AH, U.K., and L.J. Lis, Department of Physics and Liquid Crystal Institute, Kent State University, Kent, Ohio 44242.

High intensity X-rays (2 GeV, 100 mA) from the synchrotron source at Daresbury, U.K., were used to study the phase transitions in monogalactoryldiacylglycerol-water systems. Temperature jumps were provided using water baths, and the diffraction patterns were monitored continuously using a linear detector with a frame time of 100 ms. Changes in the low and high angle X-ray diffraction intensities were observed in aqueous dispersions of an equi-molar mixture of native (polyunsaturated) and fully-saturated galactolipid as the lamellar to hexagonal phase transition was induced. Within the temporal resolution of our experiment, we were able to observe a phase separation of lamellar and hexagonal phases and its transformation into a homogenous phase at high temperature. It was apparent that the phase behavior of this mixed lipid system is highly complex during the phase transition with fluctuations particularly in the structural configurations of the hydrocarbon chains with changes taking place with lifetimes in the order of several hundred milliseconds. We will compare our results to the current theories being developed to understand the temperature-induced lamellar to hexagonal phase transition in lipid-water systems.

**T-Pos193** A COMPARATIVE STUDY OF THE GEL AND LIQUID CRYSTALLINE PHASES OF METHYL SUBSTITUTED DIETHER LIPID BILAYERS BY RAMAN SPECTROSCOPY. E. Neil Lewis<sup>a</sup>, Robert Bittman<sup>b</sup> and Ira W. Levin<sup>a</sup>, <sup>a</sup> Laboratory of Chemical Physics, NIADDK, National Institutes of Health, Bethesda, MD 20892 and <sup>b</sup> Dept. of Chemistry, Queens College of the City University of New York, Flushing, N.Y. 11367.

Alterations in the inter- and intramolecular packing characteristics of aqueous dispersions of methyl derivatives of the ether lipid 1,2-di-O-hexadecyl-sn-3-glycero-3-phosphocholine (DHPC) in which the methyl group is substituted on either the 1,2 or 3 position of the glycerol backbone were sensitively monitored by changes in the vibrational frequency and intensity of selected spectral features by Raman spectroscopy. Temperature profiles constructed from spectra reflecting intermolecular order/disorder processes (C-H stretching mode region) and from those reflecting intramolecular order/disorder processes (C-C stretching mode region) provide insight into several important structural properties of diether lipid bilayers. The introduction of a methyl group in any position on the glycerol backbone eliminated the pretransition which is clearly observable for pure DHPC. Values obtained for  $T_m$  range from 43.1°C in the pure diether lipid to 41.8°C for 3 Me-DHPC, 40.1°C for 2 Me-DHPC and 38.1°C for 1 Me-DHPC, whereas the degree of disordering observed for both the gel and liquid crystalline states was measured as 2 Me-DHPC < 3 Me-DHPC < DHPC < 1 Me-DHPC. The results are discussed in terms of steric effects and torsional energy barriers associated with the packing and melting behaviour of the various structural forms of the phospholipids.

**T-Pos194** CHAIN INTERDIGITATION IN PHOSPHOLIPID BILAYER PHASES. J.P.Sheridan, Biomolecular Engineering Branch, Code 6190, Naval Research Laboratory, Washington, D.C. 20375

Two principle types of hydrocarbon chain interdigitation in gel phase lipid bilayers have now been identified: Type I, primarily manifested by lipids possessing asymmetric chains, involves interpenetration of the longer chain across the bilayer mid-plane to pack end-to-end with the shorter chain of another lipid molecule in the opposing monolayer leaflet; Type II involves full interdigitation in which the acyl chains span the entire hydrocarbon width of the bilayer. Examples of Type I are the  $L_c$  phases of asymmetric phosphatidylcholines such as 1-palmitoyl-2-myristoyl PC and the gel phases of N-stearoyl sphingomyelin\* and N-lignoceryl sphingomyelin\* (N-C24 SPM). Examples of Type II include the  $L_\beta$  gel phase of 1,3 DPPC, and 1,2 DPPC dispersed in glycerol. We have used Raman spectroscopy to investigate the structural details of these interdigitated phases. Careful analysis of the skeletal optical, methyl deformation, and C-H stretching regions reveal subtle but distinct structural differences between Type I and Type II interdigitation. In most cases, the chain interdigitation exists in only one gel phase and disappears in the next highest temperature gel or fluid phase. However, one particularly interesting case is that of the highly asymmetric N-C24 SPM. We will present spectroscopic evidence that chain interdigitation exists in both of its gel phases and that this interdigitation persists into the fluid phase.

\* The sphingomyelin samples were kindly supplied by Prof.Y.Barenholz of the Hebrew University, Jerusalem and Prof.D.Shapiro, Weizman Institute of Science, Rehovot, Israel.

**T-Pos195** DILATOMETRIC MEASUREMENTS OF ISOBRANCHED LIPIDS.

C. P. Yang\*, M. C. Wiener\*, R. N. A. H. Lewis#, R. N. McElhaney#, and J. F. Nagle\*. \*Department of Physics, Carnegie-Mellon University, Pittsburgh, PA 15213 and #Department of Biochemistry, University of Alberta, Edmonton, Canada T6G2H7.

Differential scanning dilatometry studies have been performed on aqueous dispersions of phosphatidylcholines. The hysteresis, between heating and cooling scans as a function of scanning rate, of the gel to liquid crystalline transition is measured and is found to be dependent upon whether the chain length is even or odd. The kinetics of formation of the lower temperature gel phase of these lipids is measured. We have critically tested the hypothesis suggested by McElhaney and Lewis concerning the transition mechanism of the shorter chain isobranched lipids which have only one transition from the lower gel phase to the chain melted phase accompanied by considerable hysteresis. The phase behavior of the entire sequence of lipids is summarized in terms of Gibbs free energy diagrams, with chain length as an extra parameter. The measured volume change during a transition is used to estimate changes in Van der Waals energies due to the phase transitions. Together with transition enthalpy measurements this provides estimates of the amount of trans-gauche disordering.

**T-Pos196** THERMOTROPIC AND STRUCTURAL STUDIES OF 1-EICOSYL-2-DODECYL-SN-GLYCERO-3-PHOSPHOCHOLINE (EDPC) AND 1-DODECYL-2-EICOSYL-SN-GLYCERO-3-PHOSPHOCHOLINE (DEPC). J. Mattai, N.M. Witzke<sup>+</sup>, R. Bittman and G.G. Shipley. Biophysics Institute, Boston University School of Medicine, Boston, MA 02118 and Queens College, CUNY, NY 11367.

The ether phospholipids, EDPC and DEPC, have been investigated by differential scanning calorimetry (DSC) and x-ray diffraction. DSC of hydrated EDPC shows an endothermic transition at 34.8°C ( $\Delta H=11.2$  Kcal/mol) after storage at -4°C while DEPC shows three endotherms at ~7.7°C and ~9°C (combined  $\Delta H \approx 0.4$  Kcal/mol) and 25.2°C ( $\Delta H=4.7$  Kcal/mol). Both the single transition of EDPC and the two higher temperature transitions of DEPC are reversible, while the ~7.7°C transition increases in enthalpy on low temperature incubation. At 23°C, x-ray diffraction of hydrated EDPC shows a sharp reflection at 4.2Å together with lamellar reflections,  $d=56.2$ Å. An electron density profile shows a P-P distance of 33Å indicating an interdigitated, three chains per head group, gel phase,  $L_{\beta}^*$  with no hydrocarbon chain tilt, analogous to hydrated 18/10 ester PC (T.J. McIntosh et al., (1984) Biochemistry 23, 4038). In contrast, DEPC at -4°C shows an  $L_{\beta}^*$  gel phase with tilted hydrocarbon chains ( $d \approx 61.1$ Å). This transforms at 14°C to a  $L_{\beta}^*$  phase with  $d=56.6$ Å and a P-P distance of 36Å. Above  $T_m$  both EDPC and DEPC exhibit liquid crystalline L phases with  $d=69.0$ Å and 65.6Å, respectively. The ability of both EDPC and DEPC to form triple chain interdigitated bilayers suggests that the conformational inequivalence at the sn-1 and sn-2 positions is less pronounced in the ether PCs compared to the ester PCs, where only one of the positional isomers, e.g. 18/10 PC but not 10/18 PC, forms the triple chain structure (J. Mattai, unpublished results). Thus, a different conformation around the glycerol is predicted for ether PC compared to ester PC.

**T-Pos197** MECHANISM OF SUBGEL PHASE FORMATION OF DPPC: A HIGH-PRESSURE RAMAN SPECTROSCOPIC STUDY.

P.T.T. Wong, E. Mushayakarara and H.H. Mantsch

Division of Chemistry, National Research Council of Canada,  
Ottawa, Ontario, Canada, K1A 0R6

Raman spectra of aqueous dispersions of DPPC were recorded as a function of pressure (up to 46 kbar) for samples incubated at 2°C and for non-incubated DPPC samples subjected to equally high pressure. The nature of the transition from the GII gel phase of the hydrated lipid into the subgel phase on incubation is entirely different from that of the transition from the GII gel phase into the GIII gel phase of the non-incubated lipid. The GIII gel phase has a monoclinic interchain packing, while the subgel phase exhibits a triclinic interchain structure. It is shown that pressure can not induce the transition from the GII gel phase to the subgel phase, however, it does stabilize the subgel phase above the subtransition temperature. The mechanism for the formation of the subgel phase and the complex phase behavior of the gel phase of DPPC are rationalized in terms of the dynamic properties of the acyl chains of the lipid molecule.

**T-Pos198** THE PHASE BEHAVIOUR OF 1,2-DIACYL-3-MONOGALACTOSYL-*sn*-GLYCEROL DERIVATIVES. D.A. Mannoek, Dept. of Biochemistry, University of Alberta, Edmonton, Canada T6G 2H7; A.P.R. Brain and W.P. Williams, Biophysics Department and E.M. Unit, Chelsea College, London SW3 6LX, U.K.

Monogalactosyldiacyl glycerols (MGDG) are the major polar lipid components found in the thylakoid membranes of both higher plant chloroplasts and blue-green algae. In a previous report, we described differential scanning calorimetry (DSC), wide-angle X-ray diffraction and freeze-fracture electron microscopy studies investigating the thermotropic phase behaviour of a 1,2-distearoyl MGDG derivative, which had been prepared by catalytic hydrogenation of the 1,2-dilinolenoyl derivative isolated from broad bean leaf tissue. Aqueous dispersions of this lipid were shown to exhibit complex polymorphic behaviour involving the formation of stable and metastable structural forms, whose relative proportions were dependent on the thermal history of the sample. Two distinct gel phases could be identified; a stable highly ordered form (MGDG<sub>I</sub>), which appeared only after prolonged equilibration at 290 K or after annealing the samples at higher temperatures, and a metastable form (MGDG<sub>II</sub>) which appeared on initial cooling from the liquid-crystalline state. In order to ascertain whether this pattern of phase behaviour is characteristic of MGDG derivatives in general, we have extended this investigation to include a monounsaturated form, 1-palmitoleoyl, 2-palmitoyl MGDG, isolated from the blue-green alga *Anacystis nidulans*, and its catalytically hydrogenated derivative, 1,2-dipalmitoyl MGDG. The results obtained from samples of both lipids show a pattern of phase behaviour very similar to that described for the distearoyl derivative and add further support to the earlier suggestion that the MGDG<sub>I</sub> phase is stabilized by the existence of strong interactions, probably as a result of hydrogen bond formation between neighbouring headgroups.

**T-Pos199** STRUCTURAL TRANSFORMATION IN DMPG DISPERSIONS CORRESPONDS TO SURFACE BILAYER FORMATION. N. Gershfeld and R. Nossal. National Institutes of Health, Bethesda, MD 20892

A structural transformation in bulk dimyristoylphosphatidylglycerol (DMPG)-water systems is found to occur at the temperature where "surface bilayers" (1-3) are detected by film balance techniques. The transformation temperature  $T^*$  is higher than the "gel-liquid crystal" temperature for these systems and, within experimental error, is the value predicted by thermodynamic arguments concerning correspondences between bulk and surface states (2). Several techniques, including dynamic light scattering, have been employed in these studies. The movement of suspended polystyrene beads, in particular, has been used to probe the structure of the solution. We find that below  $T^*$  the beads are inhibited from moving (the relaxation time of optical fluctuations depends strongly on bead size and only weakly on temperature), whereas above  $T^*$  the beads move freely (optical fluctuations have characteristics attributable to Brownian motion). When optical fluctuations of the lipid-water system are measured directly (without exogenous particles, similar changes in relaxation rate are discerned. However, at  $T^*$  the apparent diffusion coefficient reaches a maximum, and then falls as the temperature is increased. We interpret our measurements to indicate that below  $T^*$  the dissolved lipid forms a jelly-like slurry, whereas above  $T^*$  the system transforms to a suspension of lipid vesicles whose wall thickness and tendency to aggregate, increases as  $T$  increases. Phase contrast microscopy observations are in accord with these conclusions. 1. Gershfeld, N. L. and Tajima, K. *Nature*, 279, 708 (1979). 2. Tajima, K. and Gershfeld, N. L. *Biophysical J.*, 47, 203 (1985). 3. Ginsberg, L. and Gershfeld, N. L. *Biophysical J.*, 47, 211 (1985).

**T-Pos200** STRUCTURE AND DYNAMICS OF LYSOPHOSPHATIDYLETHANOLAMINE IN EXCESS WATER. James Slater and Ching-hsien Huang, Department of Biochemistry, University of Virginia School of Medicine, Charlottesville, Virginia 22908 and Ira W. Levin, Laboratory of Chemical Physics, NIADDK, National Institutes of Health, Bethesda, Maryland 20205.

We are currently investigating the phase behavior of a series of synthetic lysophosphatidylethanolamines in excess water. A combination of physical techniques including high sensitivity differential scanning calorimetry, phosphorous NMR and Raman spectroscopy are utilized in our approach to elucidate the thermal behavior and structural properties of these single-chained phospholipids.

Preliminary results indicate that these phospholipids exist at high temperatures in a micellar state, which transforms upon cooling to a highly ordered crystalline phase with chain interdigitation via an intermediate metastable lamellar gel state. Upon prolonged low temperature incubation, this crystalline phase which is initially formed appears to undergo further transformation, yielding additional endotherms in the calorimetric scan. The kinetics of these thermal transitions will be discussed in reference to the structural properties elucidated by NMR and Raman studies. Supported by National Institutes of Health Grant GM-17452.

**T-Pos201** DISTINCT PHASE TRANSITIONS INDUCED BY MAGNESIUM INTERACTING WITH ONE OR BOTH MONOLAYERS OF PHOSPHATIDYL SERINE VESICLES. N. Düzgüneş<sup>a,b</sup>, C. Newton<sup>d</sup> and D. Papahadjopoulos<sup>a,c</sup>. Cancer Research Institute<sup>a</sup> and Depts. of Pharmaceutical Chemistry<sup>b</sup> and Pharmacology<sup>c</sup>, Univ. of California, San Francisco, CA 94143 and Dept. of Biology<sup>d</sup>, Kalamazoo College, Kalamazoo, MI 49007.

Large unilamellar vesicles (LUV; approx. 100 nm diameter) composed of bovine brain phosphatidylserine (PS) do not fuse or release their contents in the presence of  $Mg^{2+}$  (Wilschut et al., Biochemistry 20, 3126; 1981), and provide a unique experimental system for investigating the interaction of a divalent cation with one monolayer of an acidic phospholipid bilayer. The fluorescent  $Mg^{2+}$  indicator 8-hydroxyquinoline-5-sulfonate was encapsulated in the vesicles to show the absence of  $Mg^{2+}$  entry into the vesicles. The gel-liquid crystalline phase transition endotherm of LUV(PS) in 100 mM NaCl, pH 7.4, detected by differential scanning calorimetry, was between -5 and 12 °C, with a peak at 6.5 °C. In the presence of 10 mM  $Mg^{2+}$ , the endotherm had a broad peak ranging from 11 to 15 °C, whereas multilamellar PS bilayers exposed to  $Mg^{2+}$  on both sides displayed an endotherm with a peak at 22 °C. When the LUV were frozen at -20 °C and scanned again, the endotherm shifted upward to 20 °C. LUV produced by  $Mg^{2+}$ -induced fusion of small unilamellar vesicles had a transition at 20 °C. Since this fusion is a leaky process,  $Mg^{2+}$  is expected to be on both sides of the bilayer. Indeed, when EDTA was added to the fused vesicles with  $Mg^{2+}$  inside, a broad endotherm with a peak between 10 and 14 °C was observed. Our results indicate a substantial effect due to the asymmetric distribution of  $Mg^{2+}$  across the bilayer, where the monolayer not exposed to  $Mg^{2+}$  exerts a fluidizing effect on the monolayer interacting with the cation. Supported by NIH Grant GM28117 and a Grant-in-Aid from the American Heart Association.

**T-Pos202** KINETICS AND DYNAMICS OF MEMBRANE TRANSITIONS. W.W. van Osdol and M.L. Johnson, Biophysics Program and Department of Pharmacology, University of Virginia, Charlottesville, Virginia, 22908

We are studying the kinetics of the pretransition and the main phase transition of model membranes by using a recently-developed volume perturbation calorimeter. The instrument functions by forcing a suspension of lipid vesicles to undergo small, adiabatic, bi-directional volume perturbations. The relaxation of the suspension to a new equilibrium state is monitored by measuring the temperature and pressure of the system as functions of time after application of the perturbation. Rate constants for the relaxation processes are obtained by analyzing the observables in terms of sums of exponential decays and associated amplitudes. The instrument is capable of measuring apparent relaxations in an approximate time range of 1ms to 10s.

The project has thus far concentrated on single- and multi-lamellar phospholipid systems of a single component, such as phosphatidylcholines (PCs) bearing identical, saturated acyl chains. Data about relaxations of membrane expansivity and compressibility, derived from experiments on DMPC and DPPC, will be presented to demonstrate our techniques.

We plan to extend our investigations to systems altered by the presence of impurities such as local anesthetics or cholesterol. The effect of head group structure and charge will also be studied.

The object of our investigations is to better understand how the constituent parts of a phospholipid molecule, as well as their intermolecular interactions, contribute to the dynamics of model and natural membranes.

**T-Pos203** Fractal and Non-Fractal Crystalline Phospholipid Domains in Monomolecular Layers. A. Miller, W. Knoll and H. Möhwald, TU Munich, Physics Dept. E22, D 8046 Garching

Self-similar structures are suggested to occur in physical as well as in biological systems. An example for this may be crystal growth at high supercooling and low surface tension. Both conditions can be realized for the growth of two-dimensional crystalline domains of phospholipids at the air/water interface and hence fractal structures can be expected for these model membranes.

We report on fluorescence microscopic studies of crystallization processes with a time resolution of better than 0.1 sec. The lipid investigated, dimyristoylphosphatidyl-ethanolamine (DMPE) is distinguished by an almost horizontal pressure/area diagram in the coexistence range between fluid and solid phase and can be subjected to pressure jumps up to 0.5 mN/m. Following this solid domains are formed that are fractal on the length scale between 5  $\mu$ m and 100  $\mu$ m and that exhibit a fractal dimension  $d_f$  close to a value calculated for diffusion limited aggregation (Fig. 1). Equilibrating the system leads to the disappearance of the highly carved structures after some minutes and the lengths of the boundary lines between fluid and solid of a single domain are minimized. The domain size is uniform and decreases with increasing content of a dye which was varied systematically as an impurity. During crystallization the dye distribution near the phase boundary can be determined from fluorescence intensity profiles proving that crystallization is controlled by constitutional supercooling.



**T-Pos204** EFFECT OF CALCIUM ON PHOSPHOLIPID POLYMORPHISM. A. Sen, S.W. Hui, T.V. Isac, Department of Biophysics, Roswell Park Memorial Institute, Buffalo, New York 14263, and J.M. Boggs Department of Biochemistry, Hospital For Sick Children, Toronto, Canada.

The effect of calcium on the phase property of mixed phospholipid system was studied using  $^{31}\text{P}$  NMR, x-ray diffraction, freeze fracture electron microscopy and differential scanning calorimetry. In mixtures containing negatively charged phosphatidylserine (PS)  $\text{Ca}^{2+}$  can induce bilayer to non-bilayer transition by sequestering PS. Calcium was also found to alter the bilayer to non-bilayer transition characteristics of phosphatidylethanolamine(PE):phosphatidylcholine (PC) mixtures and lamellar to hexagonal transition of phosphatidylethanolamine. In pure PE calcium was found to decrease the lamellar to hexagonal transition temperature by  $2^\circ\text{C}$ . The lowering of the transition temperature by  $\text{Ca}^{2+}$  is thought to be due to the presence of residual negatively charged PE at neutral pH since at lower pH calcium did not have any effect on the transition temperature. In lipid mixtures of PE:PC:PS and PE:PC, calcium was found to abolish intermediate structures like lipidic particles and cubic phase; direct transition from lamellar to hexagonal phase was observed in lipid mixtures in the presence of calcium. It is proposed that the removal of intermediate structures in bilayer to hexagonal transition in lipid mixtures by calcium is due to dehydration of the phospholipid mixtures by calcium.

**T-Pos205** THE THERMOTROPIC PHASE BEHAVIOUR OF 1,2 di- $\omega$ -CYCLOHEXYL PHOSPHATIDYLCHOLINE BILAYERS: DSC,  $^{31}\text{P}$ -NMR AND INFRARED SPECTROSCOPIC STUDIES. R.N.A.H. Lewis and R.N. McElhaney, Department of Biochemistry, University of Alberta, Edmonton, Alberta, Canada; C. Madec and H.H. Mantsch, Division of Chemistry, National Research Council of Canada, Ottawa, Ontario, Canada.

The thermotropic phase behaviour of a series of 1,2 di- $\omega$ -cyclohexyl phosphatidylcholines (PCs) was studied by DSC,  $^{31}\text{P}$ -NMR and IR spectroscopy. The properties of these compounds are strongly dependent on whether the acyl chains contain an odd or an even number of carbon atoms. The odd-numbered compounds exhibit a single heating endotherm which is the structural equivalent of a concomitant gel/gel and gel/liquid-crystalline phase transition. The calorimetric behaviour of the even-numbered PCs is characterized by a complex array of gel state phenomena in addition to the main chain-melting transition, and their gel states are characterized by a greater conformational disorder in the acyl chains and a greater mobility of the phosphate headgroup. The differences between the odd- and even-numbered PCs are reflected in a pronounced odd-even alternation in the characteristic transition temperatures, transition enthalpies, their heating/cooling reversibility characteristics, and their responses to the composition of the bulk aqueous phase. Moreover their chain melting transition temperatures and enthalpies are considerably lower than those of n-acyl PCs of comparable acyl chain length. These observations suggest that the presence of  $\omega$ -cyclohexyl rings in the fatty acyl chains of a PC bilayer results in a considerable disruption of the organization of both the polar headgroups and hydrocarbon chains and that these disruptions are more severe with the even numbered PCs.

(Supported by Medical Research Council of Canada and Alberta Heritage Foundation for Medical Research)

**T-Pos206** DYNAMICS AND PHASE BEHAVIOR OF MYCOPLASMA CAPRICOLUM MEMBRANE - A DEUTERIUM NMR STUDY. Tai-huang Huang, August J. DeSiervo, Stephen H. Grode, Russell W. Gillis and Alma Homola. Department of Physics, University of Maine at Orono, ME 04469.

We have incorporated (7,7,8,8-d $_4$ ) and perdeuterated palmitic acid into M. capricolum membrane by growing cells in modified Edward's medium supplemented with oleic acid, labelled palmitic acid, 5% bovine serum albumin and various amount of cholesterol. Membrane lipid compositions analyzed by 2-D paper chromatography shows that most of exogeneous palmitic acid was incorporated into phosphatidylglycerol (~60%) and cardiolipin (~35%) with the remaining present as free fatty acid or neutral lipids. The efficiency of incorporation is better than 50%.  $^2\text{H}$  NMR spectra of whole cells grown in the presence of 2.5  $\mu\text{g}/\text{ml}$  of cholesterol reveals that above  $10^\circ\text{C}$  the membrane lipids are in liquid crystalline state with the residual quadrupole splitting  $\Delta\nu_{\text{Q}}$  ~40 KHz. Between  $-10$  and  $10^\circ\text{C}$ , the spectra are characteristic of the coexistence of both gel and liquid crystalline states. At 20  $\mu\text{g}/\text{ml}$  cholesterol the  $^2\text{H}$  NMR spectra appear to be sharper with similar  $\Delta\nu_{\text{Q}}$ . Spectra of lipid extracts are also much sharper with similar  $\Delta\nu_{\text{Q}}$ . We have also measured deuterium quadrupole echo decay times,  $T_{2e}$  at various temperatures and cell-growth conditions. At growth temperature ( $35^\circ\text{C}$ ) cholesterol has no effect on  $^2\text{H}$   $T_{2e}$  of whole cells (~80  $\mu\text{s}$ ).  $T_{2e}$  decreases at lower temperatures and is longer at higher cholesterol concentrations. The implications of these data will be discussed.

**T-Pos207** THE ENIGMATIC PHASE BEHAVIOUR OF DILAUROYL PHOSPHATIDYLCHOLINE.  
M.R. Morrow and J.H. Davis, Biophysics Interdepartmental Group, Physics Department, University of Guelph, Guelph, Ontario, Canada N1G 2W1.

Nuclear magnetic resonance, differential scanning calorimetry and x-ray diffraction have been used to examine the phase behaviour of mixtures of 1,2-dilauroyl-*sn*-glycero-3-phosphocholine in excess buffer at pH 7.0. Below 0 °C, the lipids are in a solid bilayer phase, above 6 °C, they are in a fluid, liquid crystalline bilayer phase like that of longer chain phospholipids. There appear to be two "phase transitions" between 0 and 6 °C, both involving the melting of the hydrocarbon chains. While at least three explanations for this behaviour can be proposed, involving metastable phases, two-phase coexistence if buffer is not in excess, and the possibly continuous nature of the phase transitions, at present, none of these is complete nor can any be rejected.

**T-Pos208** <sup>31</sup>P NMR Spin-Lattice Relaxation Time Studies on Egg Lecithin Model Membranes. M.P. Milburn and K.R. Jeffrey, Biophysics Interdepartmental Group, Physics Department, University of Guelph, Guelph, Ontario, Canada N1G 2W1

Information on the dynamics of the choline headgroup of phosphatidylcholine liposomes may be obtained by studies of the spin lattice relaxation time as a function of temperature. For example, the correlation time of a molecular motion is often calculated from a minimum in the spin lattice relaxation time versus inverse temperature curve. Knowledge of the spin lattice relaxation mechanism of the phosphorus nuclear spin in the lipid's phosphate moiety can yield valuable dynamical information. Such knowledge may be obtained by a study of the frequency dependence of the spin relaxation as a function of temperature. The relaxation mechanism of the <sup>31</sup>P nuclear spin in liposomes of egg yolk PC has been investigated at four resonant frequencies (39 MHz, 81 MHz, 109 MHz, 145 MHz) at temperatures from -30 °C to 60 °C. Results indicate that dipolar relaxation and relaxation due to anisotropic chemical shift both contribute significantly to the relaxation.

**T-Pos209 TWO MECHANISMS FOR FORMING NOVEL TUBULAR MICROSTRUCTURES FROM POLYMERIZABLE LIPIDS.** Yager, P. and Schoen, P.E., Naval Research Laboratory, Bio/Molecular Engineering Branch, Code 6190, Washington, DC 20375-5000, and Georger, J., Price, R. and Singh, A., Geo-Centers, Newton Upper Falls, MA 02164

We have been investigating novel tubular microstructures which form from the lecithin bis(10,12-tricosadiynoyl)-sn-glycerophosphorylcholine. These structures are straight, open-ended hollow cylinders approximately 0.5 micrometers in diameter and up to several hundred micrometers in length. As the component lipid molecules contain diacetylenic groups the resultant microstructures can be rendered permanent by polymerization. These structures form within minutes when an aqueous dispersion of the lipid is cooled to the chain melting temperature, and electron microscopic studies of samples quenched during formation reveal liposomes deflating and wrapping around nascent tubules. An alternative method of formation has also been discovered that produces not only tubules, but also a precursor helical structure with overall dimensions nearly identical to those of the tubules. This alternative method has allowed rapid screening of other polymerizable lipids, some of which also produce tubules, and has great potential for discovering other lipid microstructures.

**T-Pos210 X-RAY STRUCTURAL STUDIES OF INDIVIDUAL MOLECULAR MONOLAYERS**  
V. Skita, W. Richardson, P.L. Dutton, M. Filipkowski, A.F. Garito, J.K. Blasie. Depts. of Chemistry, Biochemistry-Biophysics, Physics and the LRSM, University of Pennsylvania, Philadelphia, Pennsylvania 19104 *Introduced by John Haselgrove*

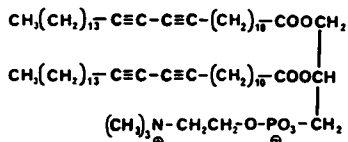
Langmuir-Blodgett multilayer films composed of various sequences of disubstituted diacetylene (D) and arachidic acid (A) monolayers deposited on glass substrates have been characterized by meridional x-ray diffraction. A polar multilayer surface can be produced by polymerizing underlying diacetylene monolayers with uv light to form a diacetylene polymer (the polymer chains being perpendicular to the monomer hydrocarbon chains) and then removing the surface arachidic acid monolayer by washing the multilayer with NaOH.

Autocorrelation functions for the DDDA and DDD multilayer profiles have been calculated. Electron density profiles for the DDDA and DDD multilayers were derived by a variant of the box refinement technique which co-refines structures simultaneously. The autocorrelation functions and electron density profiles for the DDDA and DDD multilayers clearly demonstrated the removal of the last arachidic acid monolayer.

The polar surface of the DDD multilayer can be utilized to specifically bind a monolayer of protein thereby providing a unique system for detailed structural-functional studies of membrane phenomena. The binding site on the protein may be altered by varying the polar moiety on the surface diacetylene monolayer to accommodate the surface amino acid residues of the protein and thereby unidirectionally bind the protein or protein complex. Electron density profiles could then be derived for such protein monolayer systems using the box refinement or co-refinement techniques.

**T-Pos211 INTRINSIC FLUORESCENCE OF POLYDIACETYLENIC PHOSPHOLIPDS.** Richard B. Thompson, Naval Research Laboratory, Code 6190, Washington, DC 20375-5000 and Jacque Georger, Jr. and Alok Singh, Geo-Centers, Inc., 320 Needham Street, Newton Upper Falls, MA 02164

Phospholipids having diacetylenic moieties within their acyl side chains may be photopolymerized to yield bilayer structures with novel, interesting properties. There is substantial current interest in such polymerizable lipids because of their potential use in biotechnology, their nonlinear optical properties, and their ability to form large hollow tubules. The polymer backbone can exhibit thermochromism, initially appearing blue but changing to orange or red with increased temperature. We obtained fluorescence spectra of polydiacetylenic fatty acids and phosphatidylcholines in the solid phase, as Langmuir/Blodgett films, and/or as unilamellar or multilamellar vesicles in aqueous solution. The red form emits in the orange, whereas the blue form emits very weakly in the violet with ultraviolet excitation. Phase-modulation lifetime data obtained with the recently introduced ISS multifrequency instrument suggest that the red form is a mixture of emitters with lifetimes mainly in the subnanosecond range.



(Supported by the Defense Advanced Research Projects Agency. R.B.T. is a National Research Council Research Associate.)

T-Pos212 THERMOTROPIC PHASE BEHAVIOR OF VESICLES COMPOSED OF A POLYMERIZABLE LECITHIN: A DIFFERENTIAL SCANNING CALORIMETRIC STUDY. \*Thomas G. Burke, James P. Sheridan, \*Alok Singh and Paul E. Schoen, Code 6190, Bio/Molecular Engineering Branch, Naval Research Laboratory, Washington, DC 20375-5000

The thermotropic phase behavior of aqueous dispersions of the polymerizable diacetylenic lecithin 1,2-bis(10,12-trico-s-adiynoyl)-sn-glycero-3-phosphocholine (DC<sub>23</sub>PC) was studied by differential scanning calorimetry. It has previously been shown that aqueous suspensions of monomeric DC<sub>23</sub>PC can, under certain conditions, convert from the expected spherical liposomal structures to a unique phase consisting of hollow tubules (Yager et al., Biophys. J., in press, 1985). Multilamellar vesicles were prepared by vortexing a 100 mg/ml DC<sub>23</sub>PC suspension at 60°C. Upon heating from 0 to 60°C at a scan rate of 1°C/min., a single endothermic event was observed at 43.0°C with an enthalpy of 20 kcal/mol. Subsequent cooling of this sample showed two exothermic events; one transition occurring at 38.3°C with an enthalpy of -9.8 kcal/mol. while the other event occurred at 5.3°C with an enthalpy of -9.0 kcal/mol. When the sample was cooled from 50°C to 30°C and then rescanned, an endothermic event still occurred at 43.0°C, but yielded an enthalpy of only 9.7 kcal/mol. Repeating the experimental cycle with vesicles of a different size prepared by sonication yielded similar results, with the exception that the relative enthalpies of the two exothermic events were varied, the total enthalpy remaining the same. Optical microscopy showed only vesicular structures at both 30 and 50°C with no evidence of tubule formation. The relationship between the phase transitions of these vesicles with tubule formation will be discussed.

(\*TGB and AS are employed by Geo-Centers, Inc., Newton Upper Falls, MA)

**T-Pos213** ARCHAEBACTERIAL LIPIDS: A MOLECULAR MECHANICS STUDY. E. L. Chang\*, C. Montague\*, and A. H. Lowrey†, Code 6190\* and Code 6030†, Naval Research Laboratory, Washington, D.C., 20375-5000.

Lipids derived from archaeobacterial membranes show a predominant structure composed of two glycerol-based polar headgroups connected to each other through di-biphytanyl chains. The chemical structure of the lipids suggests that a monolayer lamella may exist in the membranes of archaeobacteria. However, this has not been conclusively proven. In fact, recent low-resolution X-ray data suggest that a mixture of mono- and bilayers may coexist in the native membrane<sup>1</sup>. We have utilized a molecular mechanics algorithm, MM2<sup>2</sup>, to study the possible conformations of the various lipids derived from archaeobacteria. Both straight and folded chain conformations of "archaelipids" were examined for glycerol and nonitol headgroups. The three-dimensional local minima conformations were displayed under a molecular graphics program, FRODO, to determine the possible relationships of the structures to the membrane packing properties of the lipids.

1. A. Gulik, et al., *J. Mol. Biol.* 182, 131-149 (1985).
2. N. L. Allinger, *Advances in Physical Organic Chemistry* V13, V. Gold and D. Bethell (eds.), Academic Press (1976).

**T-Pos214** EXTENDED HYDROGEN BONDED STRUCTURES OF PHOSPHATIDYLETHANOLAMINE. A. Sen, S.W. Hui Roswell Park Memorial Institute, Buffalo, New York 14263; P.Y. Yeagle, Department of Biochemistry, SUNY at Buffalo, Buffalo, New York 14214; and H.H. Mantsch, NRC of Canada, Ottawa, Canada.

Inter and intra molecular hydrogen bonding has long been considered a possibility in some lipids like phosphatidylethanolamine (PE) but so far there has been no direct observation of such hydrogen bonded structures. In this presentation we report on our studies on the structure of phosphatidylethanolamine in a hydrocarbon environment. When PE is dispersed in hexane, the result is not a free flowing liquid as would be expected of a solution of a lipid in an organic phase, but is very viscous. The viscosity of PE in hexane (10 mg lipid/ml) is 15 centistokes as compared to 0.46 for hexane alone or 0.5 centistokes for phosphatidylcholine in hexane (10 mg/ml). Such a high viscosity suggests a gel formation and is supported by our freeze fracture electron microscopy studies which show an extensive network of fibrous structures for PE in hexane. 31-P NMR studies conducted on PE in hexane showed a almost complete immobilization of the phospholipid headgroup. The extended structures as revealed by viscosity, electron microscopy and NMR are completely abolished by the addition of a small volume of water and hydrogen bonding organic solvents like methanol and chloroform to the hexane dispersion of the lipid. Fourier transform IR measurements show major changes in the spectrum of PE in hexane after the addition of water. The changes are in the portion of the spectrum where amine and the phosphate group absorb. We propose that the extended structure of PE in hexane arises due to inter molecular hydrogen bonding between the amine and the phosphate groups of neighbouring PE molecules.

**T-Pos215** INFRARED REFLECTION SPECTROSCOPY. IN SITU MEASUREMENT OF THE SPECTRA OF PHOSPHOLIPID MONOLAYERS AT THE AIR-WATER INTERFACE. Richard A. Dluhy, National Center for Biomedical Infrared Spectroscopy, Battelle-Columbus Division, 505 King Avenue, Columbus, Ohio 43201

The past decade has seen enormous progress in the ability of vibrational spectroscopy to probe the structure and properties of organic monolayer films. Until now, however, it has not been possible to study in situ the group of monomolecular films whose native substrate is water. Such molecules include surfactants, polymers, proteins, steroids, lipids and other compounds of a biophysical nature. We wish to describe an application of external reflection FT-IR spectroscopy that utilizes the reflection properties of water in the mid-infrared spectra of monomolecular films at the air-water phase boundary.

This reflection technique has been used to obtain the infrared spectra of two synthetic phospholipids that form oriented monolayer surface films. The two phospholipids (1,2-distearoyl-sn-glycero-3-phosphocholine [DSPC], and 1,2-dimyristoyl-sn-glycero-3-phosphocholine [DMPC]) were chosen to represent two possible thermodynamic states of an insoluble surface film (i.e. the liquid-condensed [DSPC] and liquid-expanded [DMPC] surface states). These are the monolayer analogs of the gel and liquid-crystalline phases that exist below and above the first order phase transition temperature, respectively, of the bulk lipid. The polarized FT-IR reflection spectra demonstrate significant differences in the intensities in the C-H region of the spectrum as well as band splitting and frequency shifts in the PO<sub>2</sub><sup>-</sup> stretching region due to the phosphate ester. These results suggest that this reflection technique may be used to determine molecular-level changes in model phospholipid monolayer films on water.

**T-Pos216** MONOLAYERS ARE SIMPLE LIQUIDS THAT EXHIBIT TWO-DIMENSIONAL OSMOTIC PRESSURE. R.C. MacDonald and S.A.Simon (Intr. I.M.Klotz) Department of Biochemistry, Molecular & Cell Biology, Northwestern U., Evanston IL, & Department of Physiology, Duke U., Durham, NC

We have examined surface tension-surface concentration isotherms of phosphatidylcholine (PC) monolayers, prepared by addition of lipid to a constant area water surface. In the liquid-crystalline phase, the  $\gamma$ - $\Gamma$  relationship consists of broken lines, revealing the existence of 4 distinct states: 1) The vapor pressure of a liquid phase having horizontal chains. 2) A condensed liquid phase which, for dimyristoyl-PC (DMPC), extends from  $1 < \gamma < 15$  dyne/cm in tension and 4.5-9 Å in thickness. Here, alkyl chains lie on the surface, side-by-side at the high area extreme and on top of one another (2 chains thick) at the low area extreme. 3) A condensed liquid phase extending from 15 to 49 dynes/cm in tension and from 9 to 19 Å in thickness (DMPC). Chain orientation changes from horizontal to vertical within this phase. 4) A phase of constant 49 dyne/cm tension, the pressure at which bilayers are in equilibrium with the monolayer and where monolayer properties correspond closely to those of 1/2 a bilayer. The boundary between phases 2 and 3, obvious in  $\gamma$ - $\Gamma$  plots, cannot be discerned in  $\pi$ -A plots, which may explain why such states have not been observed in the past, even though they are ubiquitous features of lipid films, judging from the literature we have examined. A linear  $\gamma$ - $\Gamma$  relationship corresponds to an equation of state  $\pi A = \text{constant}$ . Application of 2-dimensional osmotic pressure formalism provides an explanation of this behavior. We assume the monolayer to be a simple 2-dimensional liquid into which water equilibrates, raising the surface pressure according to the product of the thickness and the osmotic pressure. For phases 3 and 4, the surface pressure is well approximated when one uses for the mole fraction of water, the number of water molecules known to associate with PC in bilayers.

**T-Pos217** THE EFFECT OF FREE CHOLESTEROL ON BILAYER SOLUBILITY OF CHOLESTERYL OLEATE. Paul J.R. Spooner, James A. Hamilton, Donald L. Gantz, and Donald M. Small. Biophysics Institute, Housman Medical Research Center, Boston University School of Medicine, Boston, Massachusetts 02118.

Mixtures of egg phosphatidyl choline, and cholesterol were co-sonicated with low levels of [<sup>13</sup>C] cholesteryl oleate (CO) to form vesicles in 0.56% KCl at 52°C and were analyzed by <sup>13</sup>C NMR to determine the extent of ester solubilization. CO produced a single resonance at ~37°C, attributed to the bilayer-incorporated fraction, while excess CO yielded a resonance upfield from this peak only at temperature greater than 48°C. The equilibrium intensity of the resonance at 37°C could thus be compared with that of the phospholipid carbonyl peaks to obtain the limiting bilayer solubility of CO. Incorporation of cholesterol decreased the CO solubility only slightly with respect to phospholipid, from 2.8 to 2.4 mole% over the range 0-33 mole% cholesterol. At 50 mole% cholesterol, CO solubility was reduced to about 1.3 mol% with respect to phospholipid. Further, as the cholesterol:phospholipid ratio was increased the solubilized CO peak showed significant shifts upfield, suggesting that the carbonyl group became less exposed to the aqueous environment. In summary, cholesterol up to 33 mole% with phospholipid has only a small effect on CO bilayer solubility but higher cholesterol content decreased more significantly the CO solubility and appears to push it deeper into the bilayer.

**T-Pos218** INTERACTIONS OF PHOSPHATIDYLCHOLINE, LYSOPHOSPHATIDYLCHOLINE AND CHOLESTEROL IN SURFACE FILMS. J. M. Smaby and H. L. Brockman, Hormel Institute, U of MN, Austin, MN

The interaction between 1-palmitoyl lysophosphatidylcholine (LPC), dipalmitoylphosphatidylcholine (PC) and cholesterol (C) was studied in monomolecular films at the air/water interface at 24°. As previously established, C abolished the liquid expanded-liquid condensed phase transition. The transition width decreased linearly with increasing mol fraction of C, reaching zero at a C/PC mol ratio of 0.27 (21 mol percent C). The presence of LPC in the C/PC films at LPC/C mol ratios of 1 or 2 had little effect on either the linearity of the decrease or the C/PC ratio at which the transition was eliminated. In PC/LPC mixed films, the surface pressure at which the liquid expanded-liquid condensed phase transition of PC began was increased linearly by LPC from 8.3 mN/m at LPC/PC = 0.0 to 19.4 mN/m at LPC/PC = 0.69. In ternary mixtures, this behavior was unaffected by C at LPC/C mol ratios of 1 or 2 for LPC/PC up to 0.46. Average molecular areas for ternary mixtures in the liquid expanded state were calculated using parameters obtained with binary mixtures and assuming that either the LPC/C or PC/C interaction is preferred. The results are similar but better agreement with measured values was obtained for the latter. Together, these results support the idea that PC and C form cholesterol-rich domains or a separate phase in which LPC is not miscible and that LPC and PC are miscible. Thus, while LPC/C interaction may be preferred in the presence of egg lecithin [Chauhan et al. (1984) Biochim. Biophys. Acta 772, 239-243], PC/C interaction is preferred when the dipalmitoyl species is used.

**T-Pos219** THE EFFECT OF BUTYLATED HYDROXYTOLUENE ON THE POLYMORPHIC PHASE BEHAVIOR OF PHOSPHATIDYLETHANOLAMINE Kwan-Hon Cheng\*, Philip L. Yeagle+, James P. Lepock#, and Sek Wen Hui\* (\*Biophysics Dept., Roswell Park Memorial Instit., +Biochemistry Dept., SUNY/ Buffalo, #Physics Dept., U. Waterloo, Ontario, Canada.)

The influence of butylated hydroxytoluene (BHT) on the polymorphic phase behavior of PE (transphosphatidylated from egg PC) (TPE) was investigated by P-31 NMR, differential scanning calorimetry, and freeze-fracture electron microscopy. The addition of BHT to TPE not only lowered the temperature of the gel to liquid crystalline phase transition but also resulted in an even greater decrease in the bilayer to hexagonal phase transition temperature of TPE. The BHT-induced decrease in bilayer to hexagonal phase transition temperature (from 55°C to 35°C) is dependent on the concentration of BHT (from 0 to 0.1 molar ratio of BHT/TPE). The H-2 NMR study of the BHT/perdeuterated DPPC mixtures indicated that BHT perturbs essentially the upper position of the fatty acyl chains of the phospholipid in the liquid crystalline phase of the lipid. We hypothesize that the molecular mechanism of BHT modification of the polymorphic phase behavior of TPE is associated with either the dehydration of the lipid bilayer surface or an increase in lipid volume by BHT. The destabilization of the bilayer phase could account for the previous observations of disruption of lipid containing viruses and enhancement of poly(ethylene glycol)-induced fusion by BHT.

**T-Pos220** INFLUENCE OF ACYL CHAIN LENGTH ON THE MOLECULAR PACKING OF 1,2-DIPALMITOYL-3-SHORT ACYL CHAIN *sn*-GLYCEROLS IN  $\alpha$  AND  $\beta'$ -PHASES. D.R. Kodali, D.M. Small and D. Atkinson, (Intr. by D.H. Croll). Biophysics Institute, Housman Medical Research Center, Boston University School of Medicine, Boston, MA 02118.

Thermal and structural changes in 1,2-dipalmitoyl-3-acetyl (PP2), 3-butyryl (PP4), 3-hexanoyl (PP6), and 3-octanoyl (PP8)-*sn*-glycerols were studied by DSC and x-ray diffraction. Quenching from the melt produces an  $\alpha$ -phase (hexagonal chain packing,  $d=4.05\text{\AA}$ ). For each the enthalpy of crystallization of  $\alpha$  is  $\sim 16\text{Kcal/mole}$ . While PP2 formed a bimolecular length  $\alpha$ -phase ( $D=51\text{\AA}$ ), the others packed in a uni-molecular length structure (PP4=28Å, PP6=30Å and PP8=32Å) with decreasing stability as the 3-acyl chain lengthened. At 0°C conversion to  $\beta'$  phase occurred in >8 hrs for PP2,  $\sim 2$  hrs for PP4, 15-30 minutes for PP6 and only 2-4 minutes for PP8. The  $\beta'$ -phase subcell was orthorhombic perpendicular (4.2 and 3.8Å or 4.3, 4.0 and 3.8Å) with long spacings indicating a trilayer which increased from 46 to 53Å as the 3-acyl chain lengthened. The short 3-acyl chain forms a middle layer interposed between two different layers of 1,2-dipalmitoyl chains. On incubation at the melting temperatures of the  $\beta'$ -phase, PP2 and PP4 transformed into a stable bilayered ( $D=43\text{\AA}$ )  $\beta$ -phase. In summary quenching produces a hexagonally packed  $\alpha$ -phase, unimolecular in length (exception PP2), which is probably highly disordered within and between layers leading to decreased stability as the 3-acyl chain is lengthened. In the trilayered  $\beta'$ -phase the increasing 3-acyl chain length increased the stability, facilitating  $\alpha$  to  $\beta'$  transition. When the 3-acyl chain is 4 carbons or less the trilayered structure is unstable and transforms to a stable  $\beta$ -bilayer.

**T-Pos221** STABILITY OF THE TRILAYER VS. BILAYER STRUCTURE IN 18 CARBON FA TRIACYLGLYCEROLS: THE EFFECT OF UNSATURATION AND SUBSTITUTION IN THE 2 POSITION. D.R. Kodali, D. Atkinson and D.M. Small. Biophysics Institute, Housman Medical Research Center, Boston University School of Medicine, Boston, Massachusetts 02118.

Saturated and unsaturated monoacid triacylglycerols (TG), tristearin (SSS), triolein (OOO), trielaidin (EEE, *trans*-9), trivaccin (VVV, *trans*-11) and the symmetric diacid TGs, 1,3-dioleoyl 2-stearoyl (OSO), 2-elaidoyl (OEO), and 2-vaccinoyl (OVO) glycerols were studied by DSC and x-ray diffraction. The stable  $\beta$  phase of monoacid TG (subcell triclinic //, strong 4.6Å) is a bilayered structure ( $D=45\text{\AA}$ ) whose melting point varied with chemical structure (OOO=5°, VVV and EEE=42°, SSS=73°C). On quenching from the melt the symmetric TGs OVO and OEO form a bilayered ( $D=45\text{\AA}$ )  $\beta'$ -phase (orthorhombic perpendicular subcell, strong 4.2Å and 3.8Å). However, OSO when quenched from the melt forms a hexagonally packed (strong 4.05Å), bilayered ( $D=52\text{\AA}$ )  $\alpha$ -phase. At -7°C the  $\alpha$ -phase quickly transforms to a bilayered ( $D=45\text{\AA}$ )  $\beta'$ -phase. Incubation at the  $\beta'$ -phase melting temperature transforms OVO, OEO and OSO into a trilayered ( $D=65\text{\AA}$ )  $\beta$ -phase, where the 1,3-dioleoyl chains are segregated from the vaccinoyl, elaidoyl or stearoyl chains into alternating layers. In summary, when all the acyl chains in a TG are the same (saturated, *cis* or *trans* unsaturated) the stable  $\beta$ -phase packs into a bilayered structure. However, when the 1 and 3 acyl chains are *cis* unsaturated (kinked) and the 2-acyl chain is either saturated or *trans*-unsaturated (straight) an unstable bilayered  $\beta'$ -phase can form but readily transforms to a stable trilayered  $\beta$ -phase, where the 2-acyl chains form a layer between two different layers of 1,3-oleoyl chains.

**T-Pos222** SELF-ASSOCIATION OF BILE SALTS IN ISOTONIC SALINE SOLUTIONS AT 37°C

John M. Beckerdite and E.T. Adams, Jr., Chemistry Department, Texas A&M University, College Station, TX 77843

Bile salts are natural surfactants that aid in the solubilization of lipids. We have investigated the self-association of the sodium salts of cholic (NaC), ursodeoxycholic (NaU) and deoxycholic (NaD) acids at 37°C in isotonic saline using vapor pressure osmometry. The strongest self-association was exhibited by NaD which has two hydroxyl groups. All three bile salts had similar modes of association, and they were best described by a two equilibrium constant sequential self-association, the Type IV SEK model in which odd species greater than monomer (trimer, etc.) were absent. This behavior is in marked contrast to the self-association of bile acid methyl esters in organic solvents (CHCl<sub>3</sub> and CCl<sub>4</sub>); here the trihydroxy ester (methyl cholate) showed the strongest association in each solvent.  
(Supported by NIH grant GM23877 and Welch Foundation grant A485.)

**T-Pos223** EQUILIBRIUM AND DYNAMIC PHASE BEHAVIOR OF MODEL LIPID SYSTEMS PATTERNED AFTER AQUEOUS INTESTINAL CONTENTS DURING LIPID DIGESTION. Joan E. Stagers, Olle Hernell & Martin C. Carey. Dept. of Medicine, Brigham & Women's Hospital, Harvard Medical School. Boston, MA 02115.

A series of mixtures containing oleic acid, monooleoylglycerol, egg yolk phosphatidylcholine, dioleoylglycerol, cholesterol, and a physiologic mixture of human bile salts were prepared in dilute aqueous systems to resemble the composition of human intestinal contents following a lipid meal. The condensed equilibrium phase diagram at 37°C and 150 mM NaCl was established for these lipid mixtures under the most physiologic set of conditions: pH 6.5, 1% total lipid, and a fatty acid (FA) to monoacylglycerol (MG) ratio of 5:1. The equilibrium micellar phase boundary was determined over a range of relevant pH values from 5.5-7.5, total lipid concentrations from 0.5-5%, and molar FA:MG ratios from 5-20:1. Measurement of mean lipid particle size by quasielectic light scattering (QLS) and multi-component analysis, in combination with tie-line compositional analysis, revealed that beyond the micellar phase boundary stable unilamellar vesicles (hydrodynamic radius,  $R_h = 600-800 \text{ \AA}$ ) coexist in equilibrium with mixed micelles ( $R_h = 25-125 \text{ \AA}$ ). These unilamellar vesicles formed spontaneously; and their physical state was verified by freeze-fracture electron microscopy. Kinetic analysis by QLS determined that these vesicles required 3-4 days to grow to equilibrium size. However, upon addition of mixed bile salt-lipid micellar solutions similar in composition to bile, vesicles were solubilized to mixed micelles within minutes. Human duodenal contents following a lipid meal also contained unilamellar vesicles, similar in composition and size to those in the model systems, which spontaneously converted to micelles within minutes to hours *ex vivo*. Collectively these results suggest that unilamellar vesicles coexist in metastable equilibrium with micelles under the physiologic post-prandial conditions of the intestine.